ASD-TDR-62-451

MATERIALS CENTRAL TECHNICAL LIBRARY
OFFICIAL FILE COPY

AD-292001

(Unclassified Title)

PROPERTIES OF PLASMAS AS THEY PERTAIN TO THERMAL ARC-JETS

TECHNICAL DOCUMENTARY REPORT NO. ASD-TDR-62-451
August 1962

Aeronautical Systems Division
Air Force Systems Command
United States Air Force
Wright-Patterson Air Force Base, Ohio

Project No. 1(10-3048), Task No. 30193

(Prepared under Contract No. AF 33(616)-8173
by the Plasmadyne Corporation, Santa Ana, California)

NOTICES

When Government drawings, specifications, or other data are used for any purpose other than in connection with a definitely related Government procurement operation, the United States Government thereby incurs no responsibility nor any obligation whatsoever; and the fact that the Government may have formulated, furnished, or in any way supplied the said drawings, specifications, or other data, is not to be regarded by implication or otherwise as in any manner licensing the holder or any other person or corporation, or conveying any rights or permission to manufacture, use, or sell any patented invention that may in any way be related thereto.

Qualified requesters may obtain copies of this report from the Armed Services Technical Information Agency, (ASTIA), Arlington Hall Station, Arlington 12, Virginia.

This report has been released to the Office of Technical Services, U.S. Department of Commerce, Washington 25, D.C., for sale to the general public.

Copies of this report should not be returned to the Aeronautical Systems Division unless return is required by security considerations, contractual obligations, or notice on a specific document.

#115

FOREWORD

This report was prepared by Plasmadyne Corporation under Contract AF 33(616)-8173. This contract was initiated under Project Number 1 (10-3048), Task Number 30193, "Properties of Plasmas as They Pertain to Thermal Arc-Jets". The work was sponsored by the Aeronautical Systems Division, Air Force Systems Command, USAF, Wright-Patterson Air Force Base, Ohio. The program was monitored by Mr. J. Lawler. Plasmadyne's principal investigator was Dr. Joseph Meltzer.

This report covers work conducted from 15 February 1961 to 15 February 1962. The major participants to this project were Dr. C. J. Chen, Mr. R. Greco, Mr. Q. McKenna, Dr. J. Meltzer, Mr. G. Mitcheltree, Mr. R. Price and Mr. W. Stoner.

ABSTRACT

The purpose of this study is to present information which will aid in selecting propellants for use in electro thermal engines. Several potential propellants were examined. These include hydrogen, ammonia, helium lithium hydride, nitrogen, methane, air, argon and lithium.

The report includes discussions of important propellant properties and their effect on engine performance and life. The effect of the propellant choice on the operation of the arc-jet is considered. This includes examining theoretical thruster efficiency, engine life and the effect of the engine's mission. Experiments were performed for eight propellants using Plasmadyne's one-kilowatt engine. The results of these tests are discussed.

PUBLICATION REVIEW

This report has been reviewed and is approved.

FOR THE COMMANDER:

Marc P. Dunnam

MARC P. DUNNAM, Chief
Fuels & Lubricants Branch
Nonmetallic Materials Laboratory
Directorate of Materials & Processes

(131p)(53f)(3t)(50r)

TABLE OF CONTENTS

TABLE OF CONTENTS (Cont)

LIST OF FIGURES

LIST OF FIGURES (Cont)

LIST OF FIGURES (Cont)

LIST OF TABLES

THE ELECTRO-THERMAL ENGINE

The electro-thermal engine is a propulsion device which converts electrical energy into directed kinetic energy. The incoming propellant is heated by a gaseous electrical discharge between electrodes to create the plasma. An arc is sustained between the electrodes and high energy is introduced into the propellant by Joule heating using the resistance of the gas itself. This heat or random energy is converted into thrust in a more or less conventional expansion nozzle. This device is represented in Figure 1, which is a typical DC engine. The cathode is usually placed along the axis of the engine and the nozzle acts as the anode. The incoming propellant can be used as a coolant by allowing it to flow first around the hot anode exterior before being introduced into the arc chamber. The gas is usually made to swirl and sometimes a rotating magnetic field is introduced about the anodes. These are used to increase life and give higher performance by producing a more uniform gas and thruster temperature and heating distribution.

Although the arc-jet is a somewhat simple-looking device the phenomena involved in its operation are quite complex. The efficient design involves knowledge of the inter-related effects of the arc physics, the heat transfer by both convection and radiation, the fluid mechanics of the flowing gas and plasma, the plasma kinetics and the propellant used. In addition, if the thermal arc-jet is to be considered as a useful device, the engine system must be considered. This includes the engine, propellant and storage system, controls and power supplies. In order to evaluate this system, the mission and available components for space flight must be considered. The mission under consideration has a strong influence over the selection of a propellant.

In the following report the effects of the propellant choice on the operation of the thermal arc-jet will be considered. This includes examining theoretical thruster efficiency and engine life. The ultimate goal of such a study would be an analysis of the overall system performance for some given missions. Experiments using various propellants were performed using the Plasmadyne-NASA one kilowatt thermal arc-jet engine. The results of these tests are discussed for the eight propellants investigated.

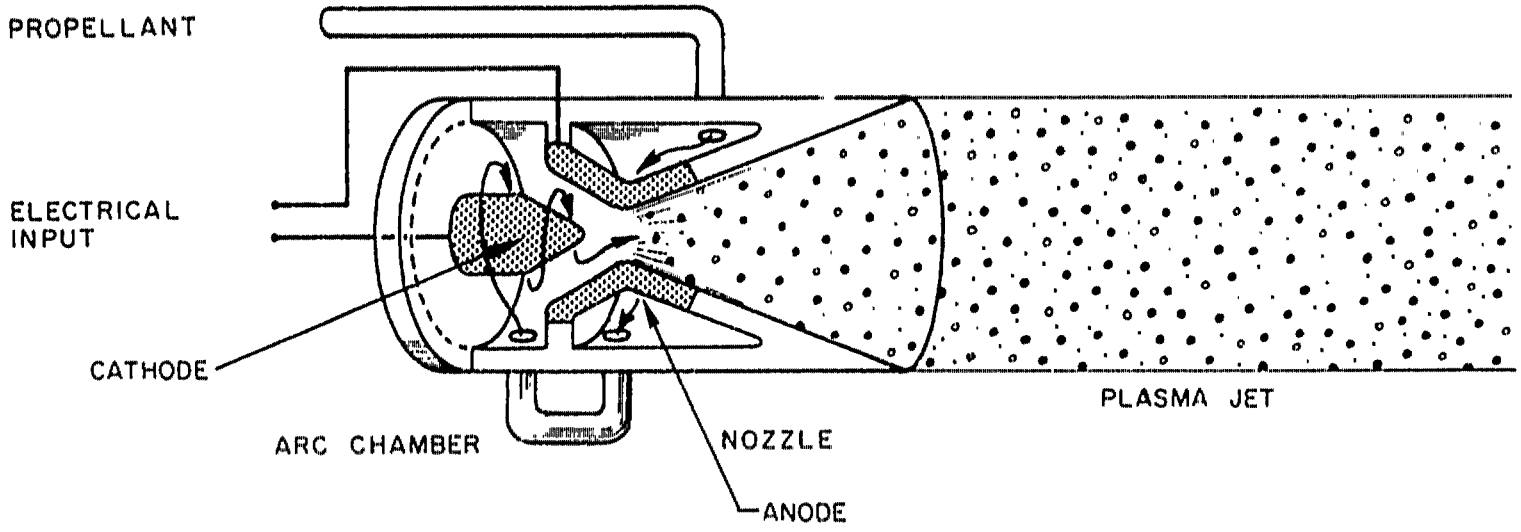

Figure 1 ELECTRIC-THERMAL ENGINE employs a high temperature arc to heat propellant. Arc electrodes are shown in solid black. Arrows indicate direction of propellant flow. Large dots represent atoms, with ionized atoms shown by the symbol o; small dots represent electrons.

THE PROPELLANT - GENERAL DISCUSSION
ON THE IDEAL WORKING FLUID OF THERMAL ARC-JETS

The propellant that will be used as the working fluid, for a single fluid system, must be capable of being ionized. This is so that the fluid can be heated by an arc mechanism. If one assumes as a first order approximation that the level of ionization is the one computed using the Saha formula for the equilibrium condition, then the ease of ionization is directly related to the ionization potential of the gas. The degree of ionization for any given temperature would become greater as the ionization potential decreased. The first requirement for an ideal arc-jet propellant would clearly be a low ionization potential. Saha's equation can be written in a simplified form for a perfect singly ionized plasma

$$\frac{\alpha^2}{1-\alpha^2} \sim \frac{(2\pi m)^{3/2}}{p\,h^3} G\,(KT)^{5/2} e^{(-E_i/KT)}$$

where: α is the degree of ionization
E_i is the $i^{\underline{th}}$ ionization potential
G is the degeneracy factor
p is the pressure
T is the temperature
m is the mass of the species
K, h are the Boltzmann and Planck constants

In addition, the ions and electrons should be capable of returning the energy invested in ionizing the particles if the temperature is lowered (this will be discussed to some extent below). This implies that the recombination rate is high and that recombination, when it does take place is by a three body non-radiative process. Thus, the ionization energy should be able to be converted to directed kinetic energy of the molecules and should not be lost in a non-thrust producing radiative process. This also applies to dissociation energies of polyatomic molecules.

The fluid used as propellant will be heated and some of the energy supplied for this purpose will be inescapably invested in excitation energy. This energy when lost from the gas by radiation will not be available to produce thrust. It is therefore important that this excitation process is not equilibrated to the translational degree of freedom. For the ideal fluid then, if this excitation should occur, it would be desirable that deactivation collisions occur in which this energy is returned to the fluid molecules by a non-radiative process.

The molecules which make up the ideal fluid should not be polyatomic. In that case, in addition to ionization losses, energy would also be absorbed in dissociation. The high energy states required in the arc-jet would make a high degree of dissociation a certainty in polyatomic molecules. This

energy is difficult to recover since the hot propellant is rapidly expanded in the nozzle. Here again, a high recombination rate process would be desirable.

The mass of the particle also plays a part in the fluid performance, particles of very light mass possess the property that they will attain very high speeds when fully expanded from a given initial temperature. It follows that particles of greater mass will expand to a lower velocity when passed through the nozzle of a thrust device. The maximum thrust for a given applied power and a given maximum operating temperature will come from working with heavy particles. However, which is more important in the possible uses of the arc-jet engine, the total impulse obtained from a given total mass ejected from the thruster will be higher for lighter particles. A higher specific impulse will be attained with light particles. The specific impulse is directly proportional to the square root of the temperature and inversely proportional to the square root of the mass and is also a function of the ratio of the specific weights.

$$I_{sp} \alpha \sqrt{T/M}$$

The choice of particle mass for the ideal fluid then depends somewhat on the desired application or mission for which it will be used.

The reliability and life of the thruster are other important criteria to be considered. In order to maintain the geometry of the engine, since changes in the geometry of the device would surely decrease its performance, it is important that the ideal fluid be chemically non-reactive. This is to prevent an attack on the electrodes, thruster and nozzle walls. Extremely high temperatures will also cause material erosion and difficulty in containing the hot plasma and arc. The heat transferred from the arc and plasma should be accomplished in a uniform manner with no local hot spots to cause extreme erosion problems. Another form of material removal from the electrodes is in the form of sputtering. Sputtering becomes a serious problem when the fluid particles acquire enough energy through the arc fall regions to be able to penetrate the solid lattice of the electrodes and displace some of the metal atoms from their lattice positions and subsequently drive surface atoms into the plasma stream.

The ideal fluid, as suggested by the above discussion, should have many non-equilibrium characteristics. All energy supplied to the fluid should be in the form of translational energy. No energy should be absorbed by the fluid in the forms of dissociation, ionization, vibration or excitation except that required for the ionization required to maintain the arc. If these processes should occur they should immediately return all energies into a directed kinetic form by a non-radiative process. Real fluids deviate markedly from the description of the ideal propellant. Most fluids being considered by arc technologists today are polyatomic with large dissociation and ionization losses involved in their usage. Only helium of the lower atomic weight class is inert. Hydrogen is diatomic and highly reactive. The recombination rates of hydrogen in the nozzle seem too slow to regain the associated loss. Other low atomic weight

atoms are quite reactive and tend to form molecules of two or more atoms. They also usually store considerable energy in the form of excitation states with long lifetimes. Real gases so far as this application is concerned absorb too much energy and release it all too slowly. They also attack electrodes and walls with considerable damage resulting. A summary of desirable properties of the "ideal propellant" (criteria of "ideality") are listed below:

1) Easily ionized by electronic excitation.

2) Thermal ionization characterized by a large temperature coefficient - thus a large degree of ionization would take place at low temperatures.

3) Thermal recombination of ions and electrons characterized by a large negative temperature coefficient - recombinations would tend to take place at higher temperatures.

4) Preferably monatomic.

5) If polyatomic, the energy of dissociation should be small.

6) Generally desired, low atomic weight.

7) Cross sections for electronic excitation below the ionization limit should be small for both electronic and heavy particle collisions.

8) Should have very little tendency to form ionic complexes.

9) Should be free of electronic or molecular metastable states of long lifetime.

10) Should be relatively inert chemically at all temperatures.

11) The ion of the parent molecule should also be relatively inert chemically.

12) Ion electron recombination should take place by non-radiative three-body processes exclusively.

13) Elastic collision cross-sections for collisions of the propellant molecules with the wall molecules should be large - thus energy is conserved in the propellant after collision.

14) Inelastic collision cross-section of the propellant molecules with the wall molecules should be small causing heat transfer from the propellant molecules to the wall to be small.

15) Inelastic collision cross-section of the propellant molecules with the cathode molecules should be large - thus heat is transferred

from the ion to cathode material and gives energy to the cathode electrons to cause emission from the surface.

16) Elastic collision cross-section of the propellant molecules with the cathode and anode molecules should be large conserving propellant energy after encounter.

17) Inelastic collision cross-section of the propellant molecules with the anode molecules should be small, decreasing heat transfer due to ion collisions in the anode fall region.

18) The ionization potential of the propellant molecules should show a large negative electron ion density coefficient. The ionization would not become more difficult as concentrations of charged particles increased and no conductivity limit would tend to be approached.

19) The propellant should liquefy at normal temperatures and should go into a relatively high density solid form at reasonable low temperatures.

20) The bulk viscosity of the liquid and gaseous forms should be low.

21) The heat of vaporization from the liquid form should be low.

22) The propellant should be free of impurities in the readily accessible forms.

A real gas will not satisfy more than a few of these qualities. Some of these properties along with tests made using various propellants will be examined to determine promising fluids for arc-jet usage.

MOLECULAR WEIGHT - THERMODYNAMIC EXPANSION

In most propulsion devices the propellant gases are heated as a mechanism of increasing the specific impulse of the device. This can be by chemical combustion, nuclear fission, a solar furnace, nuclear fusion or by an electric arc. All of these devices make use of heating a propellant under pressure and then accelerating it to a high velocity by a thermodynamic expansion to a lower pressure. As discussed above, the computations of arc-jet or even nozzle performance for a real gas is rather complex. However, to obtain a feeling for the effect of molecular weight on specific impulse, the ideal gas will be examined. For this case and at high pressure ratios which do exist in the applications considered the specific impulse is mainly a function of $\sqrt{\frac{T}{M}}$, the square root of the ratio of hot chamber temperature to the molecular weight ratio and also of γ, the ratio of specific heats. Here the temperature is considered uniform in the chamber and all through the expansion and all heat is supplied to the fluid prior to expansion. The molecular weight is the effective weight and depends not only on the initial weight of the species but also on the degree of dissociation occurring in the chamber. The degree of dissociation is best thought of as frozen in the condition imposed in the chamber. For this case the specific impulse is:

$$I_{sp} = \sqrt{\frac{T}{M}} \sqrt{\frac{2\gamma R}{g(\gamma-1)} \left[1 - \left(\frac{P_2}{P_1}\right)^{(\gamma-1)/\gamma}\right]}$$

where R = gas constant
P_2 & P_1 = the pressure in the chamber and in the atmosphere.

From this consideration, the lighter molecular weights are more desirable and the higher values of γ produce slightly lower specific impulse all other things being equal. Actually, the ionization and dissociation effects, recombination effects, viscous and heat loss effects, profile shape and real gas effects complicate the computation of I_{sp} and engine efficiencies tending towards reducing performance. Figure 2 shows the equilibrium specific impulse that is obtained for the real gases starting from an initial uniform temperature, a pressure of one atmosphere exhausted to 10^{-4} atmospheres, for several propellants. This does assume that recombination does take place in the nozzle with a resultant release of heat and further expansion because of it.

The molecular weights of the initial propellant can be misleading as it is the effective molecular weight in the state of dissociation found in the throat or nozzle which must be used in the calculations. In the table below the molecular weight, the approximate molecular weight if the molecule is completely dissociated and unionized, and the ideal specific impulse for

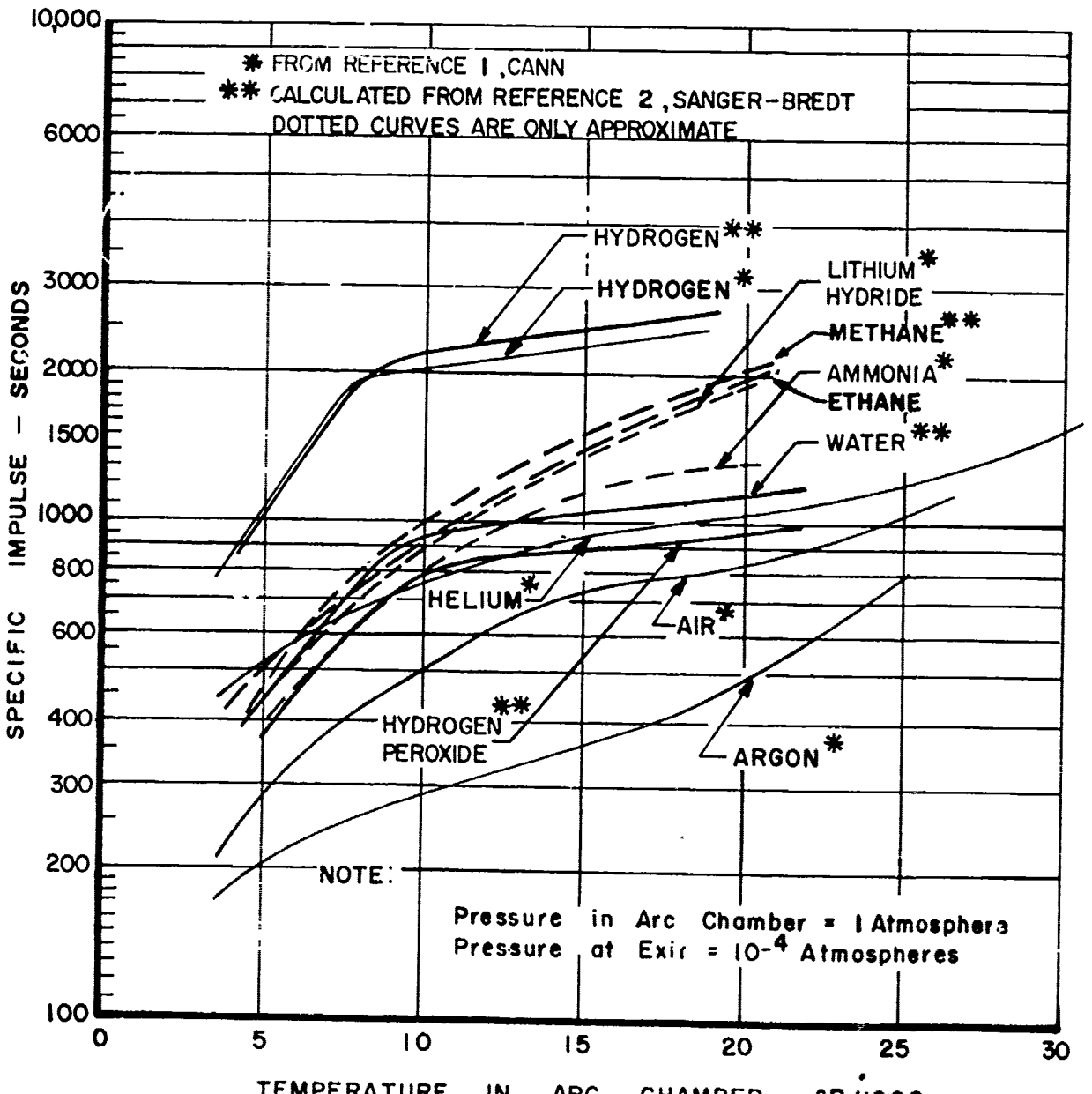

Figure 2 -- THEORETICAL EQUILIBRIUM SPECIFIC IMPULSE FOR POSSIBLE PROPELLANTS

the real gas under equilibrium conditions with an initial chamber temperature of 20,000°R are listed. At this temperature the gas is felt to be highly dissociated. The I_{sp} and the effective molecular weight do not always vary monotonously due to recombination and ionization factors.

TABLE 1

MOLECULAR WEIGHT EFFECTS

	Propellant Formula	Molecular Weight (approx)	~ Effective Dissociated Molecular Wt.	'Specific Impulse' (sec) Chamber Temp. 20,000°R
1	Hydrogen - H_2	2	1	2900
2	Methane - CH_4	16	3.2	2100
3	Ethane - C_2H_6	30	3.75	1950
4	Lithium Hydride - LiH	8	4	1900
5	Helium - He	4	4	1100
6	Ammonia - NH_3	17	4.25	1300
7	Water - H_2O	18	6	1150
8	Hydrogen Peroxide - HOOH	34	8.5	950
9	Air (.78 N_2, .21 O_2, .01 A)	29	14	830
10	Argon - A	40	40	500

DISSOCIATION

The energy required to separate atoms of polyatomic molecules is called the dissociation energy. Of the total energy supplied to the propellant by heating through the use of the arc, some then is absorbed in this manner in polyatomic fuels. This energy is lost to thrust unless it can be recovered by non-radiative recombinations in the nozzle. For the arc-jet applications now being considered, the temperatures and pressures are of a level that almost complete dissociation would be expected. Listed in the table below are the energies for atoms and molecules being considered as propellants:

TABLE II DISSOCIATION ENERGY (Ref. 3)

Bond	Propellant	Dissociation Energy Kcal/mole	Dissociation Energy Kcal/ gm
H-H	Hydrogen	103. 2	51. 6
Li-Li	Lithium	26	1. 9
Li-H	Lithium Hydride	58	7. 3
N-N	Nitrogen	225. 1	8. 1
O-O	Oxygen	117. 1	3. 6
O_2+N_2	Air	203	7
C-H	------	85. 56	----
C-H_4	Methane	348. 6	21. 8
C_2H_6	Ethane	522. 9	17. 4
N-H	------	83	----
NH_3	Ammonia	249	14. 6

This energy can be very significant, especially when operating arc engines at low specific impulse. To illustrate when dissociation losses would be significant, Figure 3 shows per cent dissociation versus temperature for several species. A pressure of one atmosphere is used in these

computations, the amount of dissociation decreases with increase in pressure (i.e., H_2 at 5000°K 1 atm, 95% at 100 atm, 30%).

The effect of dissociation energy losses on theoretical engine performance is shown by frozen flow efficiency calculation in a subsequent chapter.

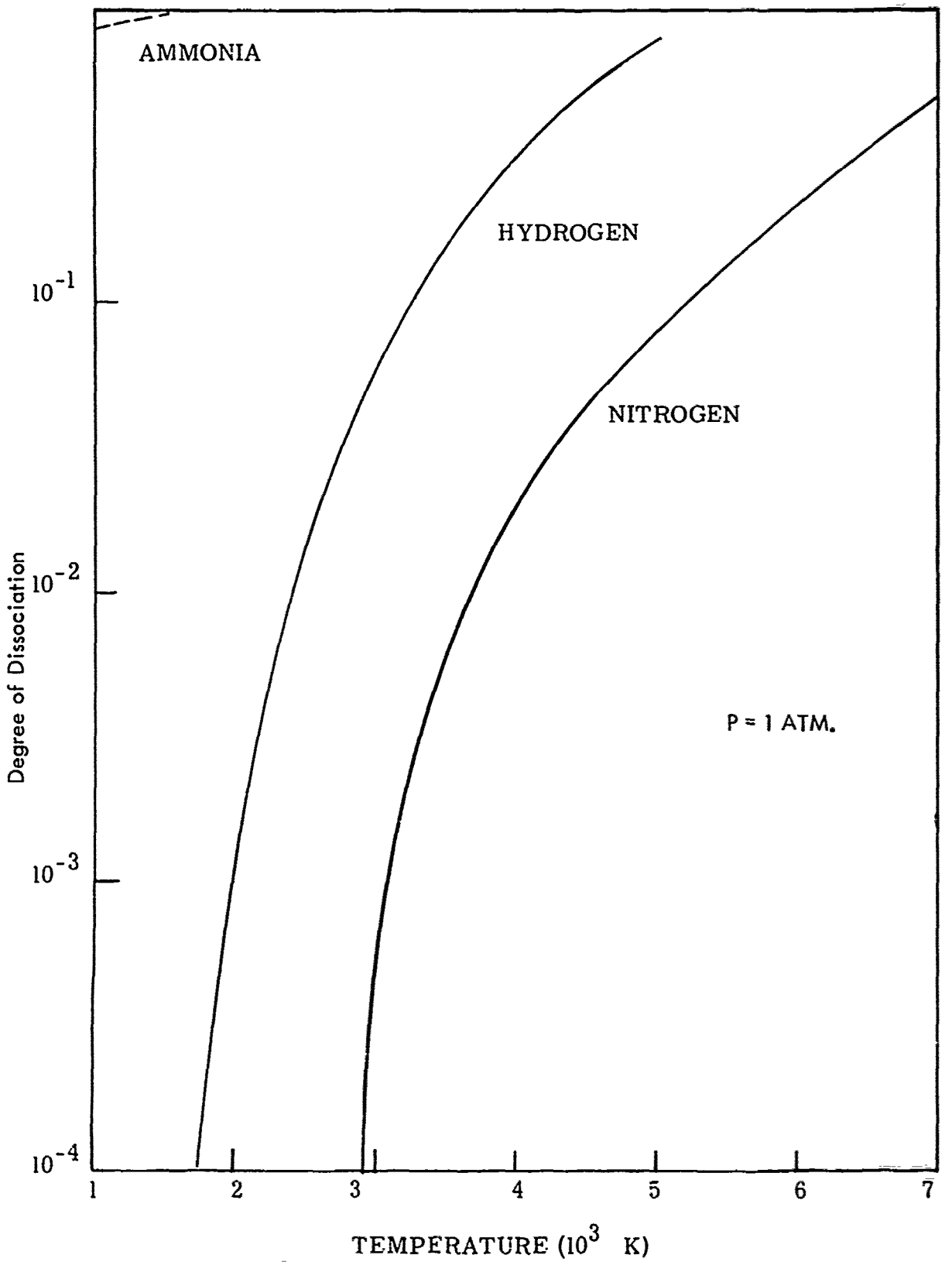

Figure 3

DEGREE OF DISSOCIATION VS. TEMPERATURE

IONIZATION ENERGY

The ionization potential represents the energy necessary to remove an electron from the atom. This energy usually designated I_1 is termed the first ionization potential. The second ionization potential, I_2, represents the energy required to remove an electron from a singly charged positive ion. Quantum mechanics has shown that periodicity is conditioned by the repetition of atomic configuration of outer electrons and properties which are concerned with the structure of the outer electrons should reveal periodicity. Thus, it is found that ionization potentials, ionic dimension, polarization, etc., when considered as a function of atomic number give a periodic like curve. Figure 4 shows such a curve and from it several generalizations can be drawn. The case when only one electron is present in outer shell will result in a low ionization potential as in the case of alkali metals such as lithium, sodium and cesium. Atoms with complete outer shells will have high I_1 values. These are the so-called inert gases, i.e., helium, neon and argon. The potential roughly increases with increasing atomic number in a single period, e.g., between atoms of lithium and neon. The ionization potential decreases with increasing atomic number for atoms of the same group, i.e., the potential of argon is lower than that of helium. The propellants considered for use with arc-jet engines are composed of atoms in the first two periods of the periodic table with the exception of argon. Of these, it can be noted that lithium is the easiest atom to ionize; helium the most difficult. The values of ionization potentials, with respect to hydrogen, of atoms with atomic numbers from 1-10 plus argon, are listed in the following table:

I_1 of Hydrogen = 13.595 electron volts = 312 K cal.

TABLE III IONIZATION POTENTIALS (Ref. 4)

Element	Atomic Number	I_1	I_2	I_3	I_4	I_5	I_6	I_7	I_8
H	1	1.00							
He	2	1.84	4.00						
Li	3	0.4	5.9	9.0					
Be	4	0.7	1.34	11.3	16.0				
B	5	0.61	1.85	2.8	19.3	25			
C	6	0.83	1.79	3.52	4.74	24	36		
N	7	1.07	2.18	3.49	5.43	7.19	40.5	49	
O	8	1.00	2.58	4.04	5.69	8.05	10.1	54	64
F	9	1.33	2.57	4.62	6.4	7.56	11.0	13	70
Ne	10	1.58	3.02	4.67					
A	18	1.16	2.05	3.01	12.6				

The amount of ionization as a function of temperature and pressure is discussed along with high temperature thermodynamic properties in a later section. The role of the ionization potential and efficiency losses caused by ionization of the fuel in the arc-jet engine is clearly shown in the next section on frozen flow efficiencies. The potential will also be examined later in connection with the electrical conductivity of the gas, a very important variable in the production of the arc itself.

PROPELLANTS CONSIDERED	
Atom	Potential eV
H	13.595
He	24.580
Li	5.390
C	11.264
N	14.54
O	13.614
A	15.755

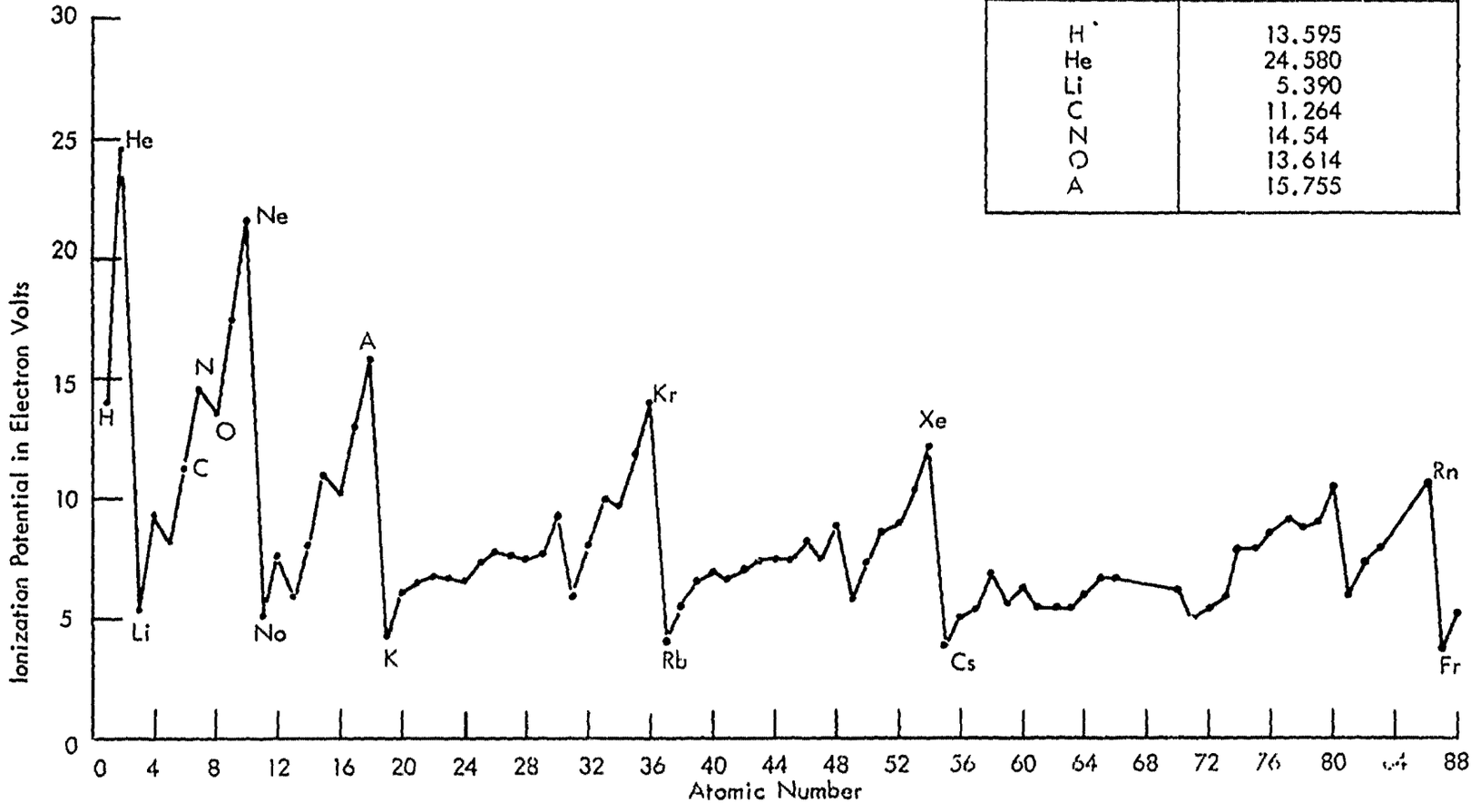

Figure 4 FIRST IONIZATION POTENTIAL

FROZEN FLOW CHARACTERISTICS

Frozen flow calculations are performed to determine the theoretical effect of dissociation and ionization losses on the operating characteristics of an arc-jet engine. This type of analysis is by no means supposed to express the overall operating efficiencies of the engine. The frozen flow efficiency calculations are a convenient means of showing the importance and maximum efficiency expected if the gas would remain in a frozen state after leaving the arc chamber. The method of computing frozen flow efficiencies is described below.

Frozen flow efficiencies considering dissociation and ionization losses frozen are shown for hydrogen, lithium hydride, argon, helium, air and lithium. In addition, calculations for some of the above are shown with excitation and vibrational energy also frozen. These analyses were performed at Plasmadyne. In addition, efficiency vs specific impulse curves are shown for ammonia and most of the elements with atomic numbers below 10.

Some general conclusions can be drawn from these types of analyses.

1. Frozen flow efficiency is increased with increasing pressure.
2. Frozen losses become less significant at very high specific impulses.
3. In the area where the arc-jet engine is being considered for use (I_{sp} 700-2000 sec) frozen losses are an important factor in determining engine performance.

Figures 5 to 16 show frozen flow results.

Computational Methods

As a gas is heated to a high temperature (in the order of several thousand degrees), molecular dissociation and ionization start to occur. This means that some of the energy imparted to the gas is expended to separate molecules from each other and electrons from the atoms. If recombination of these particles does not occur before they leave the nozzle section, this energy is not available for kinetic energy. In addition, it is also possible that the energy imparted to the molecule in the forms of vibrational and excitation energy might not be converted into kinetic energy. This implies that the kinetics of the plasma in the nozzle are such that insufficient time is available for equilibrium conditions to be reached. In these calculations, one assumes that the amount of dissociation and ionization which occurs in the arc chamber remains frozen. (Also, in some cases the vibrational and excitation states are assumed frozen.)

The frozen flow efficiency is defined as the ratio of the power delivered to the propellant minus the frozen losses divided by the power delivered to the propellant. For the case of ideal equilibrium flow, the corresponding efficiency would be 1.0.

$$\eta = \frac{\text{Power to propellant - frozen losses}}{\text{Power to propellant}}$$

In the calculations, it is assumed that there are no losses, the velocity in the arc chamber is zero, and the gas is exhausted to a zero pressure.

For the case where the degree of dissociation and ionization are assumed frozen in the nozzle, the efficiency is given by:

$$\eta = \frac{H - \Sigma \beta_j H_{D_j} - \Sigma \alpha_i H_i}{H} = \frac{\Delta H}{H}$$

where:

H = the molar stagnation enthalpy

β = the degree of molecular dissociation of the $j^{\underline{th}}$ species

H_{D_j} = dissociation enthalpy of the $j^{\underline{th}}$ molecule species

α_i = the degree of ionization of the $i^{\underline{th}}$ ion species

H_i = ionization enthalpy of the $i^{\underline{th}}$ species

The specific impulse is then given in the following form:

$$I_{sp} = \text{constant} \left[H - \Sigma \beta_j H_{D_j} - \Sigma \alpha_i H_i\right]^{1/2} = K \left[\Delta H\right]^{1/2}$$

In order to determine both the specific impulse and the frozen flow efficiency, the amount of dissociation and ionization as a function of the amount of enthalpy supplied to the propellant and the chamber pressure need be known.

This information can most conveniently be obtained from a Mollier diagram of the type prepared by Plasmadyne (see Fig. 20). These show non-dimensional enthalpy and entropy as coordinates with parameters of temperature, pressure, degree of dissociation and ionization. The method of preparation of such plasma properties will be discussed in detail in Sec. 8 of this report. The above equations for η and I_{sp} may be put in a non-dimensional form for ease of use with the diagrams.

$$\eta = \frac{\frac{H}{RT_o} - \Sigma \beta_j \frac{H_{D_j}}{RT_o} - \Sigma \frac{\alpha_i H_i}{RT_o}}{\frac{H}{RT_o}} = \frac{\frac{\Delta H}{RT_o}}{\frac{H}{RT_o}}$$

$$I_{sp} = \left[\frac{2 RT_o J}{g_o} \left(\frac{H}{RT_o} \right) \right]^{1/2}$$

where:

R = gas constant

T_o = absolute reference temperature

g_o = gravitational constant

J = conversion factor

For a particular enthalpy input temperature and pressure, both the α and β in the chamber can be found. This information plus the values of E_D and E_i (to be found in Sec. 4 and 5 of this report) is all that is required for determining η and I_{sp}. (See Figs. 5, 7, 9, 11, 13 and 16.)

Now, the case where the dissociation, ionization, vibrational and excitation energies are frozen will be discussed. (See Figs. 6, 8, 10 and 12.)

In this case, η and I_{sp} can be expressed as follows:

$$\eta = \frac{H - \beta H_D - \Sigma \alpha_i H_i - H_v - H_e}{H} = \frac{\Delta H'}{H} = \frac{\tilde{C}_p T}{H}$$

$$\eta = \left[\frac{\tilde{C}_p T}{RT_o} \right] \left[\frac{H}{\tilde{R} T_o} \right]$$

where:

H_v = vibrational enthalpy

H_e = excitational enthalpy

$\tilde{C}_p$ = effective heat capacity for the plasma mixture

$\tilde{R}$ = effective gas constant

T = absolute temperature

The specific impulse would be expressed as a function of $\Delta H'$.

For example, for a hydrogen plasma

$$\tilde{C}_p = C_{p_{electron}} + C_{p_H} + C_{p_{H_2}} = \frac{5}{2} R_H (1+\alpha)\beta + \frac{7}{2} R_{H_2} (1 - \beta)$$

$$R = (1 - \beta) R_{H_2} + \beta R_H (1 + \alpha)$$

Here again the values of α and β are taken from the Mollier diagram as a function of total enthalpy input to gas and chamber pressure.

As an outgrowth of the frozen flow calculations, the chamber temperatures versus specific impulse were also found. These were computed for both equilibrium and frozen flow conditions. Figure 17 shows chamber temperatures for both ammonia, lithium hydride and hydrogen as a function of specific impulse. At the same specific impulse, ammonia temperatures are considerably higher than those encountered using hydrogen. One also notes that the frozen flow temperatures are significantly hotter than those encountered assuming equilibrium flow conditions. Chamber temperatures are also shown for other propellants of low molecular weight in Figure 18.

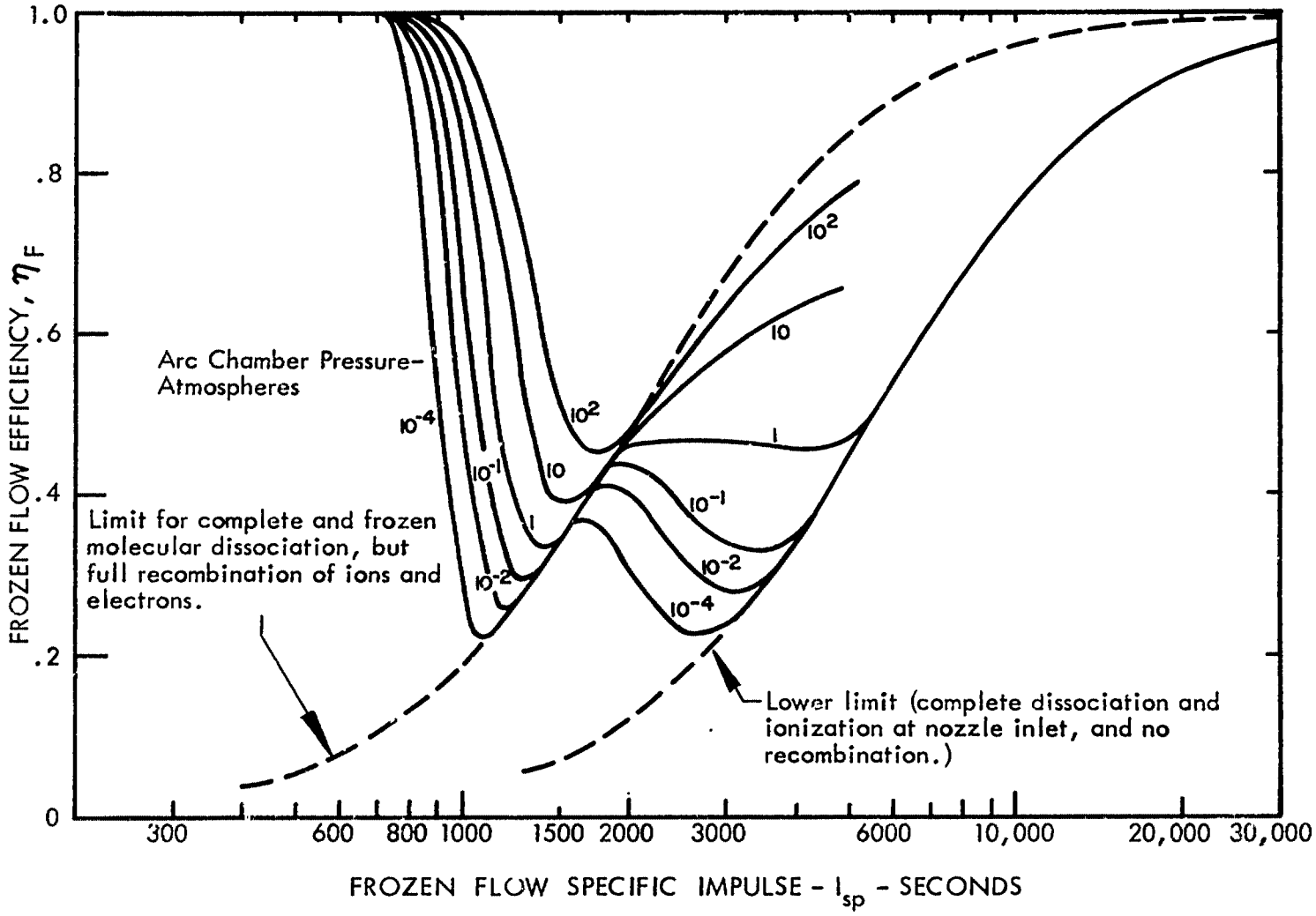

Figure 5 IDEAL FROZEN FLOW EFFICIENCY FOR A THERMAL ARC JET USING HYDROGEN WITH INFINITE PRESSURE RATIO (DISSOCIATION AND IONIZATION ENERGIES FROZEN, VIBRATION AND EXCITATION ENERGIES RECOVERED.)

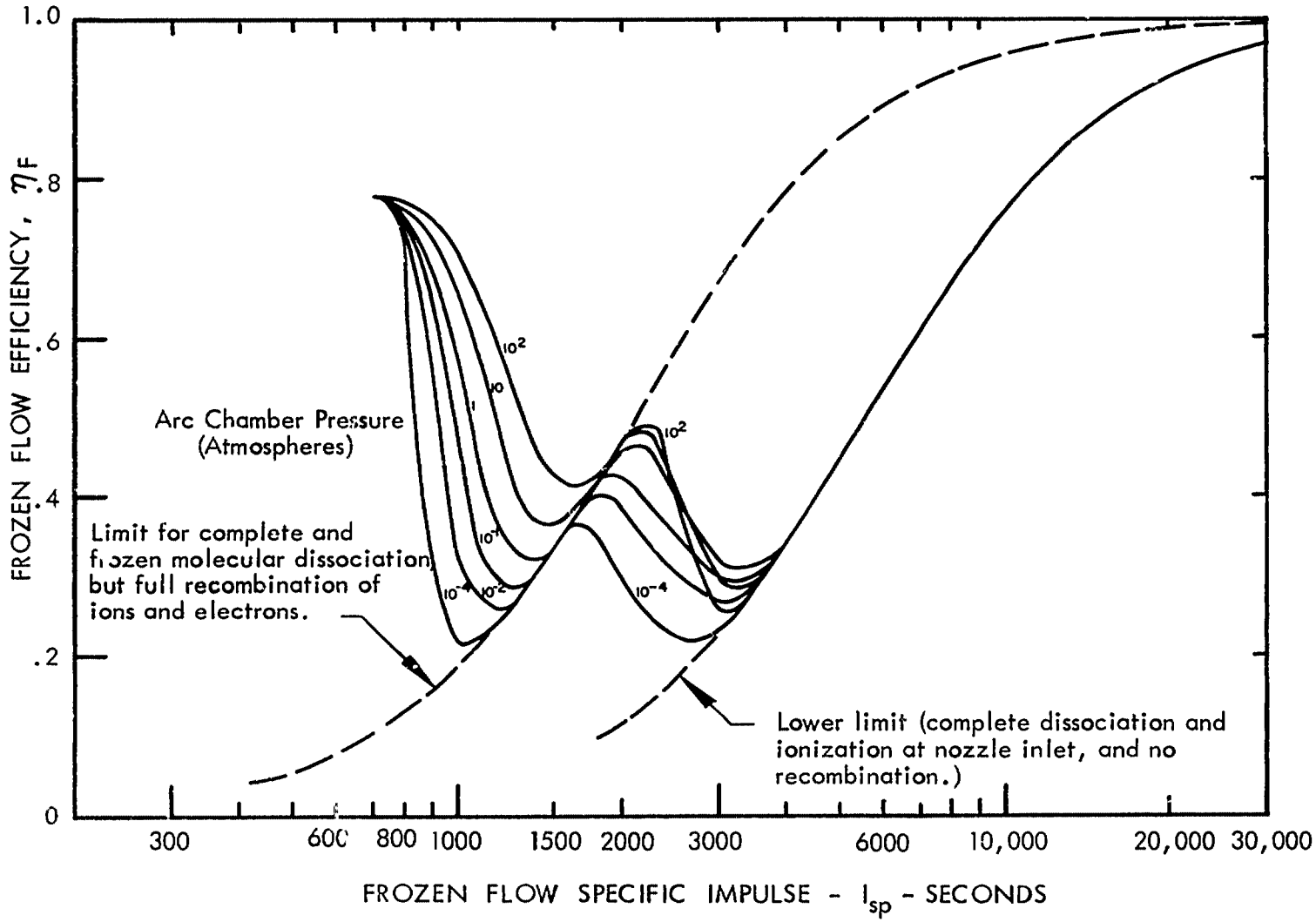

Figure 6 IDEAL FROZEN FLOW EFFICIENCY FOR A THERMAL ARC JET USING HYDROGEN WITH INFINITE PRESSURE RATIO (DISSOCIATION, IONIZATION, VIBRATION AND EXCITATION ENERGIES FROZEN.)

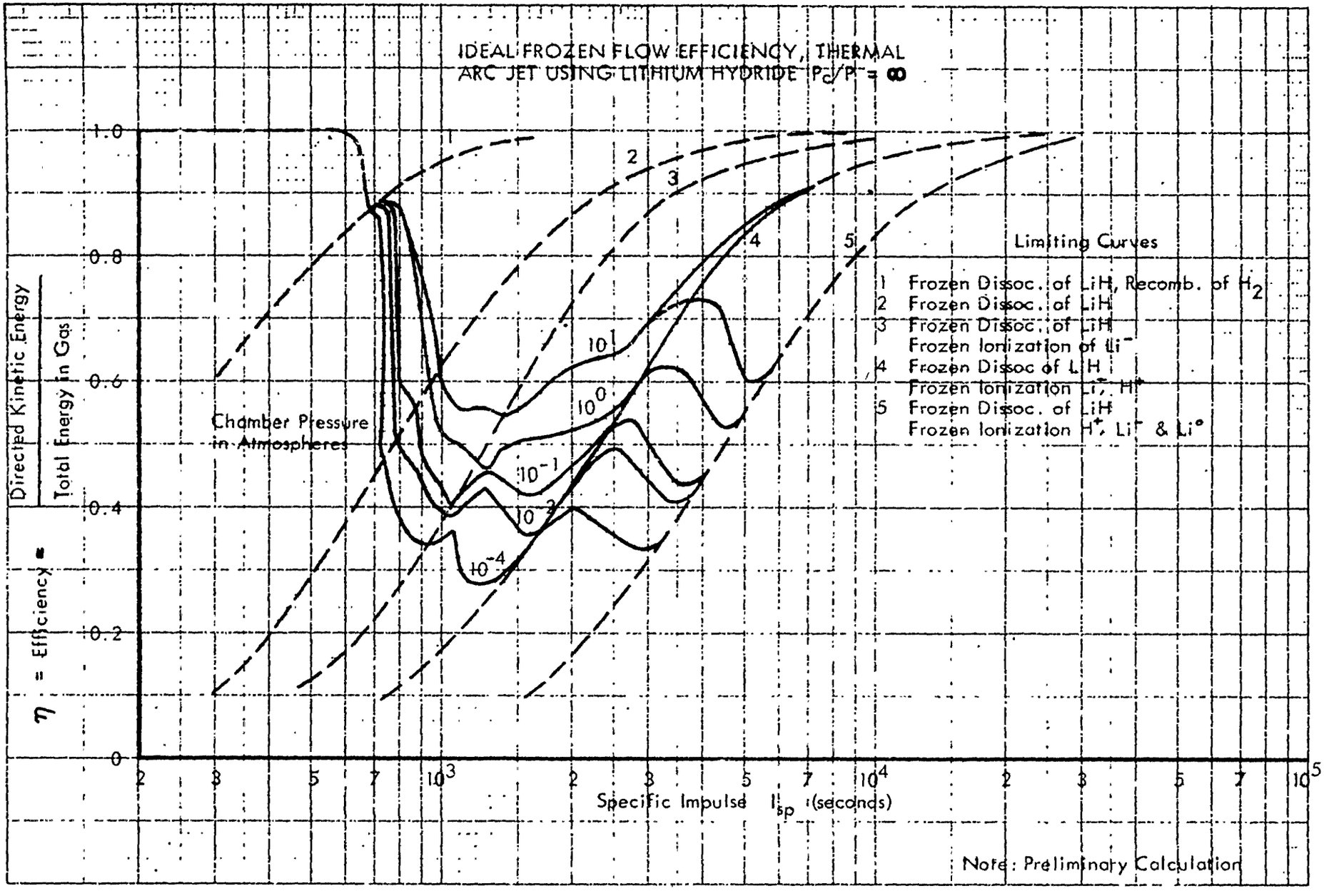
IDEAL FROZEN FLOW EFFICIENCY, THERMAL ARC JET USING LITHIUM HYDRIDE $P_d/P^- = \infty$
η = Efficiency = Directed Kinetic Energy / Total Energy in Gas
Chamber Pressure in Atmospheres
10^1
10^0
10^{-1}
10^{-2}
10^{-4}
Limiting Curves
1 Frozen Dissoc. of LiH, Recomb. of H_2
2 Frozen Dissoc. of LiH
3 Frozen Dissoc. of LiH
Frozen Ionization of Li^-
4 Frozen Dissoc of LiH
Frozen Ionization Li^-, H^+
5 Frozen Dissoc. of LiH
Frozen Ionization H^+, Li^- & Li°
Specific Impulse I_{sp} (seconds)
Note: Preliminary Calculation

Figure 7

IDEAL FROZEN FLOW EFFICIENCY FOR A THERMAL ARC JET
USING LITHIUM HYDRIDE WITH INFINITE PRESSURE RATIO
(Dissociation, Ionization, Vibration and Excitation Energy Frozen)

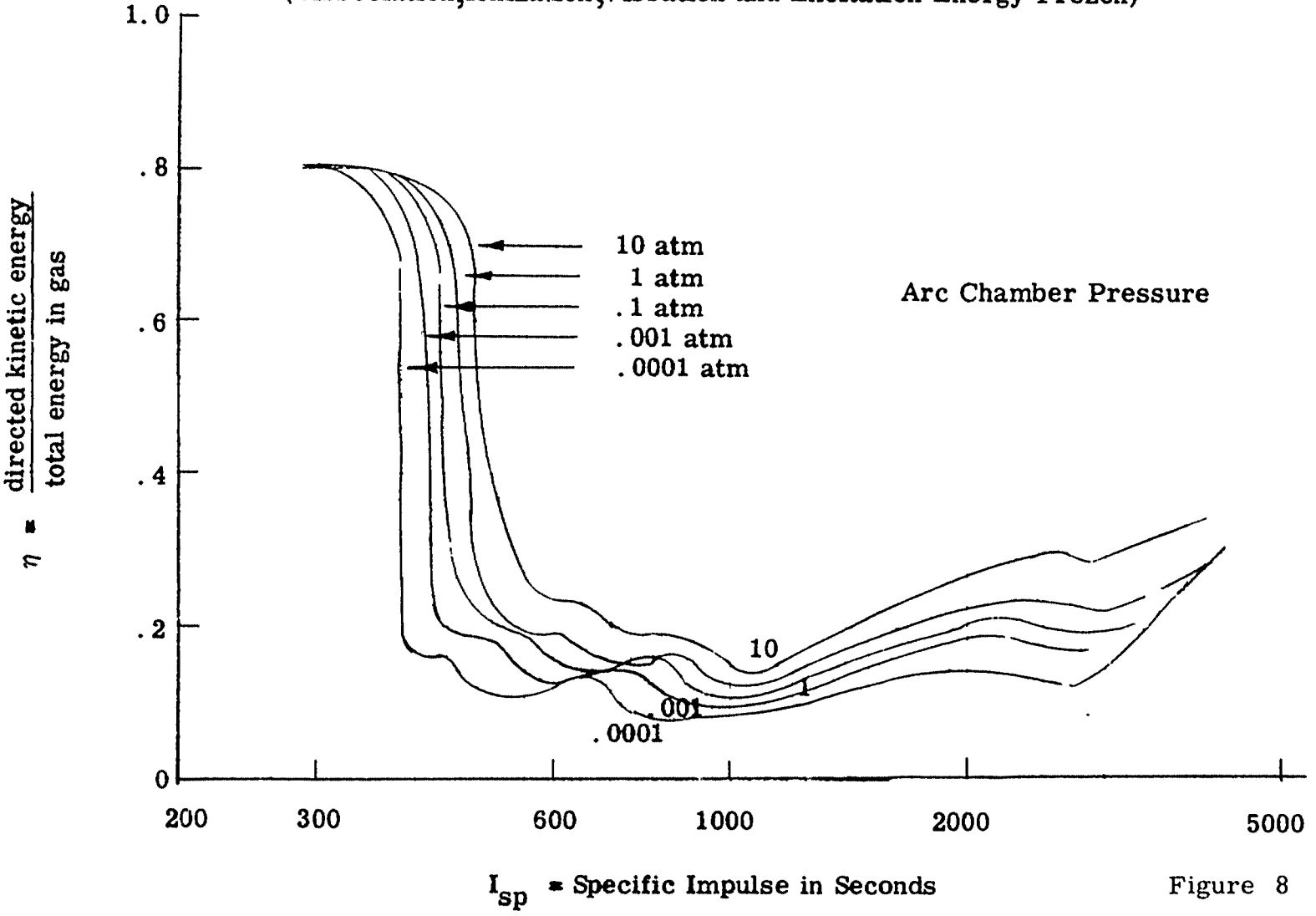

Figure 8

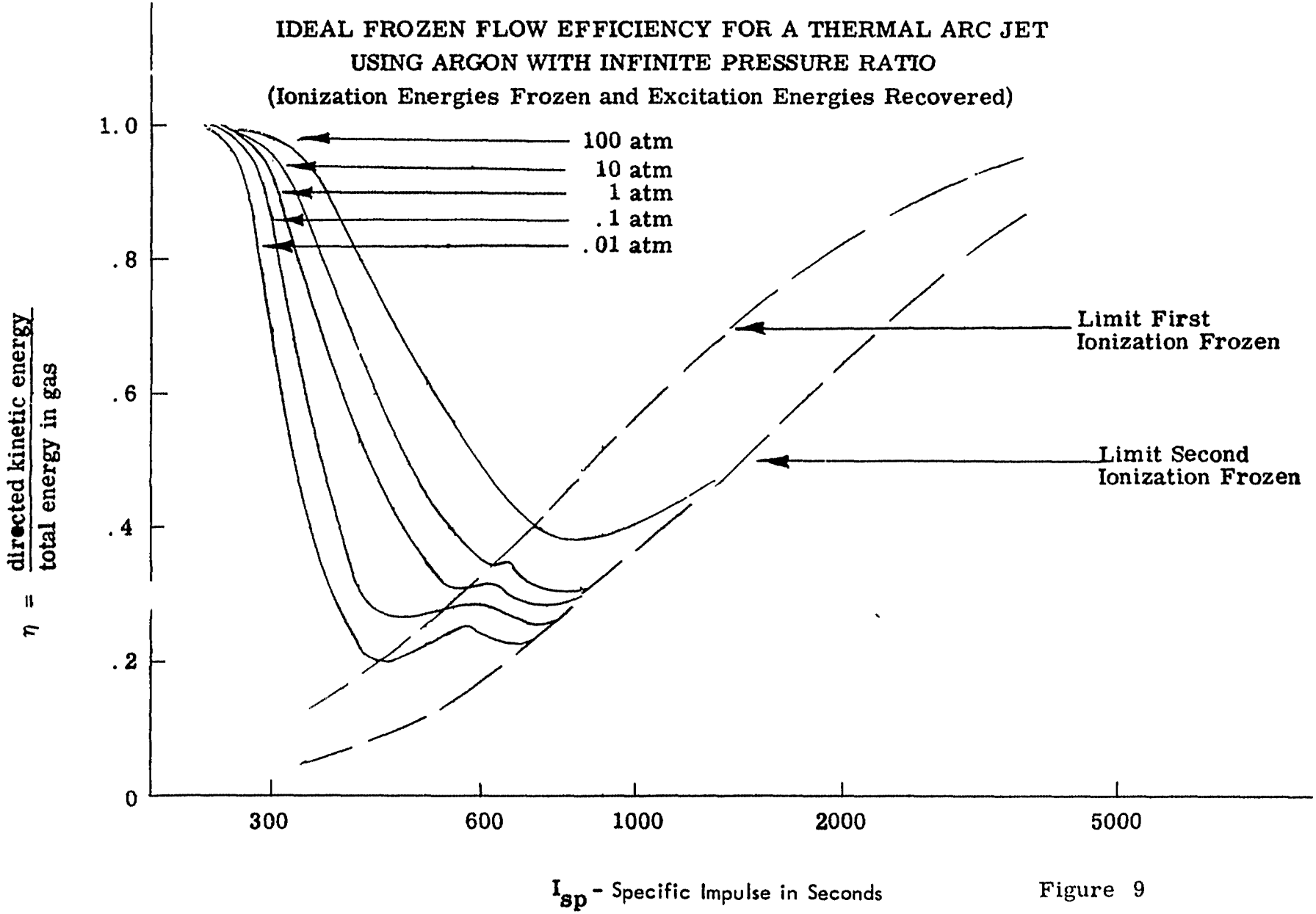
IDEAL FROZEN FLOW EFFICIENCY FOR A THERMAL ARC JET
USING ARGON WITH INFINITE PRESSURE RATIO
(Ionization Energies Frozen and Excitation Energies Recovered)
1.0
.8
.6
.4
.2
0
100 atm
10 atm
1 atm
.1 atm
.01 atm
Limit First Ionization Frozen
Limit Second Ionization Frozen
300
600
1000
2000
5000
η = directed kinetic energy / total energy in gas
I_{sp} - Specific Impulse in Seconds

Figure 9

IDEAL FROZEN FLOW EFFICIENCY FOR A THERMAL ARC JET
USING ARGON WITH INFINITE PRESSURE RATIO
(Excitation and Ionization Energies Frozen)

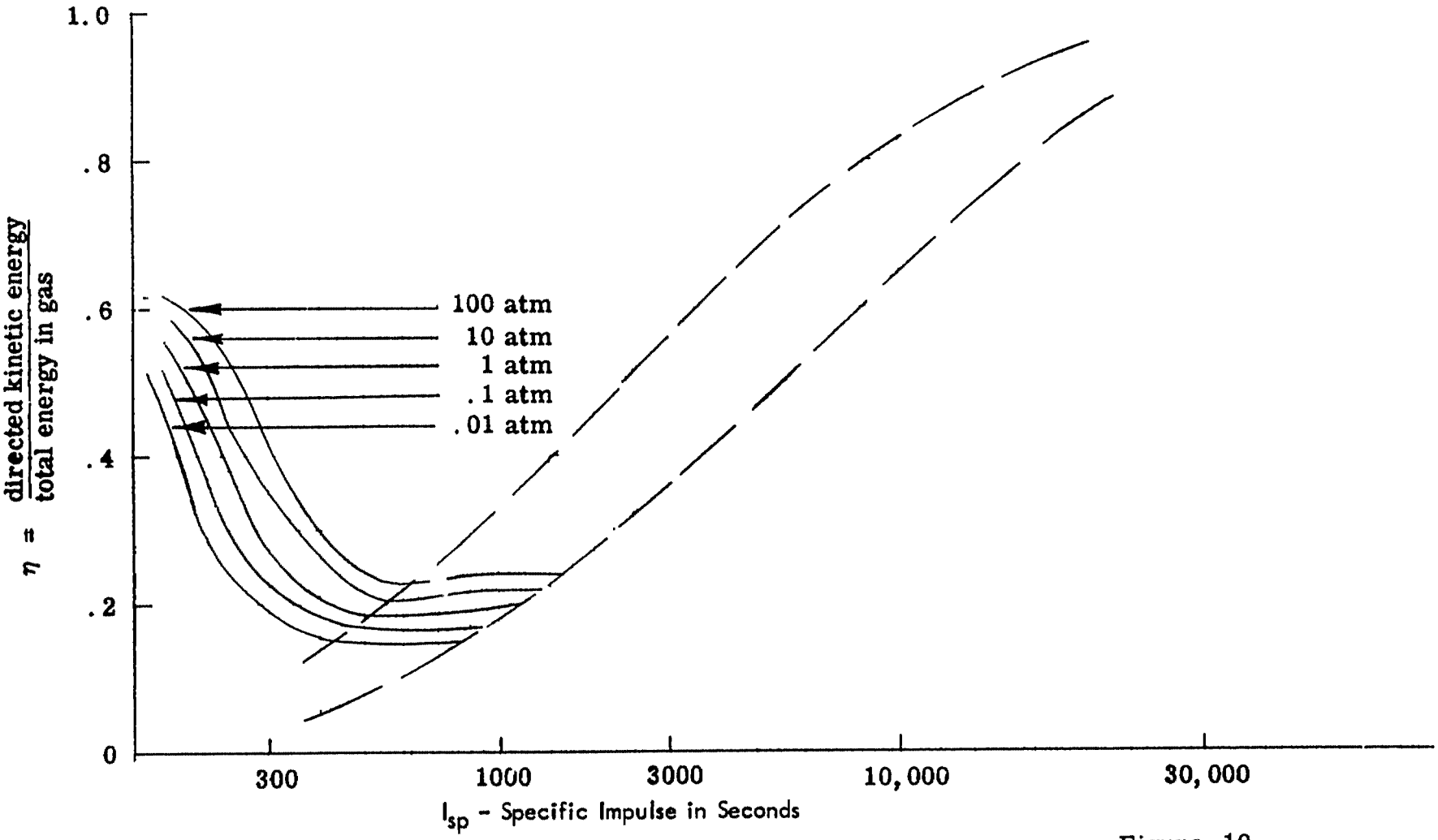

Figure 10

IDEAL FROZEN FLOW EFFICIENCY FOR A THERMAL ARC JET
USING LITHIUM WITH INFINITE PRESSURE RATIO
(Ionization Energies Frozen, Excitation Energies Recovered)

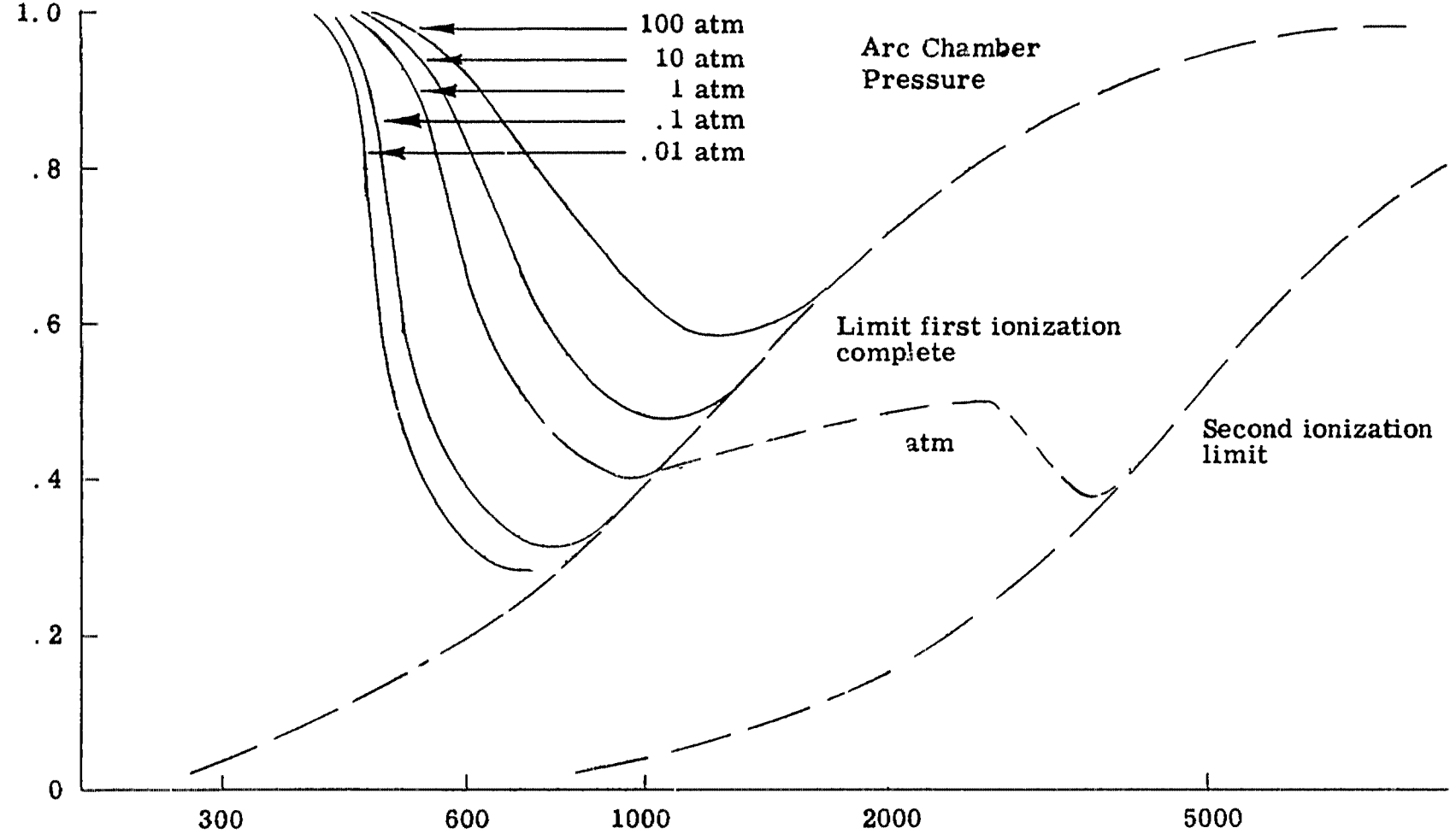

Figure 11

IDEAL FROZEN FLOW EFFICIENCY FOR A THERMAL ARC JET
USING LITHIUM WITH INFINITE PRESSURE RATIO
(Excitation and Ionization Energies Frozen)

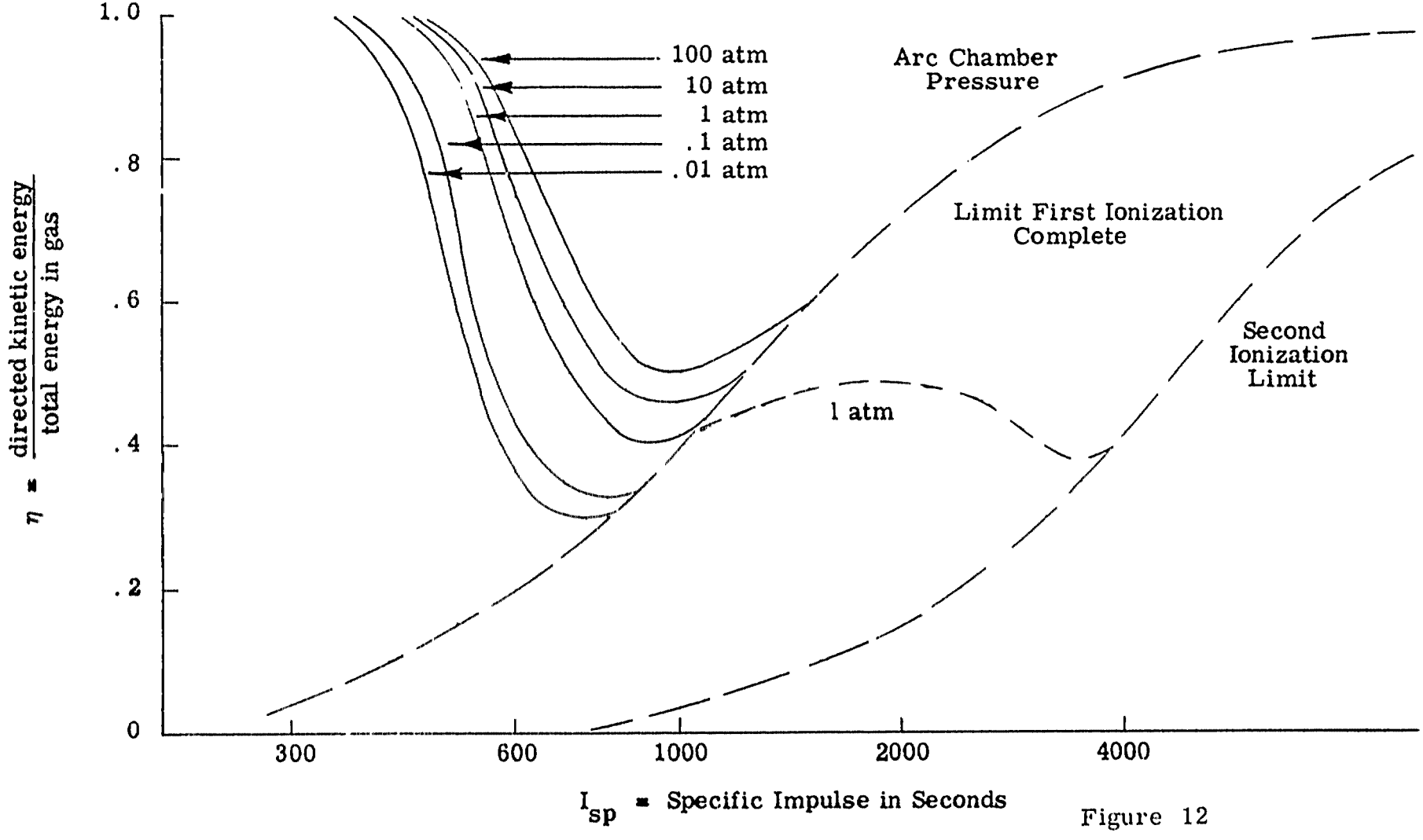

Figure 12

IDEAL FROZEN FLOW EFFICIENCY FOR A THERMAL ARC JET
USING AIR WITH INFINITE PRESSURE RATIO

(Dissociation and Ionization Energy Frozen)

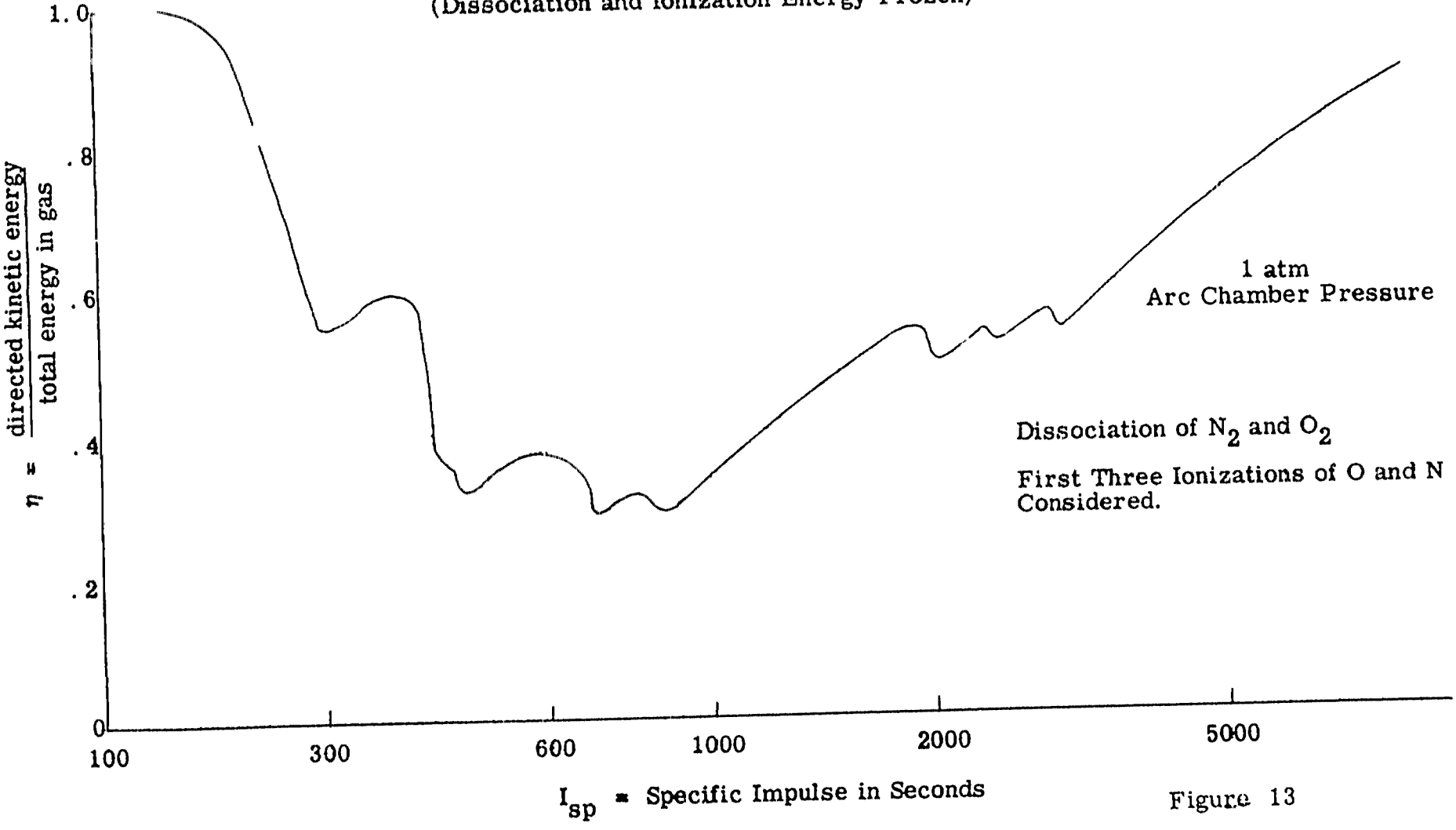

Figure 13

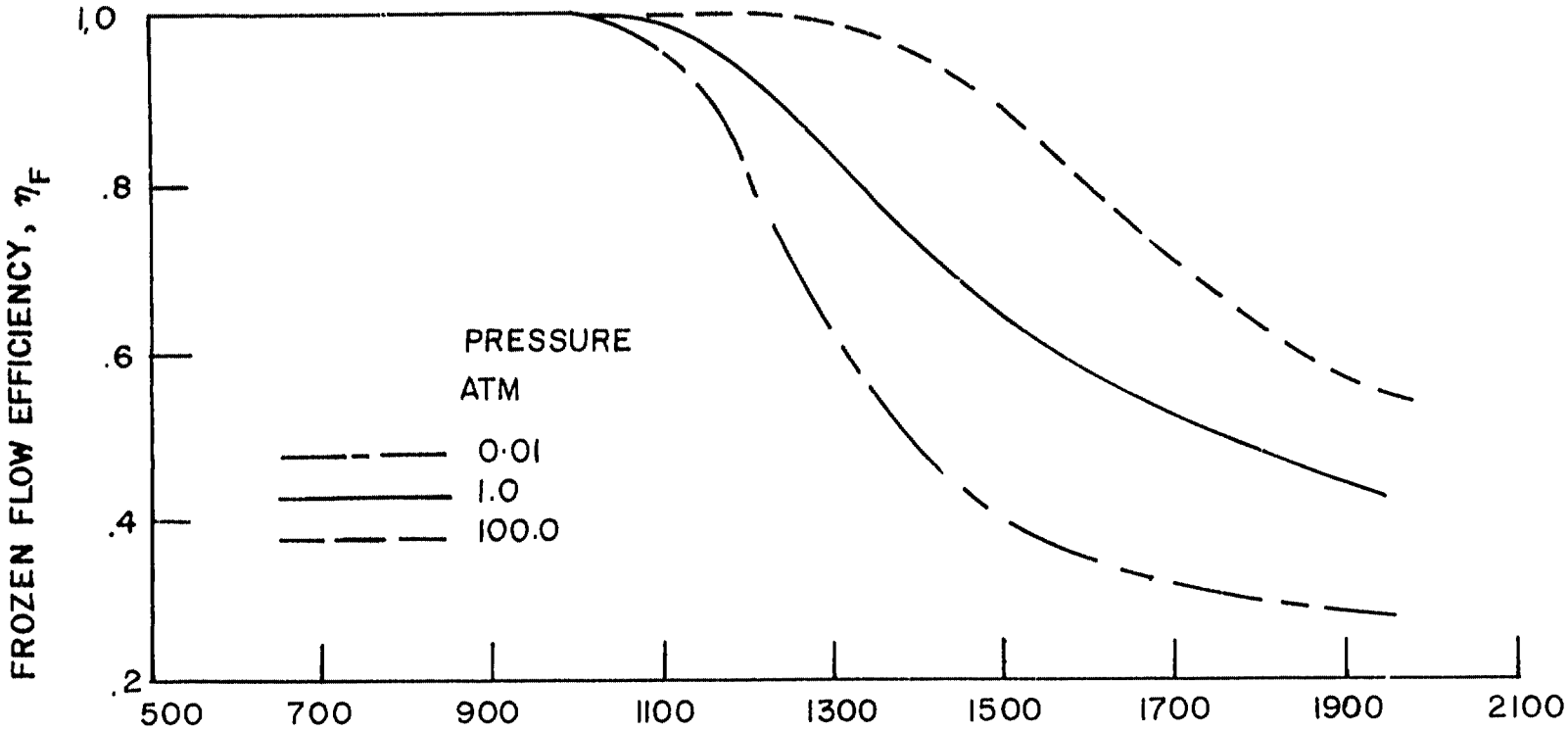

Figure 14 EFFECT OF PRESSURE ON FROZEN FLOW EFFICIENCY

(from Ref. 6)

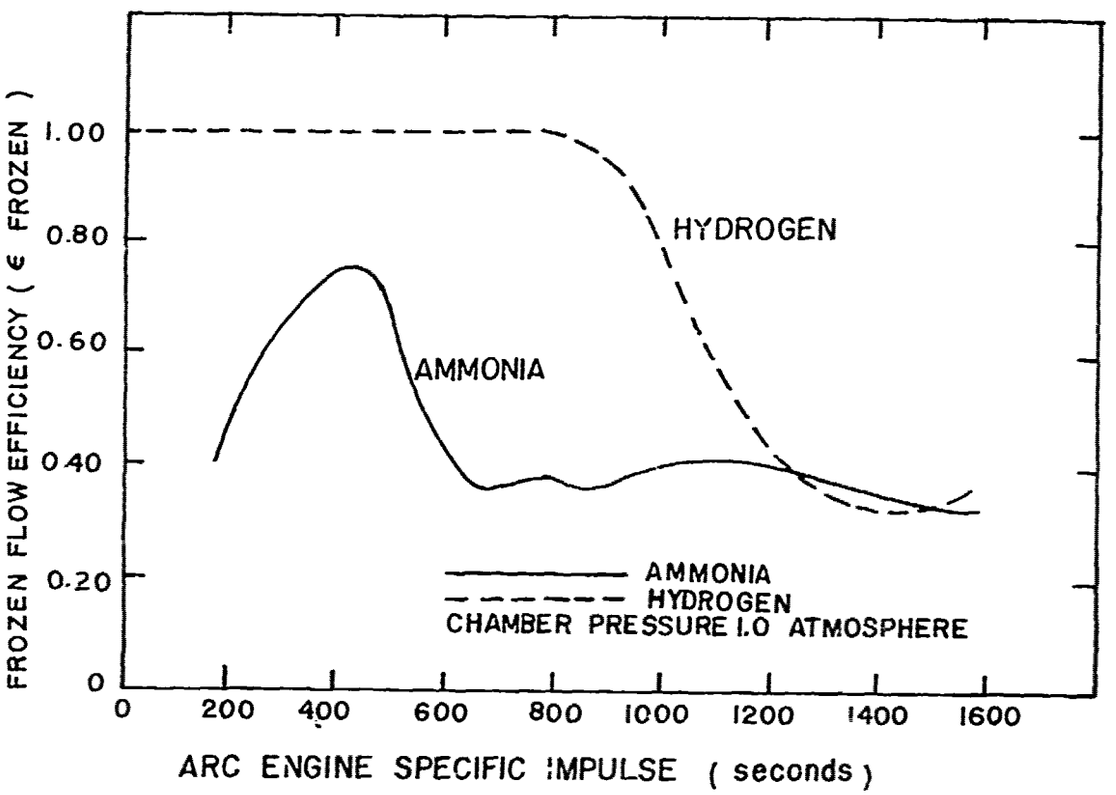

FROZEN FLOW EFFICIENCY VERSUS SPECIFIC IMPULSE--
AMMONIA AND HYDROGEN

Figure 15

(from Ref. 5)

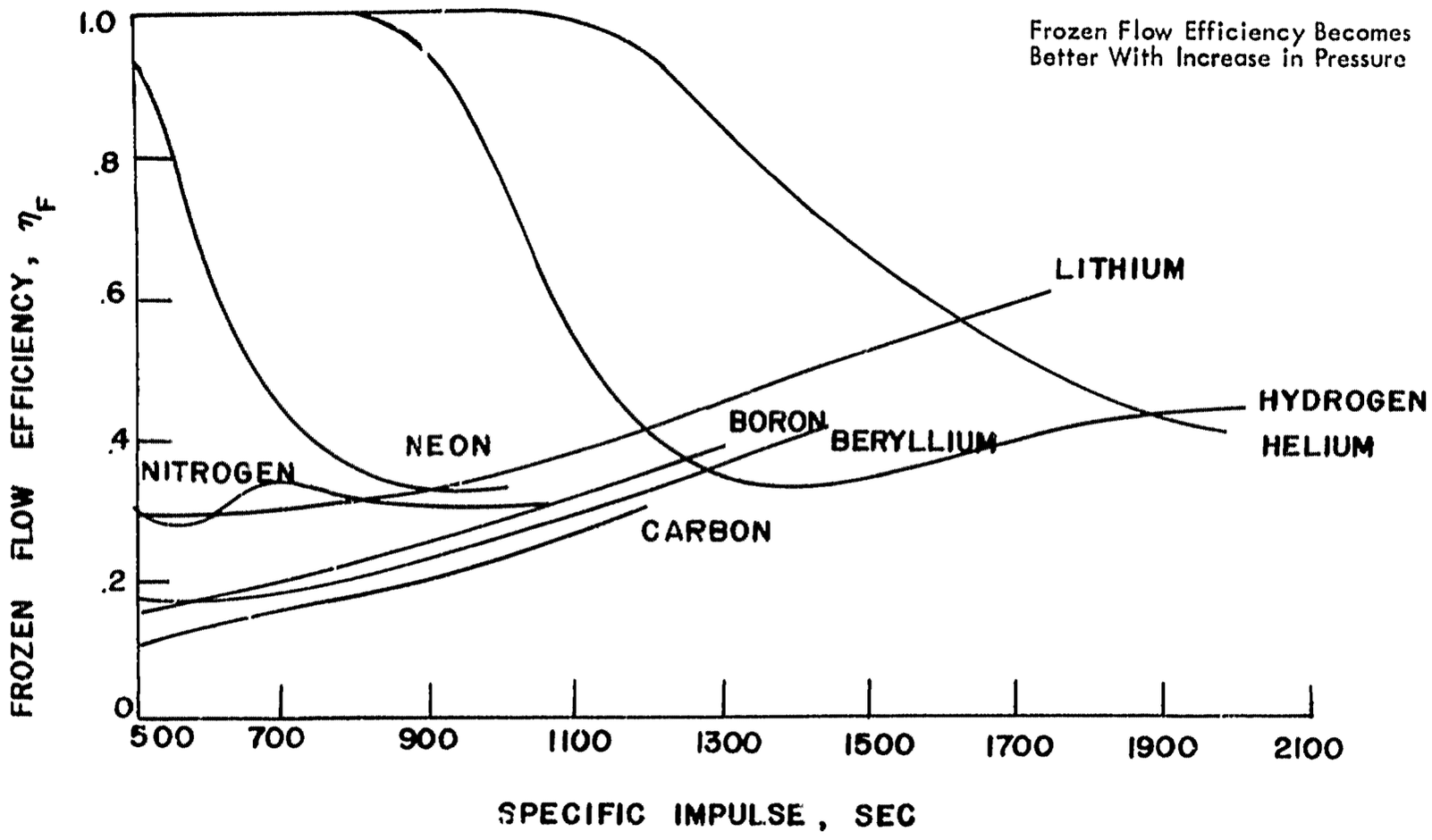

Figure 16 FROZEN FLOW EFFICIENCIES FOR VARIOUS PROPELLANTS, PRESSURE, 1 ATMOSPHERE

(from Ref. 6)

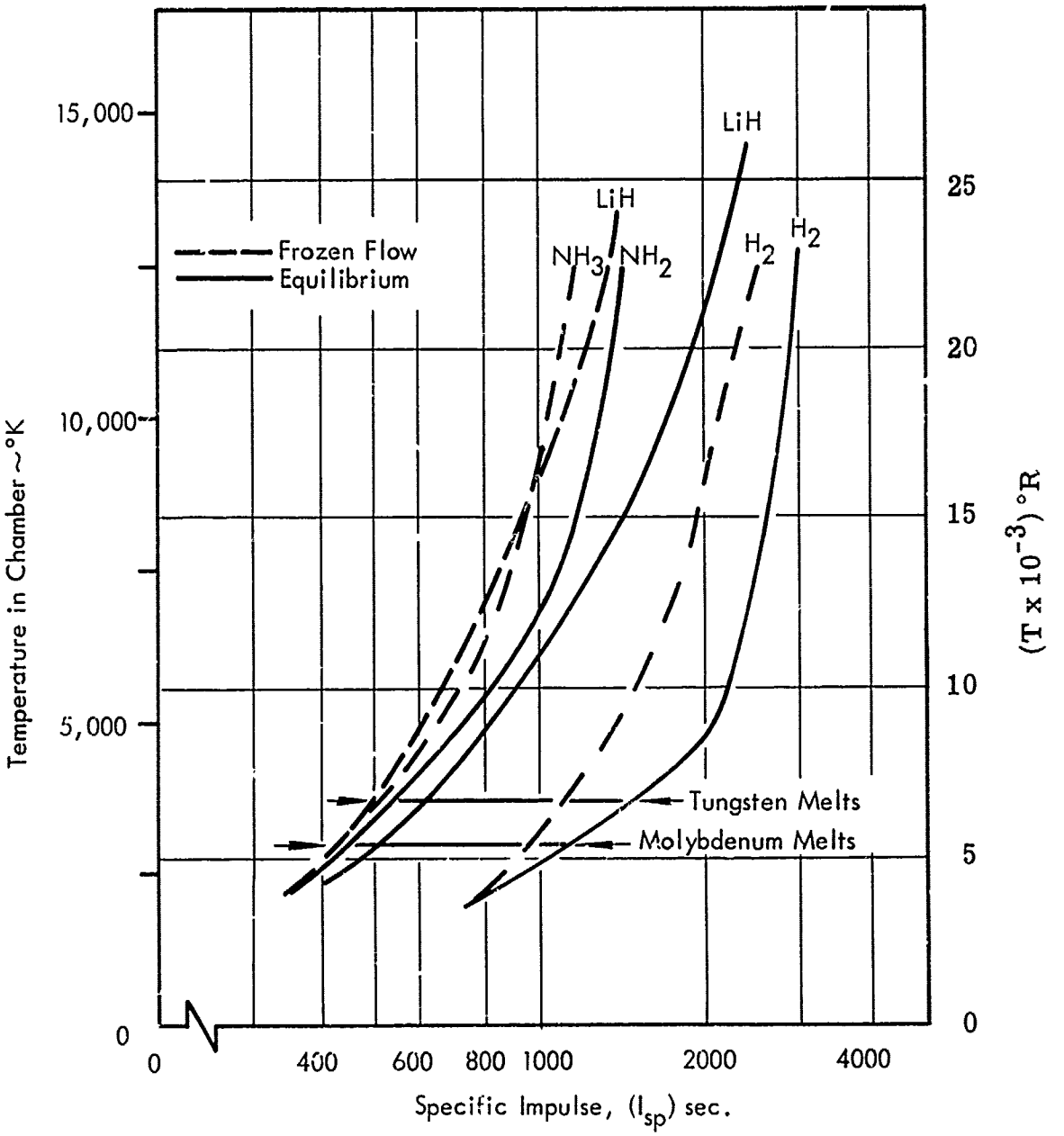

Figure 17 THEORETICAL CHAMBER TEMPERATURE VS. SPECIFIC IMPULSE

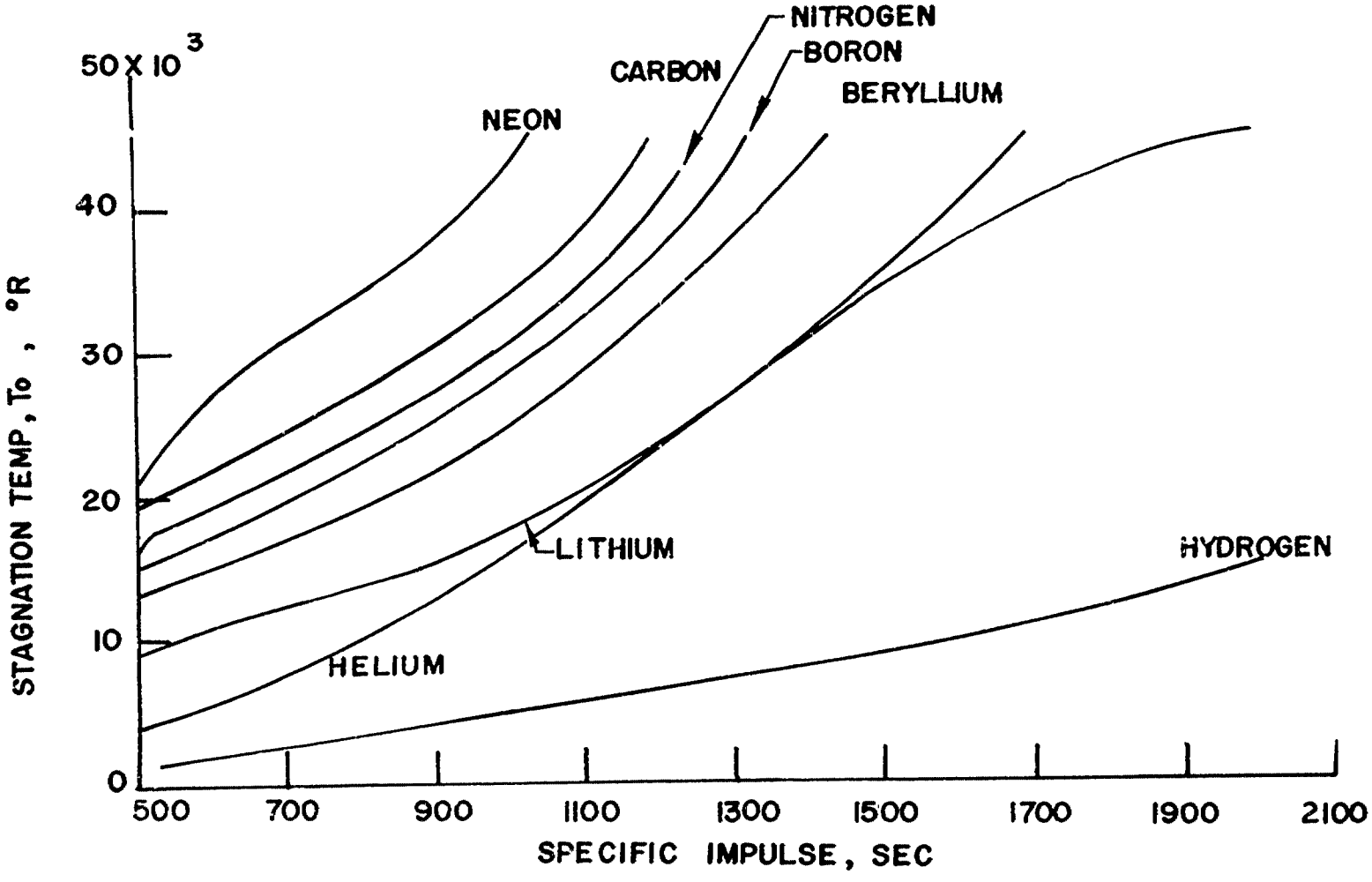

STAGNATION TEMPERATURES FOR VARIOUS PROPELLANTS. PRESSURE, 1 ATM.

Figure 18

(from Ref. 6)

PROFILE EFFECTS

The ideal frozen flow efficiency is normally calculated for the case with uniform conditions across the jet. In an actual thruster, there is a radial enthalpy profile across the jet which can have an important effect on performance. The central portion of the plasma is considerably hotter than that near the wall. This is true independent of the propellant used. The magnitude of the profile effect depends on the shape of the radial distribution, the per cent ionization and dissociation as a function of enthalpy and the level of operation of the engine. Plasmadyne has written a computer program for determining this profile effect. The effect of the radial distribution is an important parameter in determining the theoretical performance of a thruster. Figure 19 shows the result of this effect for a single family of profiles. The calculation shown is for hydrogen, starting with a chamber pressure of about three atmospheres. For hydrogen and for the range of profiles shown, one can realize as much as a forty per cent variation in efficiency due to profile shape. The effect of profile shape and one's ability to control it can play an important part in propellant selection.

Computations should be made using a profile determined experimentally. The effect might raise or lower the predicted efficiency depending on the propellant used and shape established.

The procedure used in computing the effect of profile shape on frozen flow is as follows:

The enthalpy profile is represented by a series

$$H = H_o (1 + C_1 \dot{m} + C_2 \dot{m}^2 + C_3 \dot{m}^3 + \ldots C_{10} \dot{m}^{10})$$

where:

H_o = enthalpy at the center line

C = arbitrary constants chosen to give desired profile shape

$\dot{m}$ = non-dimensional mass flow varying from zero at the center line to one at the wall $\dot{m} = f(r)$ r being the radius. $\dot{m}$ is the ratio of the mass flow occurring in the area r = o to r divided by the total mass flow

The energy profile is introduced in the arc chamber. The fluid is next isentropically expanded under equilibrium conditions to an intermediate pressure at which the gas composition freezes. The gas is assumed to remain frozen in this state during the remaining expansion.

For the calculations --

(1) Adiabatic conditions were assumed.
(2) The Plasmadyne Mollier charts were used to determine equilibrium conditions (degree of dissociation and ionization).
(3) Enthalpy entering chamber is zero.
(4) Frozen particles are assumed to obey the perfect gas assumption with the dissociation and ionization fractions held constant, but vibrational energy recovered. Average effective values for the specific heats (including vibrational energy) were estimated for the temperature range involved in the expansion using Figure 15-1 of Sears' "Thermodynamics" Addison-Wesley Publishing Company.
(5) The gas constant is evaluated using information from the Mollier chart for the gas composition by particle species.

The thrust is given by

$$F = \int v \, d\dot{m} + \int p \, \frac{dA}{d\dot{m}} \, d\dot{m} = \int_0^{\dot{m}} \left(v + \frac{p}{\rho v} \right) d\dot{m}$$

where:

v = velocity
p = pressure
ρ = density

$\left(v + \frac{p}{\rho v} \right)$ is a function of the total enthalpy for a given pressure ratio. This function has been expressed as a power series to fit a series of points determined as described below.

The velocity at the exit is obtained directly from the total enthalpy change. If the density and velocity at the exit are known, the area is computed from the continuity equation. The pressure-area contribution to the thrust is similarly evaluated. The thrust is obtained by integrating over the exit area.

The power in $P_{in} = \int_0^{\dot{m}} H \, d\dot{m}$

The efficiency is given by

$$\eta = \frac{\dot{m} \; V^2_{eff}}{2 \; P_{in}} = \frac{I_{sp}^2 \; g_o^2 \; \dot{m}}{2 \; P_{in}}$$

where:

I_{sp} = specific impulse = $F/_{\text{weight flow}}$

V_{eff} = effective velocity

The exit area is given by

$$A = \int_0^{\dot{m}} \frac{d\,\dot{m}}{\rho\, v}$$

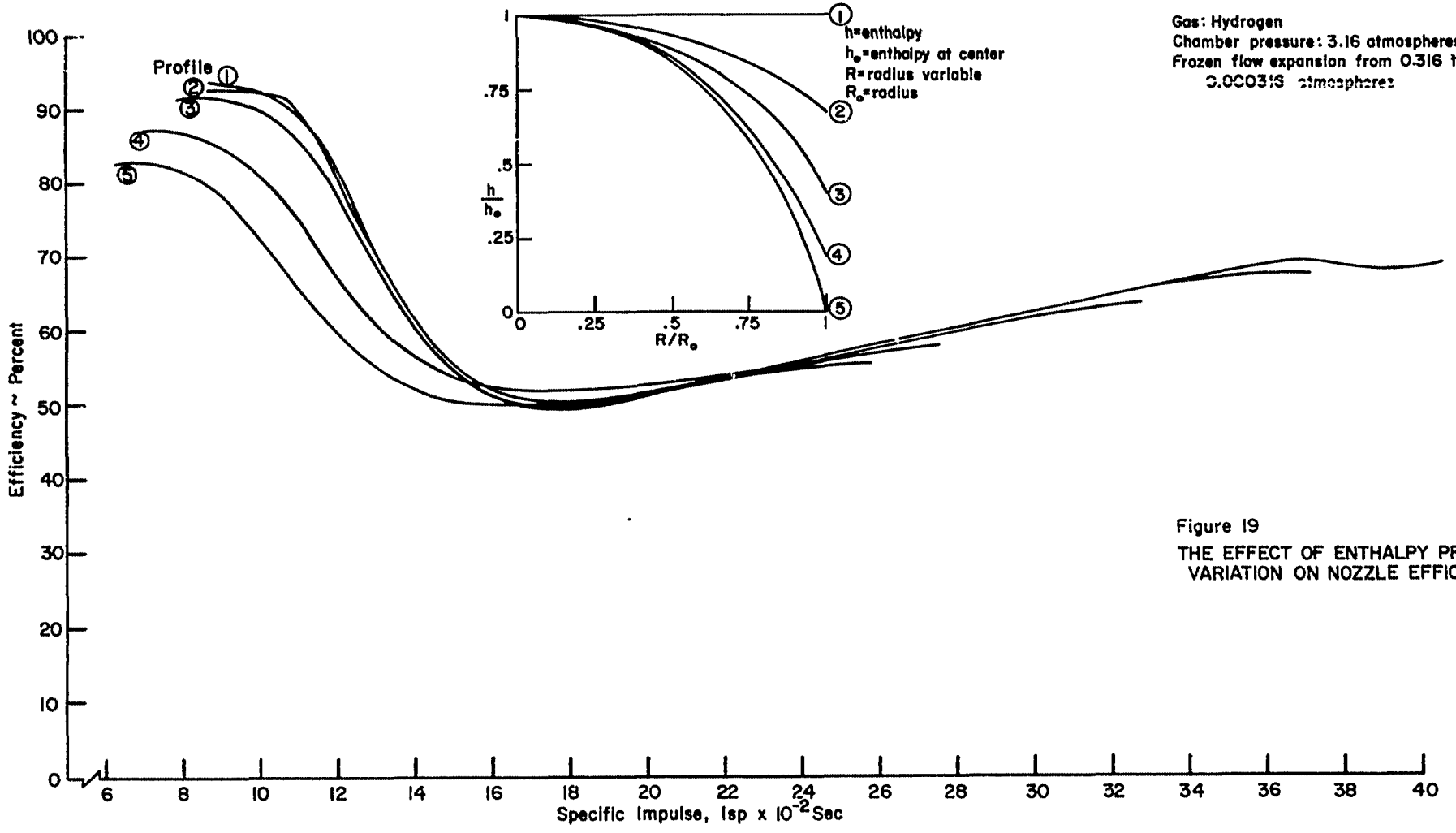

Figure 19
THE EFFECT OF ENTHALPY PROFILE VARIATION ON NOZZLE EFFICIENCY

HIGH TEMPERATURE THERMODYNAMIC PROPERTIES

Before theoretical studies can be carried out on arc-jet performance, it is first essential that information be available concerning the equilibrium thermodynamic properties of propellants at high temperatures. The studies include the evaluation of ideal efficiency versus specific impulse, computation of transport properties of plasma and recombination studies. Computation of the equilibrium properties were carried out in 1959 and 1960 at Plasmadyne for five potential propellants. The argon, lithium, helium and hydrogen work was performed under Air Force Contract AF 49(638)-54 and lithium hydride analysis under AF 49(638)-766. The results of this work are presented in the form of mollier charts of non-dimensional enthalpy versus entropy. Constant temperature, pressure, per cent dissociation and/or ionization are the parameters plotted on the curves. To illustrate the type and extent of this work, see Figures 20 and 21.

A series of reports is now being prepared by Ling-Temco-Vought on high temperature properties. The enthalpy, pressure, temperature and density relationships are depicted in these reports. In addition, values of various molar concentrations, speeds of sound and specific heats are presented as functions of temperature and density. This work presently includes studies of methods of computing partition functions and analysis for air and argon. Future work includes calculating properties of nitrogen, oxygen, helium and hydrogen plasmas. (Ref. 7 to 9)

Heller and McGee of Marshall Space Flight Center (NASA) have set up several extensive programs to compute thermodynamic properties. The first deals with hydrogen, helium and lithium plasmas, the second is a general computational scheme for plasma property evaluation (Refs. 10 and 11).

The Rand Corporation has done several studies on high temperature properties. This includes Gilmore's work on air and Krieger's work on ammonia, water, lithium hydride, methane and methanol (Refs. 12 and 13). These were done as part of a parametric investigation of low-molecular-weight high-hydrogen content compounds for use as propellants for nuclear powered rockets.

Many more computations of these properties have been performed, especially noticeable are the German contributions to this area. These include computations for air, hydrogen, hydrogen peroxide, water, helium and ammonia (Ref. 14).

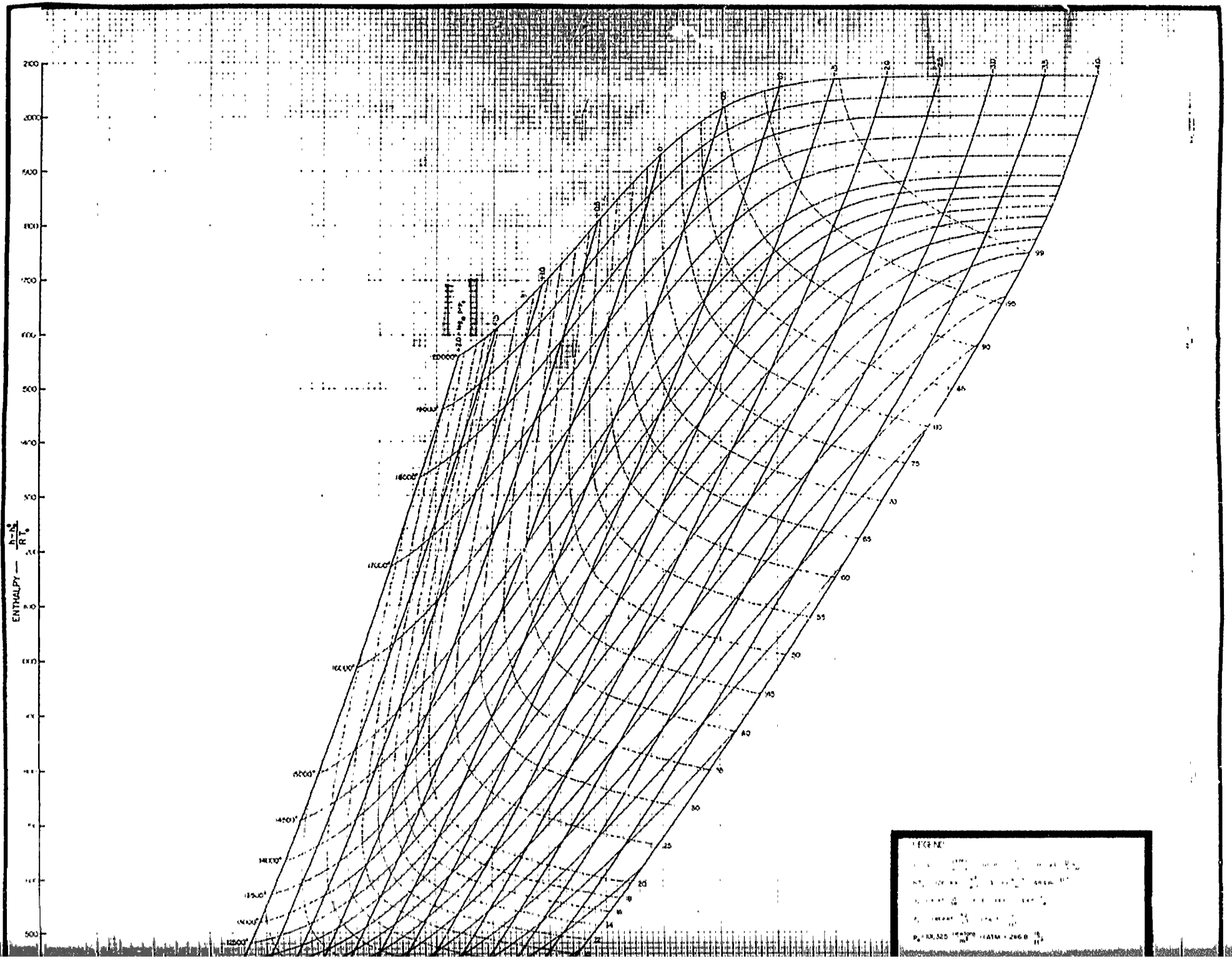
ENTHALPY — $\frac{h-h_0^\circ}{RT_0}$
LEGEND

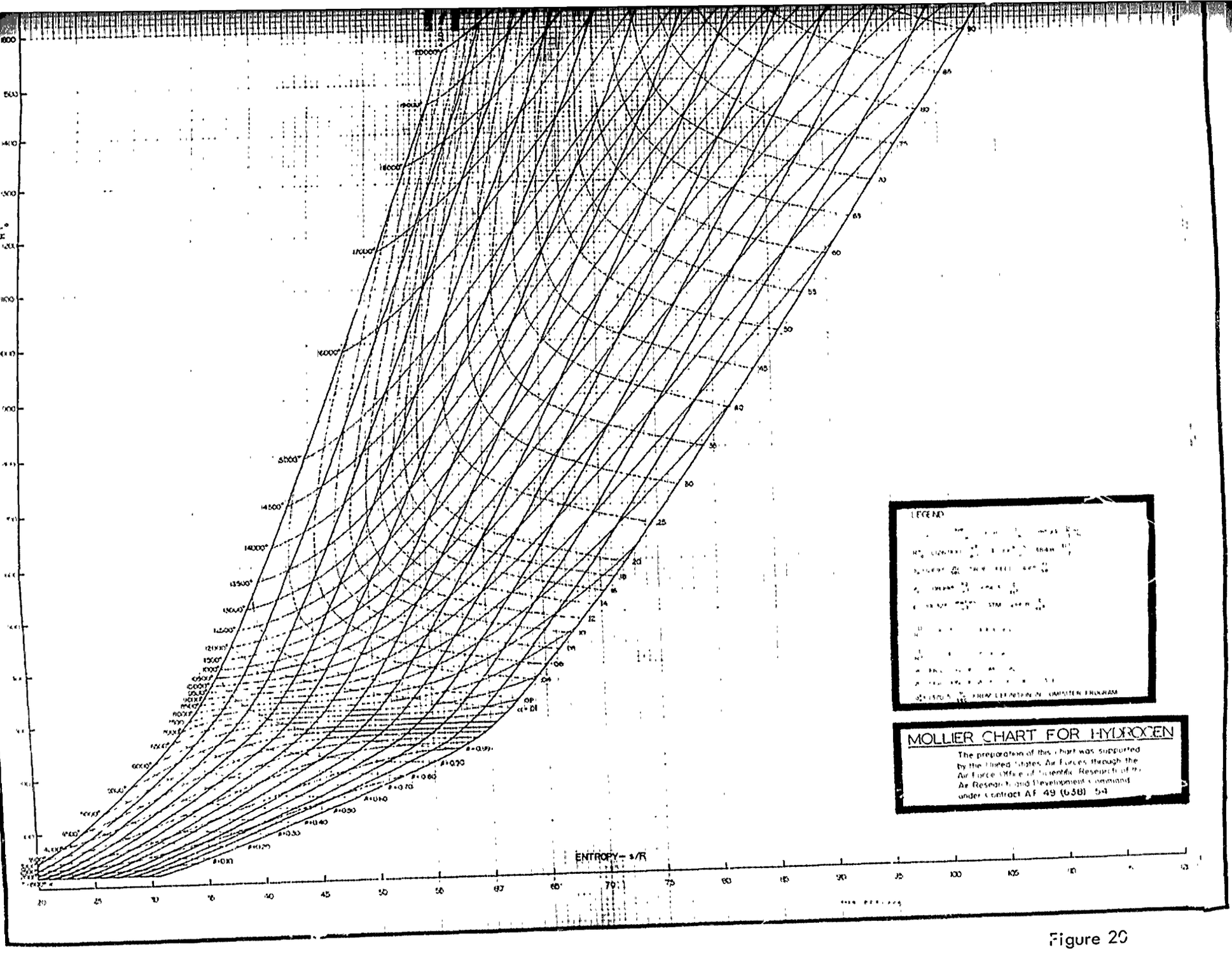
ENTHALPY — $\frac{h-h^\circ}{RT^\circ}$
ENTROPY — s/R
LEGEND
MOLLIER CHART FOR HYDROGEN
The preparation of this chart was supported by the United States Air Forces through the Air Force Office of Scientific Research of the Air Research and Development Command under Contract AF 49 (638) 54

Figure 20

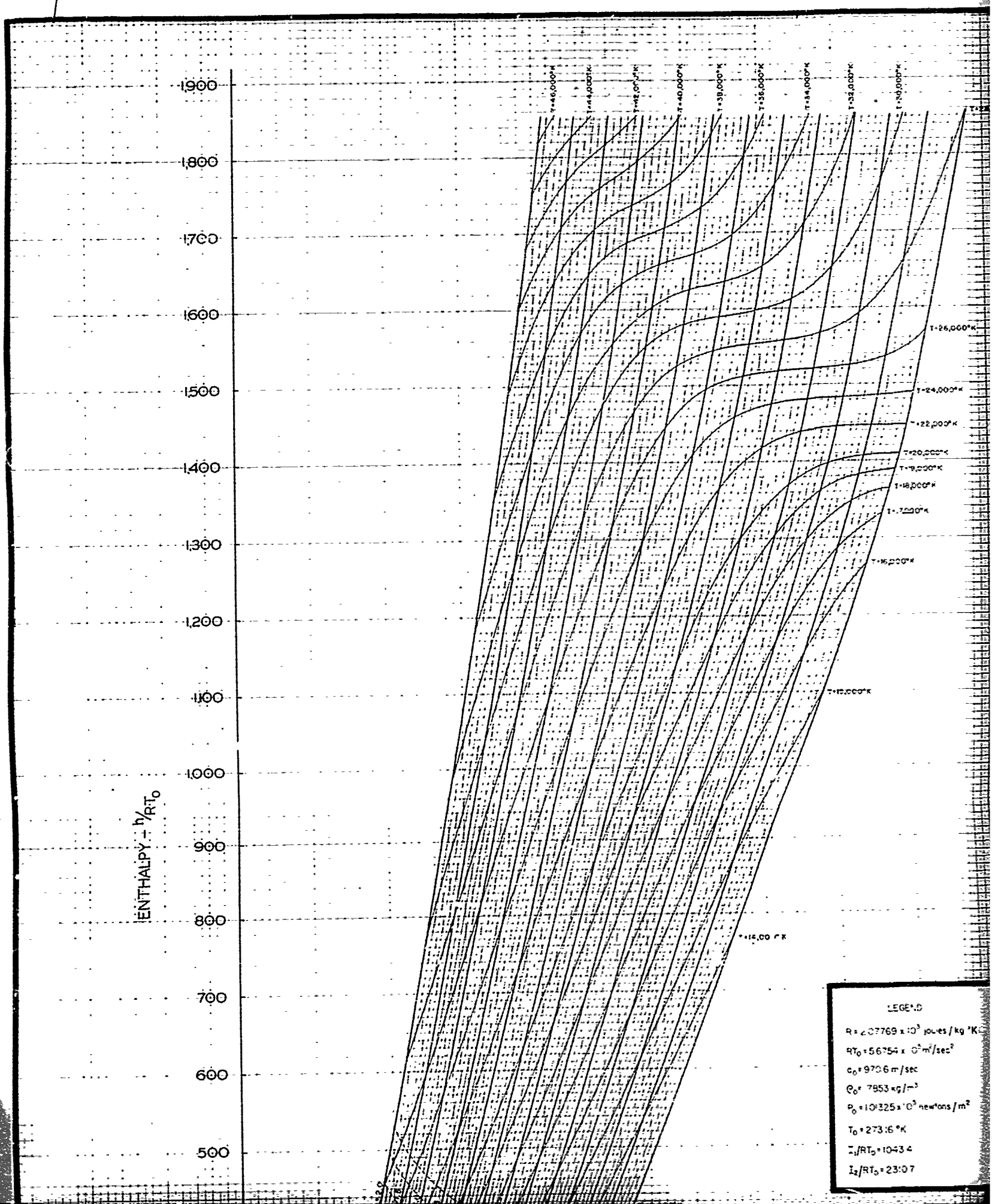
ENTHALPY = h/RT_0
1,900
1,800
1,700
1,600
1,500
1,400
1,300
1,200
1,100
1,000
900
800
700
600
500
T=46,000°K
T=44,000°K
T=42,000°K
T=40,000°K
T=38,000°K
T=36,000°K
T=34,000°K
T=32,000°K
T=30,000°K
T=26,000°K
T=24,000°K
T=22,000°K
T=20,000°K
T=19,000°K
T=18,000°K
T=17,000°K
T=16,000°K
T=15,000°K
T=14,000°K
LEGEND
R = 2.07769 x 10³ joules/kg °K
RT_0 = 5.6754 x 10⁶ m²/sec²
c_0 = 970.6 m/sec
ρ_0 = 7853 kg/m³
P_0 = 10.1325 x 10⁵ newtons/m²
T_0 = 273.16 °K
I_1/RT_0 = 10.434
I_2/RT_0 = 23.07

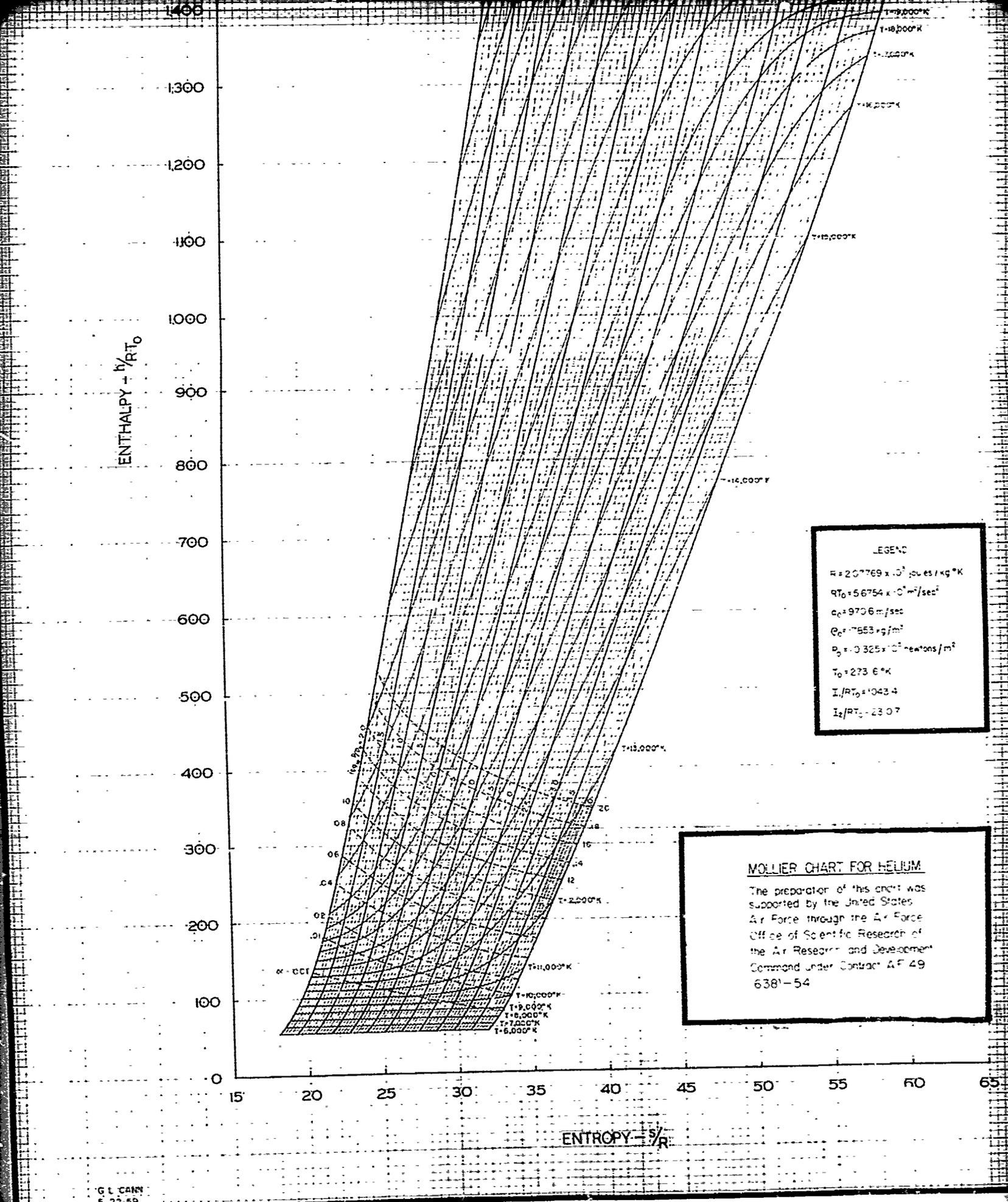
ENTHALPY = h/RT_0
ENTROPY = S/R
1400
1300
1200
1100
1000
900
800
700
600
500
400
300
200
100
0
15
20
25
30
35
40
45
50
55
60
65
T=19,000°K
T=18,000°K
T=17,000°K
T=16,000°K
T=15,000°K
T=14,000°K
T=13,000°K
T=12,000°K
T=11,000°K
T=10,000°K
T=9,000°K
T=8,000°K
T=7,000°K
T=6,000°K
T=2,000°K
LEGEND
R = 2.07769 x 10³ joules/kg °K
RT₀ = 5.6754 x 10⁶ m²/sec²
c₀ = 9706 m/sec
ρ₀ = .7853 kg/m³
P₀ = 1.0.325 x 10⁵ newtons/m²
T₀ = 273.6 °K
I₁/RT₀ = 1043.4
I₂/RT₀ = 23.07
MOLLIER CHART FOR HELIUM
The preparation of this chart was supported by the United States Air Force through the Air Force Office of Scientific Research of the Air Research and Development Command under Contract AF 49 638-54
G. L. CANN
5-22-59

Fig

THERMAL CONDUCTIVITY AND HEAT CAPACITY

The thermal conductivity and heat capacity are important arc jet performance variables. They are important in determining the operating temperature of the engine and the heat transfer rates from the arc to the propellant and chamber and nozzle walls. The heat capacity should be high for arc-jet operation. That is, a high capacity would allow a greater amount of energy to be added to a gas for a smaller increase in temperature. As a general rule the lower the molecular weight of a species, the higher its heat capacity. The heat introduced into the propellant should be recoverable. The heat absorbed in dissociating polyatomic molecules is essentially non-recoverable. An effective capacity must be considered in the case of dissociation. It is composed of the sum of the translational, rotational, vibrational and excitation contributions plus the heat absorbed during dissociation. Figure 2 illustrates the fact that low operating temperature can be correlated with low molecular weights, and that this is because of their associated high capacity. The effect of molecular dissociation on the heat capacity is illustrated in Figure 22. High thermal conductivity is also associated with low molecular weight. Thermal conductivities of several monatomic and diatomic species are shown in Figures 24 and 25.

The difference in operation of the arc with monatomic and molecular propellants will be discussed. The basic differences regarding the variation of specific heat and thermal conductivity with temperature results in quite different temperature distributions across the arc-column cross section (discussion taken from Ref. 15). Generally low temperature gradients occur in regions of high thermal conductivity.

The temperature distribution for a molecular gas has the form shown in Figure 23 for nitrogen. Near the boundary, the temperature is low, and thus, in accordance with Figure 24 the thermal conductivity is low, resulting in a steep temperature gradient. Farther inside the arc column, the temperature rises to the level where the degree of dissociation steeply increases, and therefore the thermal conductivity becomes high. The temperature profile flattens out because the same flow of heat is maintained with a smaller temperature gradient. In the regions of still higher temperatures, however, the thermal conductivity passes its first maximum and decreases again, resulting in steeper temperature gradients. As ionization sets in, the temperature curve once again starts to level off, reaching a maximum at the axis of the column. The electrical conductivity (Fig. 26) in this case remains quite low until the second upturn of the temperature curve, and then rises sharply; hence, the current is confined almost entirely to a small region near the axis.

In the case of a monatomic gas, the situation is less complicated. The temperature distribution of the arc column in this case has a shape similar to that shown in Figure 23 for mercury. The two temperature distributions for nitrogen and mercury given in Figure 23 are typical for all molecular and monatomic gas columns carrying higher currents (Ref. 16). Again, in

the case of the monatomic gas, near the boundary of the column the temperature and the thermal conductivity are low, and there is a steep temperature gradient. As the temperature increases, however, ionization sets in and the thermal conductivity rises; as a result the temperature gradient decreases. The temperature again reaches its maximum at the axis.

The electrical conductivity of the plasma increases with increasing ionization; the current-density distribution across the column thus has a form similar to the temperature distribution.

The advantages of high heat capacity and thermal conductivity during the continuous operating condition for the arc-jet appear as disadvantages as far as arc initiation are concerned. The maximum amounts of thermal energy are extracted from the arc column by heat conduction and convection during the "zero-current" period and thus tend to prevent ignition.

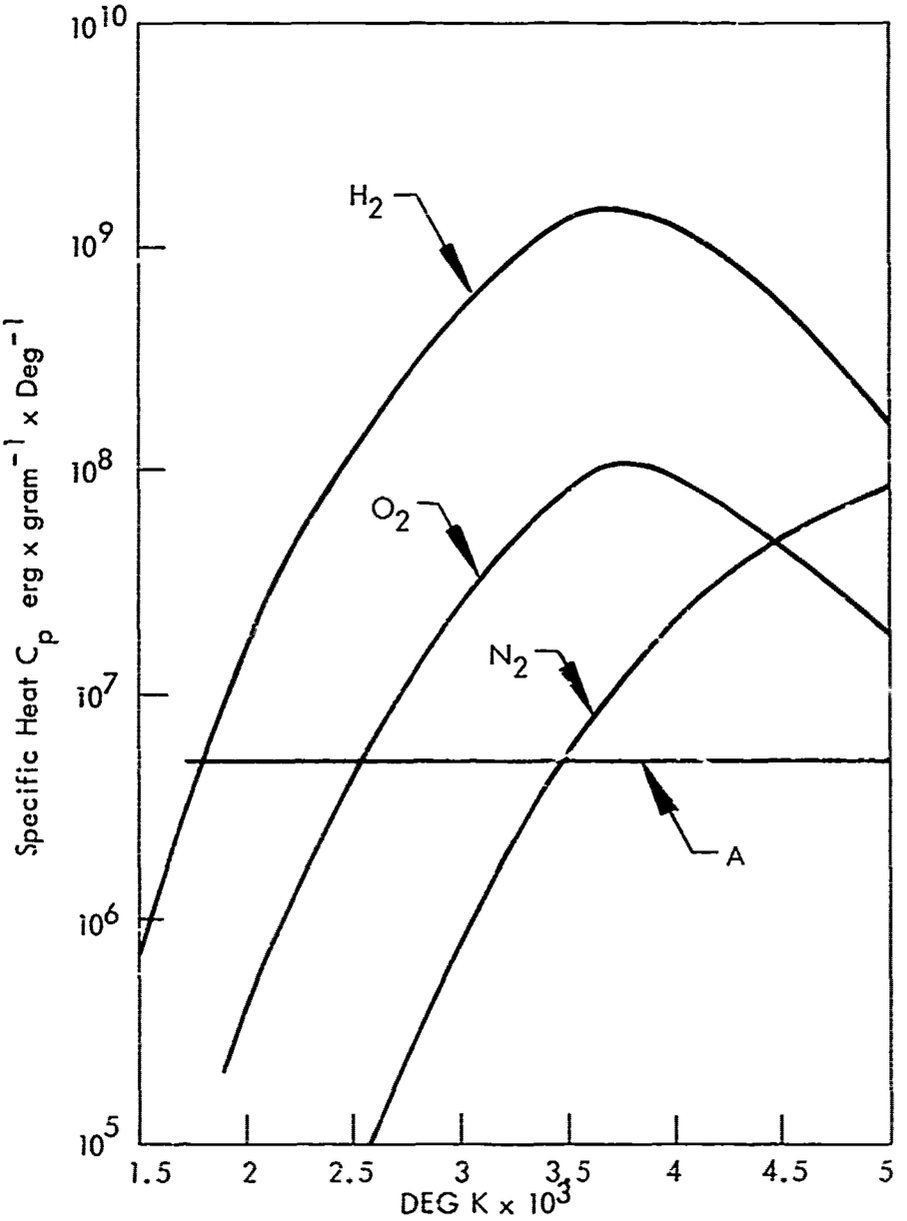

Figure 22 FRACTION OF SPECIFIC HEAT DUE TO MOLECULAR DISSOCIATION FOR 1 ATM. FOR HYDROGEN, OXYGEN, AND NITROGEN AS A FUNCTION OF TEMPERATURE (REF. 17). FOR COMPARISON, THE SPECIFIC HEAT FOR ARGON IS PLOTTED (REF. 18).

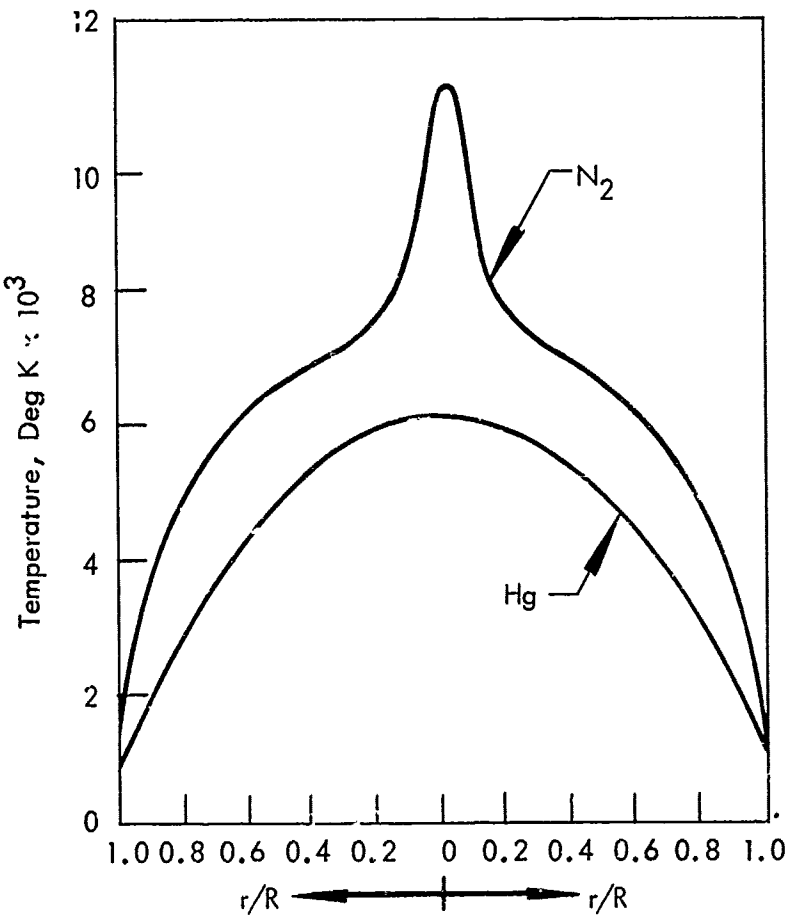

Figure 23 TEMPERATURE DISTRIBUTION ACROSS THE ARC COLUMN FOR A DIATOMIC NITROGEN (REF. 20) AND A MONATOMIC (MERCURY, (REF. 22) PROPELLANT.

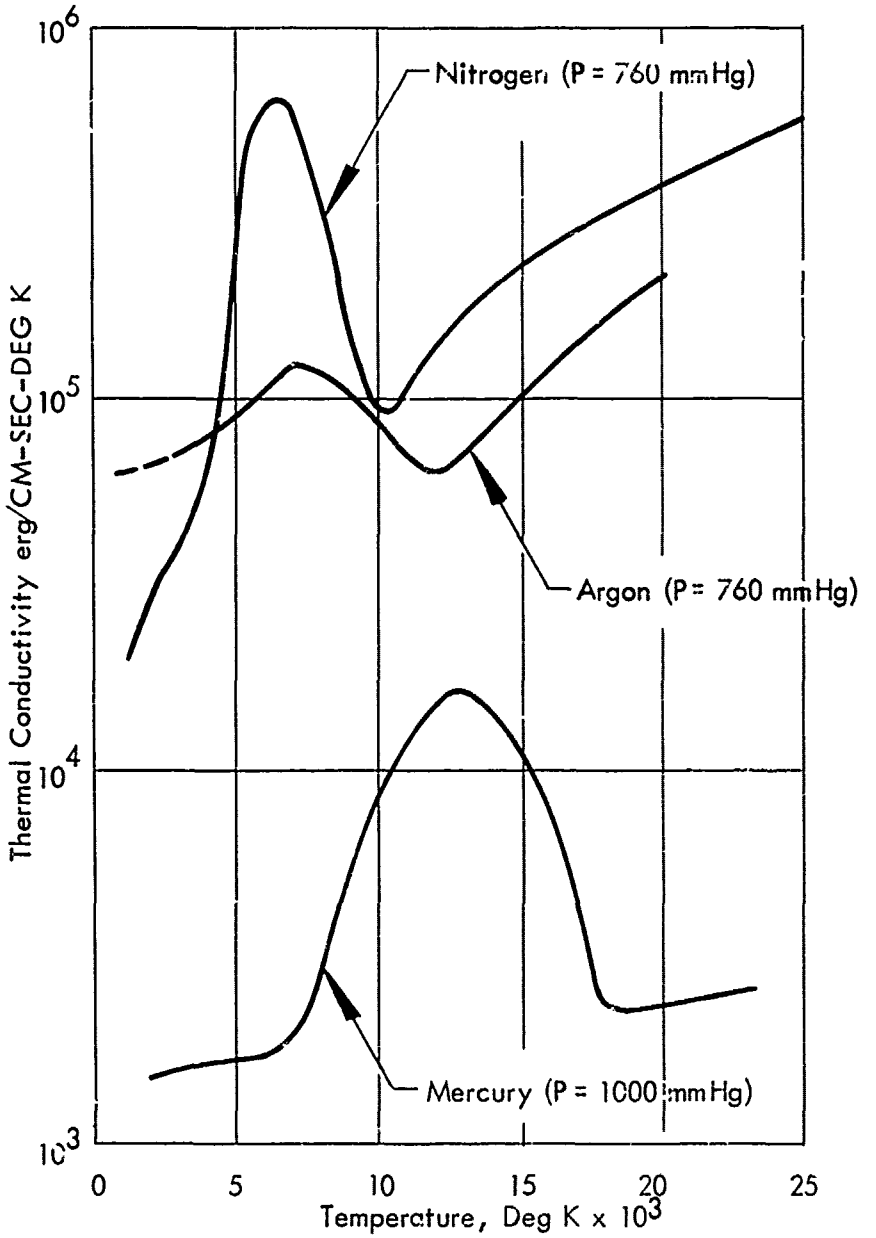

Figure 24 TEMPERATURE DEPENDENCE OF THE THERMAL CONDUCTIVITY FOR NITROGEN, ARGON (REF. 21) AND MERCURY (REF. 19)

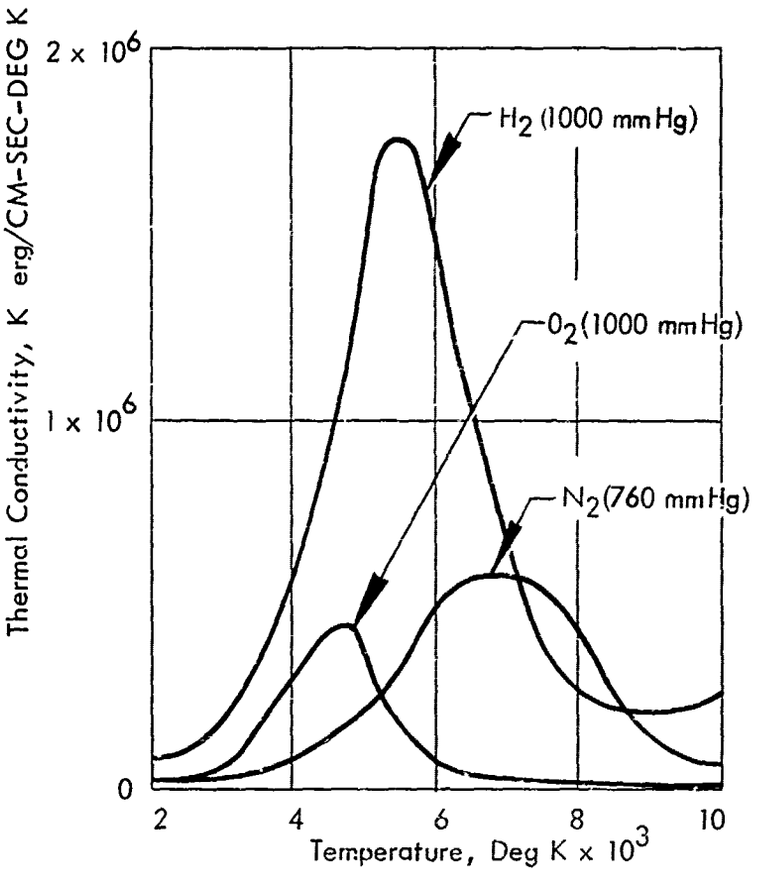

Figure 25 THERMAL CONDUCTIVITY FOR HYDROGEN, OXYGEN, AND NITROGEN AS A FUNCTION OF TEMPERATURE, THE DIFFUSION OF DISSOCIATION ENERGY INCLUDED (REF. 19 AND 20)

ELECTRICAL CONDUCTIVITY

The electrical conductivity can simply be related to the amount of ionization in the gas. As a first approximation Saha's equation can be used to determine this ionization degree. Saha's equation can be written as

$$\frac{x^2}{1 - x^2} \quad p = CT \; 2.5_{\epsilon xp} \left(\frac{- e V}{K T}\right)$$

Where

$$x = \frac{N_j}{N} = \frac{\text{Number of Ions}}{\text{Original Number Atoms}}$$

p = Total pressure
c = Constant and K = Boltzmann constant
T = The absolute temperature
$e V_i$ = Ionization energy of the atoms

The amount of ionization is a strong function of temperature and pressure. Increases in temperature increase the ionization and increases in pressure decrease this value. If the ionization potential of the atoms is low as in the case of alkali metals ionization will take place more easily at a given temperature.

The electrical conductivity of the plasma increases with increasing ionization; the current-density distribution across the column thus has a form similar to the temperature distribution. (See Fig. 23)

The distributions of current density of a monatomic gas and of electrical conductivity of a molecular gas are compared in Figure 26. The current-carrying cross-section of the arc column shall be defined as bounded by that diameter at which the current density is one-tenth of its value at the axis. With this definition, the effective current-carrying cross-sectional area of the molecular gas column is only about one-ninth of that of the monatomic gas column, provided that both columns have equal over all diameter and total current. In order to conduct the same total current through the molecular gas column with its restricted current-carrying cross-section, either the electrical conductivity and hence the temperature, or the longitudinal voltage gradient must be correspondingly higher. Usually both the temperature and the voltage gradient are higher.

The higher operating temperatures which accompany higher molecular weight propellants give rise to higher conductivity arc columns. For this case, higher current operating conditions for a given power will be observed.

The ignition of the arc-jet engine is a very important phase of its operation. The ease of engine start-up can be roughly measured by the sparking

or breakdown voltage for the gas-electrode system. This voltage is that potential difference between electrodes above which the gas acts as a conductor. Early work by Paschen showed that this potential is a function of the product of gas pressure, p, and electrode separation, d. The shape of the electrodes, the nature of the external circuit, the specific gas used and the electrode material also play a strong role in determining the breakdown voltage. Impurities in the electrode material have very great effects on the phenomena. At very low pressures, short gaps and very high gas density "Paschen's Law" fails.

The table below is a compilation of minimum sparking potentials (V_{min}) for various gases

Propellant	Cathode Material	V_{min} Volts	pd_{min} (mm of Hg x cm)
He	Fe	150	2.5
Ne	Fe	244	3.0
A	Fe	265	1.5
N_2	Fe	275	0.75
O_2	Fe	450	0.7
Air	Fe	330	0.57
H_2	Pt	295	1.25
CO_2	--	420	0.5
Hg	W	428	1.8
Hg	Fe	520	~2
Hg	Hg	330	---

(Refs. 23 and 24)

Helium has a very low sparking voltage and for experimental tests arcjet engines are usually started using it. The propellant to be run, usually H_2 or NH_3, is then introduced into the engine and the helium flow stopped.

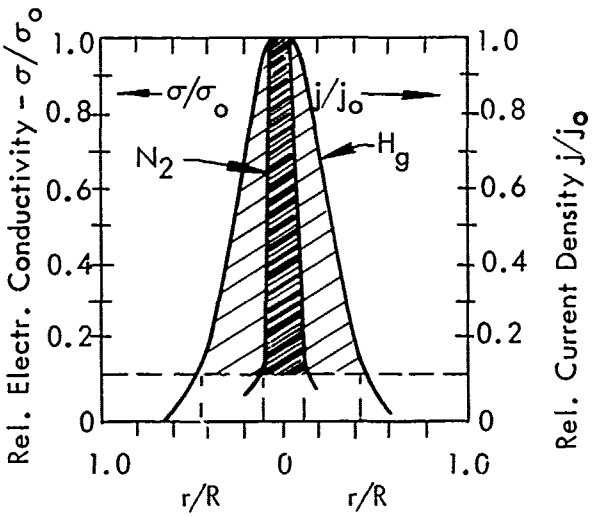

Figure 26 ELECTRICAL CONDUCTIVITY AND CURRENT DENSITY DISTRIBUTION ACROSS THE ARC FOR A MONATOMIC (MERCURY, REF. 22) AND A DIATOMIC (NITROGEN, CALCULATED ACCORDING TO REF. 20) PROPELLANT.

LATENT HEATS

The most convenient method of feeding the propellant into the arc-jet engine is in the gaseous state. The fuel may be stored prior to use in a solid liquid or gaseous condition. If it is stored as a gas at high pressure, of course, no heat need be supplied to the stored material to get useful propellant flow to the engine. However, if stored as either a liquid or a solid, heat must be supplied from an external source to transform it into the gaseous state. In the case of a stored liquid two distinct conditions can exist: first where the temperature at which phase transition occurs is below ambient temperature and the second where it is above that temperature. In the first case, this heat may be supplied from the atmosphere. If the proper insulation is used the heat leak into the storage tank can be used to control the production of gas and no system penalty need be charged to the heat supplied for this purpose. In the second case, heat must be supplied from an internal system source at a penalty to the overall efficiency to cause the desired phase change.

In the case where the propellant is stored as a solid but supplied to the engine as a gas, heat must be supplied for this purpose. The solid must be heated to the melting point, the latent heat of fusion supplied to bring it to a liquid state, the liquid must be heated to the vaporization temperature and finally, the latent heat of vaporization must be supplied to bring it into the gaseous state. Figure 27 illustrates this case for lithium at one atmosphere pressure.

This energy supplied to the propellant in the form of latent heats and liquid or solid heating is essentially lost as far as useful thrust. As an example of the significance of this factor for the solid storage propellant like lithium or lithium hydride, about 15-20 per cent of the total energy required for a specific impulse of 500 seconds would go into pre-heating in the storage tank.

It is conceivable that these latent heats need not be completely lost. If ingenious methods of using this energy as a means of cooling hot operating portions of the engine, a double advantage could be gained. At present, as stated early in this report, the incoming cool gas is used as a means of cooling the electrode regions while reducing the overall heat loss to the enviornment from the engine.

To illustrate the magnitudes of the latent heat and temperatures that these phase changes occur, they are listed for one pressure (1 atm) in Table IV.

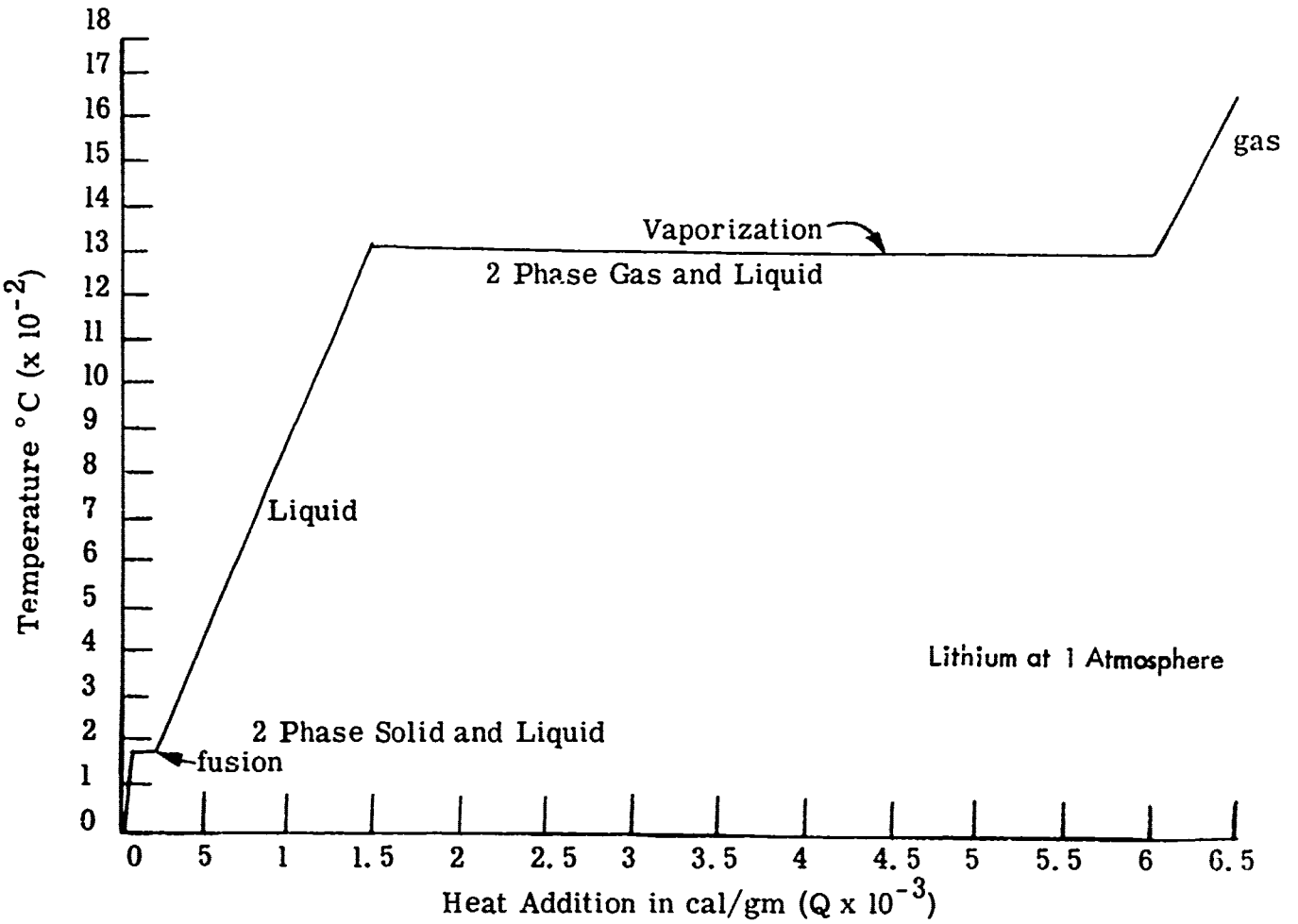

Figure 27 LATENT HEATS OF LITHIUM

Table IV LATENT HEATS (Refs. 25 - 27)

Propellant	Melting Temperature °C	Heat of Fusion cal/mole	Boiling Temperature °C	Heat of Vaporization cal/mole
Hydrogen	-259.2	28	-252.7	216
Helium	-271.4	~6	-268.4	22
Lithium	179	1100	1372	32250
Lithium hydride	680 (± 19%)	**	*840-930	**over 40,000
Ammonia	-77.7	1352	-33.4	5581
Methane	-182.5	224	-161.4	2040
Oxygen	-218.9	106	-183	1629
Nitrogen	-210	172	-195.8	1336
Argon	-189.3	290	-185.8	1590

* Li-H dissociation is believed to start to occur at a temperature below the so-called boiling temperature.

** Not known with any degree of accuracy due to chemical changes occurring below the gaseous state.

From this table we can observe that lithium or lithium hydride would have to be stored as solids and a great deal of heat must be supplied to them to bring them into the gaseous state. All other propellants listed could be stored as a cryogenic liquid stored at a lower than ambient temperature. They could also be stored as high pressure gases. This subject of storage is covered more fully in another section.

STORAGE PROBLEMS

The weight of the propellant and storage tank required to perform a particular mission is an extremely important portion of the system analysis. The fact that a particular propellant has the best engine performance is not a sufficient reason for its selection; the entire system must be considered. The amount of fuel required, its storage density, the weight of the storage tank, and the size of the tank are all important factors. The propellant can be stored as a solid, a gas or a liquid and in some cases as a cryogenic. The actual amount of propellant stored in the tank depends on the mission, the engine performance using a particular propellant, and the leakage required in some cases for insulating purposes. The tank itself contains the propellant, its required ullage space, and also acts as an insulating shield when the propellant is stored below ambient temperature. The details of the storage analysis can be quite lengthy and only a very brief explanation is included in this report.

Solid storage is possible with propellants such as lithium or lithium hydride which have high melting temperatures at the storage pressures considered for arc-jet usage. The density of this material is relatively high and the tank walls are needed only to contain the material. The difficulty in using the solid is in design of a feed system. Heat must be supplied from the system if the feed is liquid or gaseous. The high temperatures involved in using these fuels (see section on latent heats) causes serious material problems.

To keep lithium in a gaseous state at one atmosphere, temperature in excess to 1300° C must be maintained throughout gas-flow system. Storage density is listed in the table below for these solids.

The storage density of the propellant should be high so that the tank weight is low. In order to obtain a higher density in a number of potential propellants the storage temperature must be quite low. The table below shows some selected properties of cryogenics for electrothermal engines. To help accomplish this, insulating materials must surround the tank and usually a protective tank must cover the insulating material. The weight of the tank can be significantly increased by using the insulated tanks. The greater the amount of propellant that is required for the mission, the more favorable is the total weight of storage tank plus propellant to the usable propellant (Wt/W_u). The system of cryogenic stored propellant using a vapor cooled shield will be illustrated to give a feeling for the problem. Figures 28 and 29 show the ratio Wt/W_u as a function of storage time for 173 lb. and 7776 lb. of stored usable propellant. The first conclusion that can be drawn from this work is that a very high storage weight penalty is paid to carry the helium. This is because of its very low density and the very low temperature required for its storage. Heat insulation becomes a very major problem. The ammonia methane and ethane are easily stored; ammonia giving the lightest tank weights. Ammonia can be stored without

any difficulty with thermal problems. The storage of hydrogen is somewhat intermediate in its difficulty.

The tests to date on arc-jets show that the best performance can be achieved using hydrogen as a propellant. Ammonia gives reasonable performance followed by helium and the hydrocarbons are the least satisfactory. Helium, because of its lower performance and heavy storage weight penalty does not seem desirable for space usage with the arc-jet.

Aside from the storage of solids, hydrogen and ammonia must be evaluated further. Because hydrogen has better arc-jet performance but is more difficult to store than ammonia, each is better for some missions. Less hydrogen weight is needed for a particular mission; and for a given storage time and for a given amount of required propellant both systems can be equal in weight. In general, the analysis of these two systems results in a curve as shown below.

Figure 30

Comparison Between Liquid Hydrogen and Liquid Ammonia Storage Tank on a Weight Basis

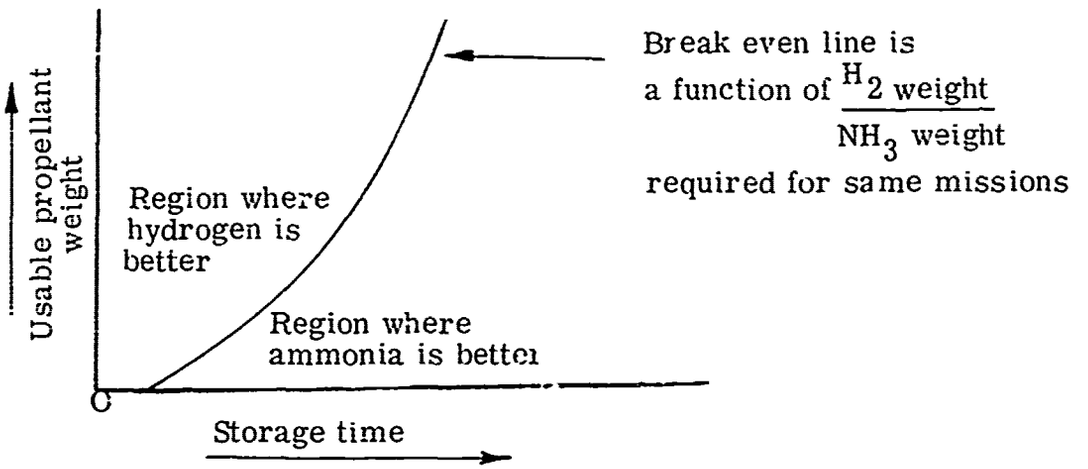

For shorter storage times and higher rate propellant usage hydrogen would be superior. And for longer storage times ammonia results in a lighter total storage system.

More efficient methods of cooling cryogenic tanks for long durations are presently under development. Improvements in insulation materials would decrease some of the weight penalties associated with low temperature storage. At present, "super" insulators with conductivity values in the order of 4×10^{-5} Btu/ft hr °F are available. Airesearch Corporation is developing a very lightweight refrigeration system which will eliminate the need of sacrificing some of the propellant as a means of cooling the insulation. The refrigeration is a closed system and allows zero heat transfer to the propellant. This system shows very significant weight reduction in the storage systems using hydrogen for long periods of time.

STORAGE DENSITIES

Table V — SOLID

Propellant	Storage Temp.	Pressure	Storage Density
Lithium	Ambient	1 atm	$\sim$ 33 lb/ft^3
Lithium hydride	Ambient	1 atm	$\sim$ 49 lb/ft^3

Table VI — CRYOGENIC

Propellant	Critical Temperature and Pressure	Density At Critical Pt. lb/ft^3	Boiling Temperature °F	Liquid Density at Boiling Pt. lb/ft^3
Hydrogen	- 399.8°F 188 psia	1.87	-423	4.43
Helium	- 450.6°F 32.2 psia	4.3	-452	7.82
Methane	-116.7°F 673 psia	10	-258.9	26.48
Ethane	89.8°F 716 psia	13.1	-127.5	34.12
Ammonia	270.3°F 1639 psia	14.7	-28.1	42.57
Argon	-308°F 705 psia	33.2	-303	----
Air	-366°F 588 psia	21	-323	$\sim$54

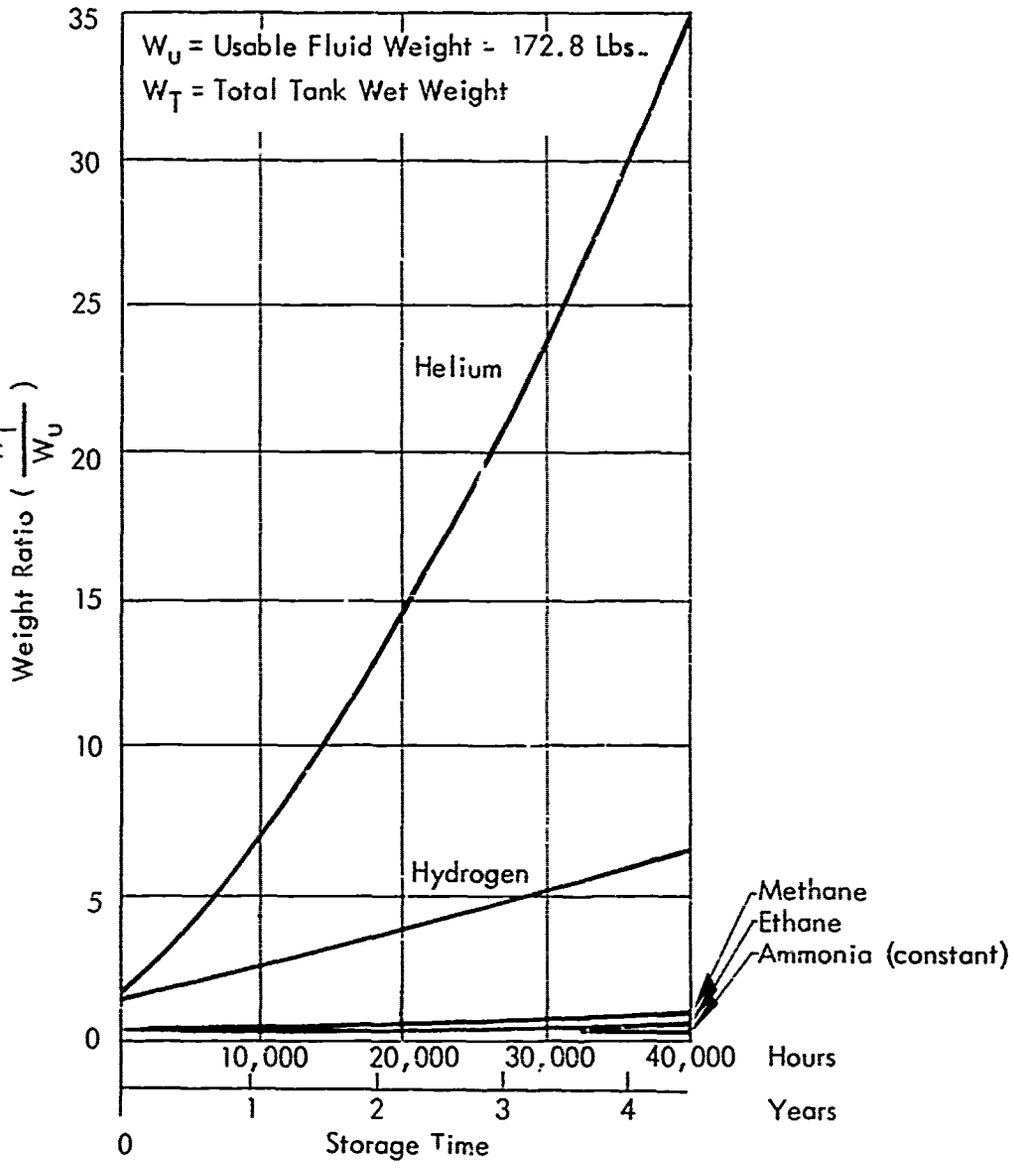

Figure 28 VAPOR-COOLED SHIELD-OPTIMUM WEIGHT RATIO

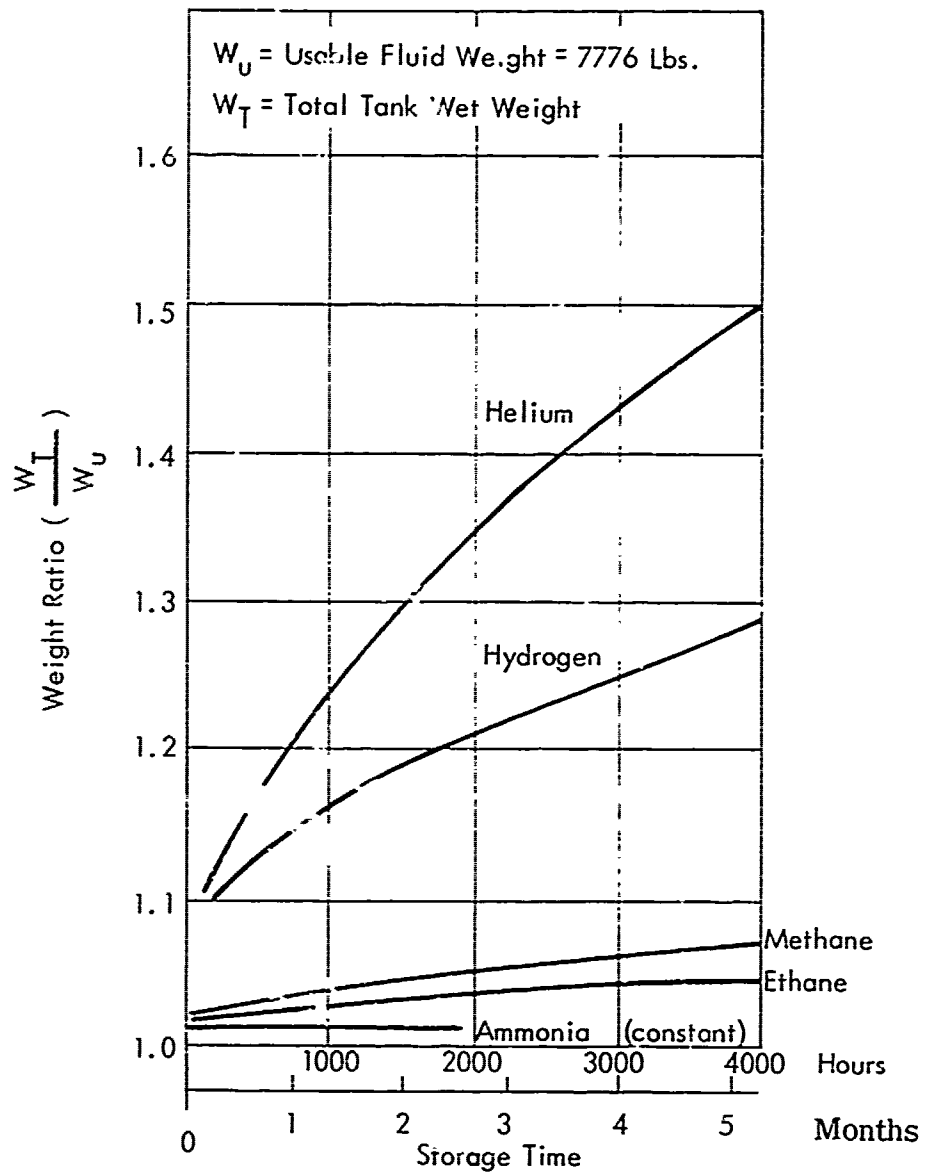

Figure 29 VAPOR-COOLED SHIELD-OPTIMUM WEIGHT RATIO

(from Ref. 28)

ENGINE LIFE

The life of the arc-jet is limited by the erosion rate of the anode-nozzle in the typical configurations used presently. This erosion can take place by several mechanisms: The mass loss due to vaporization, localized heating in the anode fall region, sputtering, and chemical reactions between the propellant fluid and the wall.

The amount of electrode material loss due to vaporization can be obtained from elementary kinetic theory (Refs. 29 and 5). The maximum mass flux from the surface is given by

$$\dot{M}_{vap} = KP_{vap}\ M/T$$

where K = constant

P_{vap} = vapor pressure

M = molecular wt.

T = surface temperature ° Absolute

The vapor-pressure temperature relations were obtained from References 30 and 31. $\dot{M}_{vap}$ is shown as a function of surface temperature in Figure 31. The temperature at the wall depends strongly on the operating temperature of propellant. Thus, for example, the wall temperature for a hydrogen operated engine would be considerably cooler than with one operating on ammonia for the same I_{sp}. The rate of vaporization would be lower and the life longer using hydrogen. This is, of course, if vaporization was the major phenomena controlling life. Reference 5 reports that maximum wall temperatures operating at an I_{sp} of 1000 seconds with a radiation cooled engine were 1600°K for hydrogen and 2600°k using ammonia.

The amount of erosion caused by the anode foot region depends on the current and current density in that region. The exact analysis of this effect is complicated by the fact that the arc has various operating modes and frequently moves rapidly over the anode surface. This phenomena is discussed at greater length in a subsequent chapter. The life of the thruster has been found to increase (using various propellants) with a decreased current for a given power operation. The material loss due to sputtering becomes a serious problem when the fluid particles acquire enough energy through the fall region to be able to penetrate the solid lattice of the electrodes and displace some of the metal atoms from their lattice positions and subsequently drive surface atoms into the flow stream.

The relative effects of the different mass removal mechanisms is not at all clear at present. These must be understood before significant increases in engine life can be achieved.

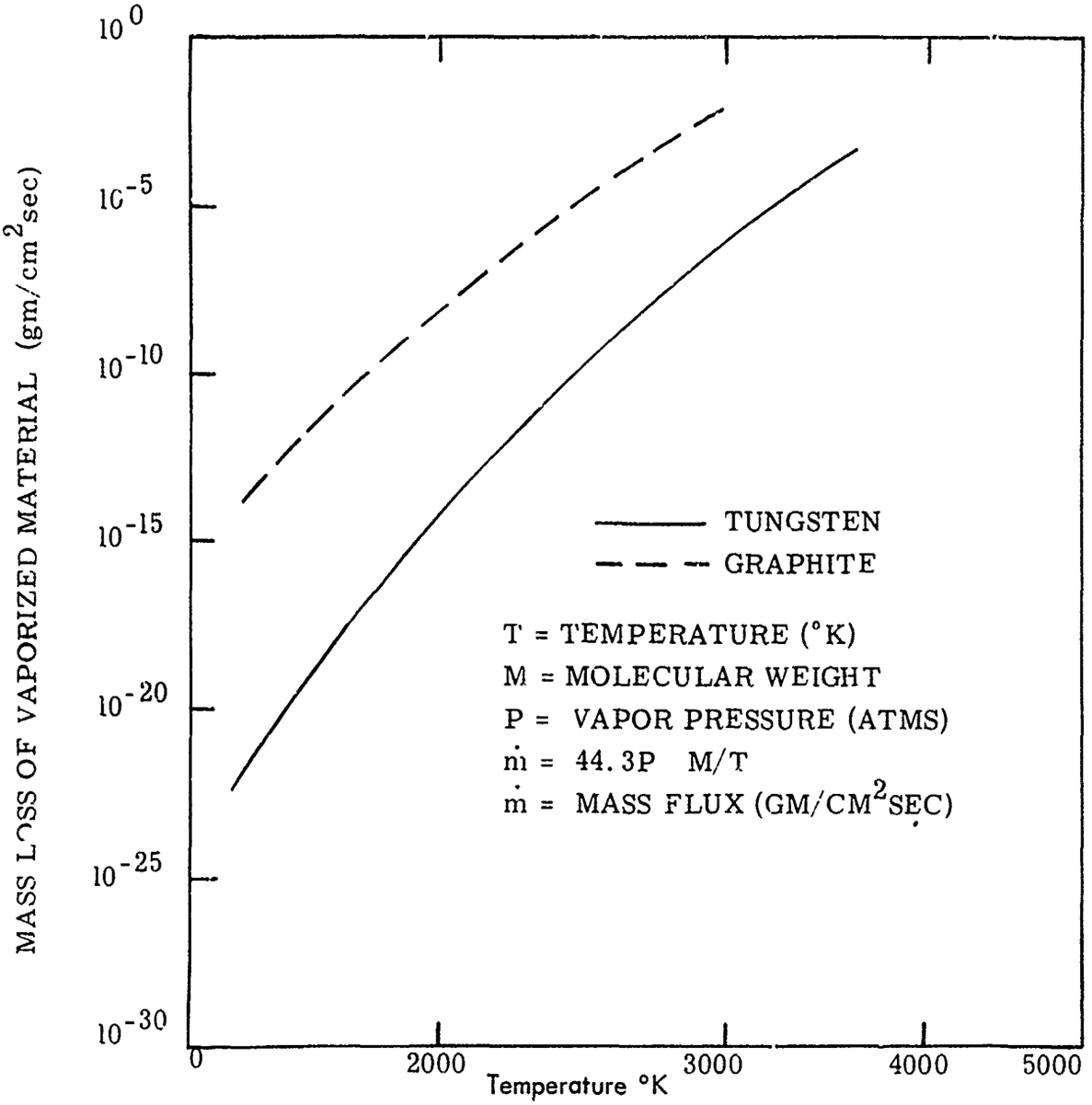

MASS FLUX OF VAPORIZED MATERIAL VERSUS MATERIAL SURFACE TEMPERATURE

Figure 31 (Ref. 5)

THE MOVING ARC FOOT AND ENGINE LIFE

Recently an arc phenomenon was observed which can be used to increase the life and performance of the thermal arc-jet. It shows that at certain operating regimes and using certain propellants the arc attachment region travels axially and periodically along the anode surface. This is for geometries similar to those presently used in most D-C arc-jets. The arc initiates at the upstream end of the cylindrical anode and the foot is swept downstream by gas flow repeatedly over the same path. The life of the anode can be increased by forcing the arc foot to move rapidly over the entire surface of the anode in such a manner that the path is different for each repeating cycle. This reduces the concentration of heat flow due to losses in the anode fall region and thus markedly reduces anode erosion rates.

In thermal arc-jets as they are designed now, the permissible running conditions for the unit and the operating life obtainable are limited by the erosion of the anode. This is true even in cases where the electrode drop loss at the anode is small compared to other thermal losses in the unit, and this is a direct result of the fact that the anode drop heat loss enters the wall in a very concentrated form. A reduction of the concentration of anode heat loss would permit improvements of thermal arc-jet performance in several ways including the ability to attain higher specific impulse and arc chamber pressure. Higher average wall temperature could be attained since localized hot spots would not be formed in the anode. The higher wall temperature would cut down on convective heat transfer to the walls. The higher arc chamber pressure would increase the usually very low Reynolds number and reduce dissociation losses.

High frequency fluctuations were first noted in the arc-jet at Plasmadyne in 1959 when arc voltage and current were monitored using an oscilloscope. The voltage was found to vary in a saw-toothed pattern with voltage increasing gradually and dropping abruptly at very high frequency (5 - 200 kilocycles). These voltage fluctuations were observed on many occasions. Wheaton and Dean* have carefully studied these voltage fluctuations and have demonstrated that they are caused by an operating pattern in which the arc initiates at the upstream end of the anode and is swept downstream over the anode surface by the gas flow. The voltage increases as the arc grows longer until it is high enough to cause breakdown again at the upstream end of the anode. This cycle repeats at high frequency and keeps the foot of the

---

* John R. Wheaton and Robert C. Dean, Jr., "On Anode Gas Sheath Electrical Breakdown in a High Pressure Arc Plasma Generator," Dartmouth Research Report, October, 1961. (Ref. 32)

arc moving rapidly in an axial direction over the anode surface. Since the arc will tend to break down at the same circumferential position at the beginning of each cycle, the arc is expected to follow down the same path on the anode with each cycle until the geometry is changed enough by erosion to modify the breakdown conditions. Figure 32 shows an oscilloscope trace of the voltage across the electrodes of a typical Plasmadyne arc-jet. The fluctuations shown are similar to those reported by Wheaton and Dean.

In addition to axial motion of the arc, tangential motion is frequently induced by the use of whirl in the gas flow and/or an axial magnetic field. This tangential motion combined with the axial motion described in the preceeding paragraph results in a spiral path which the arc follows down the anode. Since the arc still breaks down at the beginning of each cycle, the arc repeatedly retraces the same spiral path on the anode. When enough erosion occurs to permit the arc to break down at a new position at the upstream end of the anode, the arc starts along a new spiral path. This seems to explain the spiral erosion marks which are frequently observed on cylindrical anodes.

To avoid concentrated heat flow into the anode it would be desirable to spread the arc over the anode in a non-repeating pattern for the condition at which the above fluctuation take place. This can be controlled, it is believed, by several means such as:

1. Using a pilot arc to force the initiation point
2. Using a variable strength magnetic field around the anode
3. Using a transverse magnetic field around the anode
4. Using segmented electrodes to force the location of the initiation point
5. Using physical rotation of arc-jet engine parts to control the arc foot relocation point.

Details of this phenomenon and its control to increase life are too lengthy to include in this study but will be supplied in other Plasmadyne reports.

The phenomenon was only observed in diatomic gases such as nitrogen and hydrogen. Repeated tests with monoatomic propellants such as helium or argon revealed no such occurrence.

This arc foot movement might be an important factor in the life of an engine and the choice of a propellant which can exhibit this phenomenon might be an important factor in its selection.

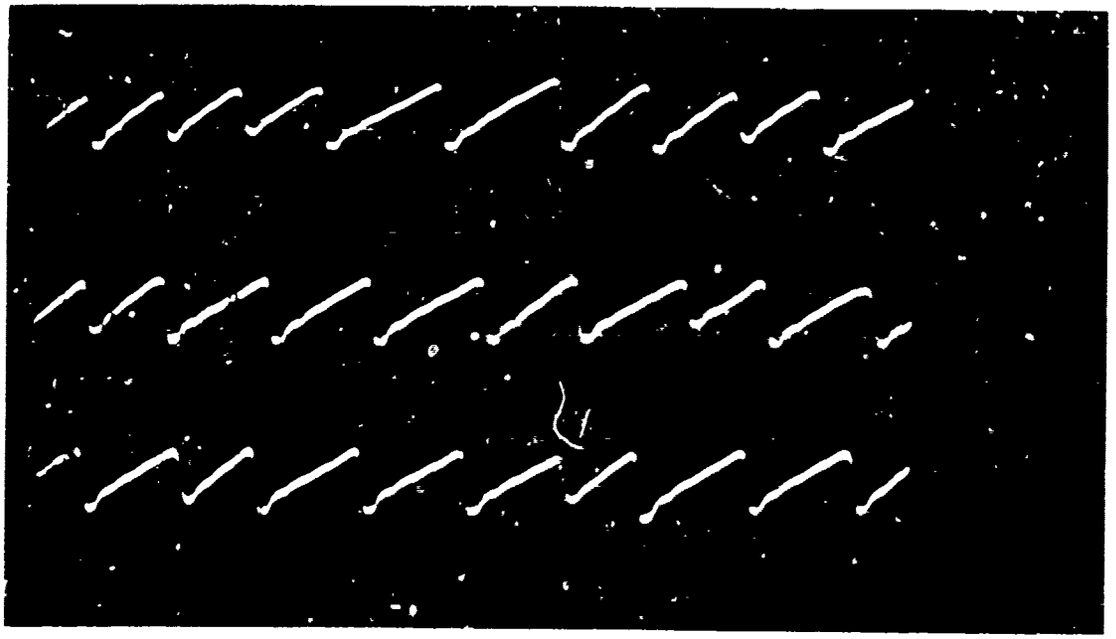

Figure 32a -- VOLTAGE TRACES WITH HYDROGEN
75 Amps, 98 Volts (Average), 0.16×10^{-3} Pounds Per Sec.
50 Volts Per Centimeter, 5 Microseconds Per Centimeter

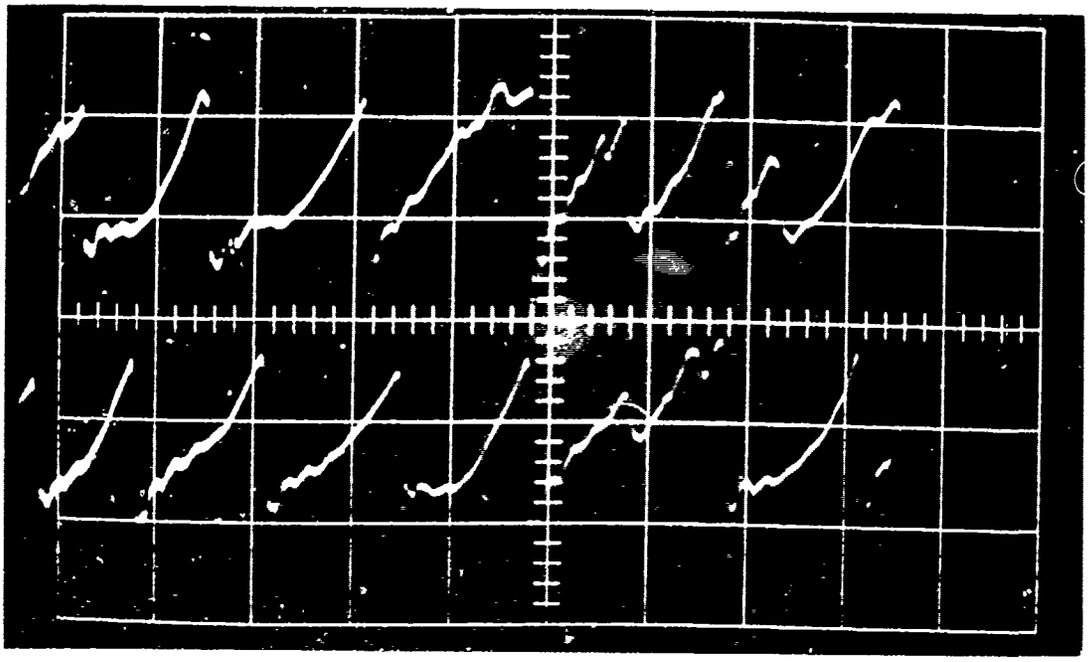

Figure 32b -- VOLTAGE TRACES WITH HYDROGEN
45 Amps, 162 Volts (Average), 162 Volts (Average)
0.54×10^{-3} Pounds Per Second, 50 Volts Per Centimeter
5 Microseconds Per Centimeter

CHEMICAL INTERACTIONS BETWEEN MATERIALS OF CONSTRUCTION AND PLASMA JET PROPELLANTS

The design of high intensity electric arc devices has for many years concentrated on the use of inert gases in order to circumvent the chemical problems involved with gases other than the "noble" gases. It was recognized early that the usual electrode materials such as graphite were readily attacked by air, water, CO_2, etc. Thus, in order to study arc behavior and arc phenomena without the complicating chemical factors pure helium and argon were used. The result, of course, has been the development of numerous high intensity arc devices which have important commercial applications.

Electric propulsion for space vheicles is one such application now being seriously considered and investigated. One type of electric propulsion involves the use of a plasma stream heated by an electric arc. It is of importance to the investigators in this field to consider the use of gases and compounds other than argon or helium as the propellant in a plasma jet engine. Theoretical considerations indicate that better performance should be obtained from propellants such as hydrogen, ammonia, and lithium hydride. Other factors to be considered in the choice of propellants for a plasma jet engine are the ease with which the "fuel" can be stored, its storage density, and the weight of the vessel required. It follows then that the cryogenic propellants (H_2, N_2, A, He, O_2, etc.) creat design problems which may be alleviated if fuels such as NH_3 or LiH could be used. It is obvious from this that chemical activity of the materials of construction of an arc-jet engine with respect to the various proposed propellants is of significant importance.

If one attempts to predict the chemical behavior of a given material in the presence of a specific propellant, factors such as wall temperature and the boundary layer conditions must be known. These factors are controlled by such conditions as engine configurations, power input, mass flow rate of propellant, and the thermophysical properties of both the material and the propellant. This represents a vastly complex situation and is beyond the scope of the comments to follow.

Without regards to novelty of design (i.e., complicated cooling systems for the materials of construction of a plasma jet engine), a group of materials having superior high temperature properties will be compared and their resistance to attack from various propellants will be described.

Thoriated tungsten is a superior electrode material based on its electrical and thermal conductivity, high melting point and low vapor pressure, and its resistance to thermal shock. The following table presents the chemical resistance of thoriated tungsten to various propellants.

Table VII

THORIATED TUNGSTEN

Propellant	Remarks
Nitrogen	Tends to disolve N_2, solubility of N_2 is 0.19×10^{-4} wt. % at 1600° C and 0.38×10^{-3} wt. % at 2400° C.
Hydrogen	No reaction up to melting point
Ammonia	No reaction up to melting point
Li & LiH	Should be similar to Na, NaK, and Cs metals which do not react up to 900° C
CH_4 or C_2H_6	Begins to react at 1200° to form WC and a eutectic (1.5 wt. % C) which melts at 2475° C
Air	Begins to oxidize at 400° C, rapid at 650° C

The best materials one might use as an uncooled housing material for the arc-jet engine are tantalum and molybdenum metal. This is based on their good electrical and thermal conductivities, high melting points and low vapor pressures, high resistance to thermal shock, and ease of fabrication. The resistance to the propellants in Table VII is described in Tables VIII and IX for these materials.

Table VIII

TANTALUM

Propellant	Remarks
Nitrogen	Nitrides at 300° C: rapid at 1100° C to form hard skin. At 2000° C in high Vacuum all N_2 is evolved.
Hydrogen	Absorbs H_2 above 250° C ; above 800° C in high vacuum all H_2 is evolved.
Ammonia	Same as with N_2
Li & LiH	Good up to 1000° C.
CH_4 or C_2H_6	Reacts between 1700-2500° C to form TaC Eutectic (0.8 wt. % C) melts at 2800° C oxidizes readily above 550° C

Table IX

MOLYBDENUM

Propellant	Remarks
Nitrogen	Forms nitride skin above 1100° C
Hydrogen	Inert at all temperatures
Ammonia	Same as N_2
Li & LiH	Good up to about 1000° C
CH_4 & C_2H_6	Forms carbides at elevated temperature and an eutectic (1.8 wt. % C) which melts at 2200° C
Air	Oxidizes readily above 650° C

Three materials which can be used as ultra-high temperature electrical insulators are Al_2O_3, BeO, and BN. The choice of these three materials is based on their high melting points, high electrical resistivity, good thermal stability, and thermal shock resistance. The behavior of these substances with the propellants in the previous tables is listed in Table X.

Little has been said up to this point about the phenomena taking place at an emitting electrode surface. In certain cases high erosion rates of tungsten electrodes have been obtained with helium and argon gases even though conventional chemical phenomena can be ruled out. It has been empirically shown that such high erosion rates can be greatly decreased by proper electrode spacing and configuration, cooling-channel design, and proper matching of power input and gas mass flow rate. Here again the complexity of the emission phenomena places any detailed discussion beyond the scope of this brief study.

However, it should be pointed out that electrochemical phenomena may be important. For example, List and Jones, and Skolnik and Jones (References 33 and 50) have shown that uncooled graphite electrodes operate in N_2, O_2, Air, and H_2 such that a voltage drop occurs which coincides with the formation of compounds such as: CN, NO, CO, CO_2, and CH_4. The ionization potential of these compounds being lower than those of the gases mentioned thus influences the anode voltage. List and Jones, and Skolnik and Jones could not observe a voltage drop for metal electrodes, but suggest that this effect was obscured because the ionization potentials of metals such as tungsten, copper, and iron are lower than any compounds which could form. It appears then that there can be a definite influence on the voltage-current characteristics of the arc depending on the electrode material and the propellant used. Thus, it is possible that electrochemical phenomena may play an important part in the operating characteristics of an arc-jet engine and the life of the electrodes.

Table X

ALUMINUM OXIDE, BERYLLIUM OXIDE, AND BORON NITRIDE

Propellant	Remarks		
	Al_2O_3	BeO	BN
Nitrogen	No reaction to melting point (2050°C)	No reaction to melting point (2570°C)	Good to 2900°C (Pure BN) Good to 1400°C (Commercial BN)
Hydrogen	Same as N_2	Same as N_2	Same as N_2
Ammonia	Same as N_2	Same as N_2	Same as N_2
Li & LiH	Reaction at 200°C (Li). Reaction at 500°C (LiH).	Similar to Al_2O_3 behavior	Serious reaction at high temperatures as with graphite
CH_4 & C_2H_6	No reaction to melting point	Reacts above 1800°C to form Be_2C; carbide dissociates to Be+C at 2200°C	Reacts to form B_4C at 2000°C
Air	No reaction to melting point in dry air	No reaction to melting point in dry air	Reacts at 1500°C (Pyro-BN) Reacts at 1000°C (Commercial BN)

The foregoing information describing the compatibility of selected materials with a group of propellants is based on literature data taken under essentially static conditions. It should be realized that little is known about the reaction kinetics under conditions of varied mass flow, heat flux density, and boundary layer conditions in an arc-jet engine. It is important, therefore, that research efforts should be instigated in which propellant and materials be studied together.

The results of interaction of propellant and container materials in arc-jet engines will be summarized. Hydrogen has the lowest deterioration effects on all the materials considered. The carbon containing propellants and air have serious containment problems at the higher temperature. Alkali metal propellants are not seriously active until above 1000° C; however, these propellants usually will be operated above this temperature because of their high vaporization temperature. The nitrogen containing chemicals are moderately active and can be used with certain of the container materials.

This discussion is not concerned with the temperature at which the arc-jet will operate using different propellants. The higher the operating temperature required to obtain the desired engine performance, obviously, the more serious will be the materials problems involved in their design.

SPUTTERING

The erosion of metallic surfaces by positive ion bombardment is called sputtering. Measurements of this phenomenon are generally reducible to a "sputtering ratio" which may be defined as the ratio of ejected metal or target atoms to the incident bombarding ions. This defined, the sputtering ratio is characteristic of target material and bombarding ion, but may vary with ion energy and angle of incidence.

If the weight loss of the target is a true measure of the amount of sputtering and the integrated current is a true measure of bombarding ions, the sputtering ratio can be expressed as

$$S = W/I_t = N_i/N_j = 96500\ W/A\ I_t$$

where

W = Weight loss in milligrams

I_t = Integrated Target current (Ma-Sec)

N_i = Target atoms lost

N_j = Bombarding Ions

A = Constant = 63.5 for a copper target

The sputtering rates are higher for more massive ions and except for the case of hydrogen ion H+, the total weight of ions striking the target (for the experimental data shown) is a small fraction of the observed weight loss. The amount of sputtering is also sensitive to the pressure. The variation with pressure appears to be due to the formation of a surface layer which inhibits the emission of sputtered target atoms from the surface. At pressures in excess of 10^{-4} mm of Hg the number of neutral particles from the residual gas striking the target is orders of magnitude greater than the number of ions. The surface layers are self renewing at higher pressures. A doubling of the pressure usually results in a decrease in sputtering of 10-15%.

The table below exhibits sputtering ratios for various ions incident on copper at 50 kev of energy. Some results using argon and various target material are presented in Table XII. This data is taken from Reference 34 and are only shown for relative effects of sputtering variations. Figure 33 shows the effects of ion energy and molecular weight on the sputtering ratio.

Table XI

SPUTTERING OF COPPER BY ION AT 30 Kev

ION	^{n}MOLECULAR WT	SPUTTERING RATIO
H^+	1	0.011
D^+	2	0.03
He^+	4	0.13
N^+	14	5.28
Ne^+	20	3.61
A^+	40	9.02
Cu^+	63.5	9.6

Table XII

SPUTTERING BY ARGON ION AT 30 Kev

TARGET	SPUTTERING RATIO
Ta	2.7
Mo	3.31
Cu	9.02
Al	2.38

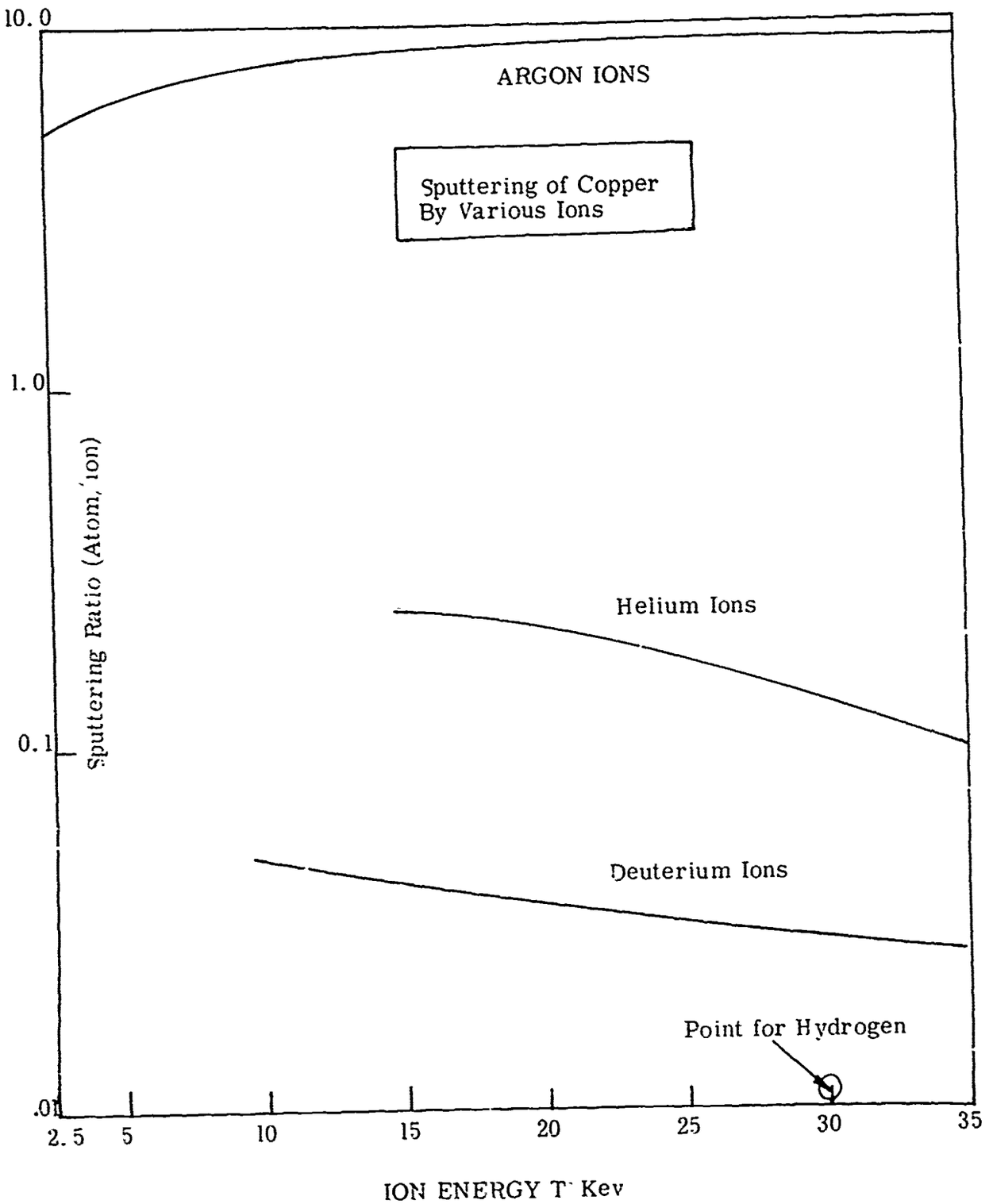
10.0
ARGON IONS
Sputtering of Copper
By Various Ions
1.0
Sputtering Ratio (Atom/Ion)
Helium Ions
0.1
Deuterium Ions
Point for Hydrogen
.01
2.5
5
10
15
20
25
30
35
ION ENERGY T Kev

Figure 33

RECOMBINATION

The energy transferred to the propellant in the arc region of an arc thruster is sufficient to cause a considerable number of propellant molecules to dissociate. If recombination into molecules can be achieved within the diverging portion of the exhaust nozzle, then the energy captured in the dissociation process will be released to the gas particles in the stream, increasing their thermal energy, and consequently, the amount of momentum they transfer to the nozzle walls, i.e., "thrust".

An accurate evaluation of the recombination characteristics of propellants in an arc-jet thruster can be accomplished only by experimental measurement. Experimental data for chemical reaction rates in nozzle flow are extremely scarce. Accordingly, any theoretical calculation of recombination rates or relaxation times in nozzle flow involves many assumptions. Such calculations may be in error by orders of magnitude and must therefore be regarded only as very crude estimates.

Preliminary calculations of the molecular recombination rates of hydrogen, lithium hydride and ammonia were carried out, using simple collision theory. The increase in recombination rate caused by the injection of foreign particles into the exhaust flow was briefly investigated. Some experimental results from a recent Plasmadyne study of hydrogen nozzle recombination are presented.

Energy Absorbed in a Dissociation Process

A diatomic dissociation process may be represented by the equation

$$A_2 \rightleftharpoons A + A \qquad (1)$$

The degree of dissociation α is defined as the ratio by mass of the atoms in the mixture to the total mass of atoms and molecules. Therefore for diatomic dissociation

$$\alpha = \frac{N_A}{N_A + 2\,N_{A_2}} \qquad (2)$$

where N_A is the number of atoms and N_{A_2} is the number of molecules present in the mixture.

The energy distribution in the atom-molecule system can be evaluated as follows, by assuming the energy to be in two forms only - dissociation and thermal:

$$E = (N_A + N_{A_2})\,E_T + \frac{N_A}{2}\,E_D \qquad (3)$$

where E is the total energy in the gas, E_T is the thermal energy of each particle, and E_D is the dissociation energy.

Equation (3) can be rewritten as

$$E = N E_T + N \left(\frac{\alpha}{1 + \alpha} \right) E_D \qquad (4)$$

where N is the total number of particles. The percentages of thermal energy and dissociation energy in the system are respectively:

$$\% \text{ thermal energy} = \frac{E_T}{E_T + \left(\frac{\alpha}{1 + \alpha} \right) E_D} \times 100 \qquad (5)$$

and

$$\% \text{ dissociation energy} = \frac{\alpha E_D}{(1+\alpha) E_T + \alpha E_D} \times 100 \qquad (6)$$

For the case of hydrogen at chamber conditions of 1.0 atmosphere pressure and 3000°K. ($I_{sp} \approx 1000$ sec.), $\alpha \approx 0.08$, $E_T \approx 0.5$ ev, $E_D = 4.7$ ev and

$$\% \text{ thermal energy} = \frac{0.5}{0.5 + \frac{0.08}{1.08} \times 4.7} \times 100 = 60\%$$

$$\% \text{ dissociation energy} = \frac{0.08 \times 4.7}{1.08 \times 0.5 + 0.08 \times 4.7} \times 100 = 40\%$$

Thus, 40 per cent of the energy present in the gas is unavailable for producing thrust if no recombination occurs within the nozzle.

RECOMBINATION RATE CALCULATION

Symbol Definition

a, b	Activation energies
M	Molecular weight
n	Number density
P	Steric factor
R	Universal gas constant
T	Temperature
u	Third body
μ	Reduced mass of binary system = $\frac{m_1 \; m_2}{m_1 + m_2}$
σ	Diameter of species particle
σ_{AA}, σ_{Au}	Effective diameter of the temporary particles formed by binary collisions $\approx$ 88 per cent of the sum of the diameters of the two colliding particles.
τ	Mean duration of collision
( )	Concentration of species

Karl F. Herzfeld (Ref. 35), George P. Wood (Ref. 36) and others have derived expressions for the rate of recombination of atoms into molecules, based on simple collision theory. Wood's analysis was followed in the present discussion.

Two atoms can form a stable molecule only if a part of the sum of their respective energies is absorbed by a third body and momentum is conserved. With no third body present during their collision, two atoms would merely "bounce off" each other, without forming a molecule. In order to make his calculation, Wood assumed that recombination can occur in two ways: during the collision of two atoms a third body collides with them, causing recombination; or, during the collision of an atom with a third body, another atom collides with them, causing recombination.

Wood derives the following equation for the recombination rate of atoms into molecules ($A_2 \rightleftharpoons A + A$):

$$\frac{d(A_2)}{dt} = 2(2\pi RT)^{1/2} \left[(AA)(u) \left(\frac{\sigma AA + \sigma u}{2} \right)^2 \left(\frac{M_{AA} + M_u}{M_{AA} \; M_u} \right)^{1/2} P_{AA \cdot u} e^{-a/RT} + \right.$$

$$\left. + (A_u)(A) \left(\frac{\sigma_{Au} + \sigma_A}{2} \right)^2 \left(\frac{M_{A_u} + M_A}{M_{A_u} \; M_A} \right)^{1/2} P_{Au_A} e^{-b/RT} \right] \quad (7)$$

(AA) is the concentration of pairs of A atoms in the act of colliding with each other and (Au) is the concentration of A and u particles in the

act of colliding with each other. The steric factor P_{AA} • u is a measure of the efficiency of u as an absorber of energy and momentum from a pair of A atoms, while $P_{Au,\ A}$ is similarly a measure of the "third body efficiency" of u when u is in collision with an A atom and they collide with another A atom. The energies involved in the collisions must be greater than the activation energies a and b, for the reaction to occur.

The concentrations (AA) and (Au) were considered to be equal to the rate at which collisions occur multiplied by the mean duration of a collision. This leads to the expressions:

$$(AA) = \tau_{AA}\,(A)\,(A)\,\sigma_A^{\,2}\,(2\pi RT)^{1/2}\left(\frac{2}{M_A}\right)^{1/2} \qquad (8)$$

and $$(Au) = 2\tau_{Au}\,(A)\,(u)\left(\frac{\sigma_A+\sigma_u}{2}\right)^{2}(2\pi RT)^{1/2}\left(\frac{M_A+M_u}{M_A}\frac{}{M_u}\right)^{1/2} \qquad (9)$$

Wood's assumed values for the mean collision duration, $\tau = 6\times10^{-9} \times \left(\frac{\pi\mu}{8RT}\right)^{1/2}$ seconds and for the activation energies a = b = 0 (i.e., a and b were considered to be small compared with RT) were used. Experimental data give values for the steric factor P from 0.01 to 1. Wood's assumed value of 0.1 was used in our calculation.

Hydrogen

For hydrogen, both H and H_2 can act as third bodies and the recombination rate was computed using equations (7), (8), and (9), which reduce to

$$\frac{d\,(H_2)}{dt} = 10^{-36}\,n_H^{\,2}\,T^{1/2}\,(9.43\,n_H + 17.8\,n_{H_2})\ \frac{\text{molecules}}{\text{cm}^3\text{sec}} \qquad (10)$$

where the n's are the number densities.

Lithium Hydride

Above 1400°K an appreciable number of LiH molecules probably cannot exist (Ref. 37) and accordingly the rate of recombination of LiH would be very low above this temperature. For the present estimation only the recombination rate of the hydrogen liberated from the LiH dissociation reaction was computed. The available third bodies are H, H_2, and Li, and the rate equation becomes

$$\frac{d\,(H_2)}{dt} = 10^{-36}\,n_H^{\,2}\,T^{1/2}\,(9.43\,n_H + 17.8\,n_{H_2} + 18.8\,n_{Li})\ \frac{\text{molecules}}{\text{cm}^3\text{sec}} \qquad (11)$$

Ammonia

Ammonia decomposes readily at a few hundred degrees Kelvin. Since the gas in an arc-jet thruster is always at a temperature higher than this, there is little chance of achieving NH_3 recombination. However, recombination can occur in the reactions

$$H + H \longrightarrow H_2$$

and $$N + N \longrightarrow N_2$$

with H, H_2, N and N_2 acting as possible third bodies.

For ammonia the rate equations reduce to

$$\frac{d(H_2)}{dt} = 10^{-36} n_H{}^2 T^{1/2} (9.43 n_H + 17.8 n_{H_2} + 7.25 n_N + 18.0 n_{N_2}) \frac{\text{molecules}}{\text{cm}^3 \text{sec}} \quad (12)$$

and

$$\frac{d(N_2)}{dt} = 10^{-36} n_N{}^2 T^{1/2} (19.7 n_H + 41.8 n_{H_2} + 16.2 n_N + 31.7 n_{N_2}) \frac{\text{molecules}}{\text{cm}^3 \text{sec}} \quad (13)$$

The number densities were determined from the equilibrium constants given in Reference 38 according to the method outlined by Penner (Ref. 39).

Equations (10), (11), (12) and (13) are plotted in Figures 34 to 36 for a total mixture pressure of 0.1 atmosphere, in each case.

Pressure Dependence

The above stated equations show that recombination rate varies as the cube of pressure for an ideal gas ($p = nk T$).

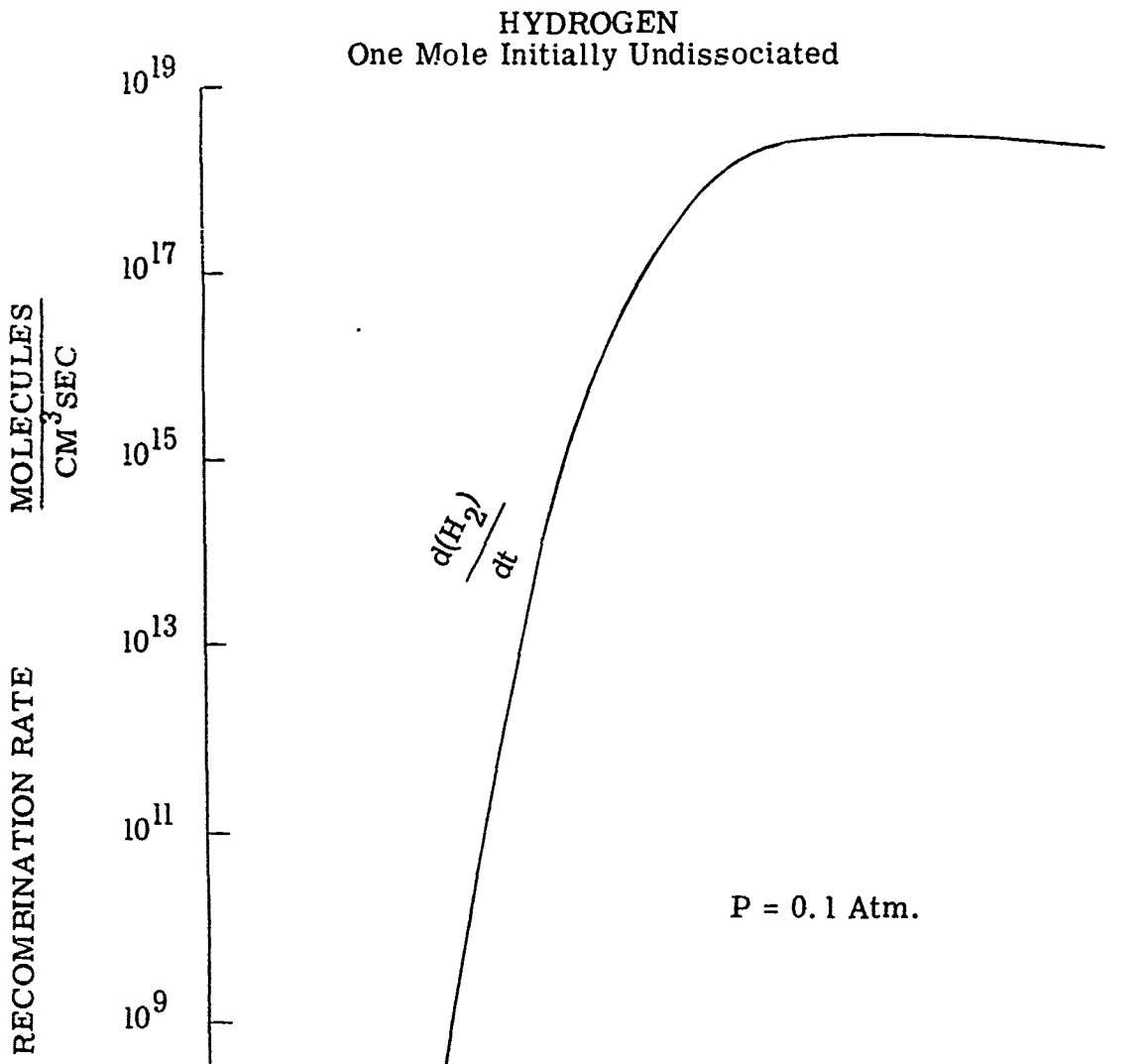
HYDROGEN
One Mole Initially Undissociated
MOLECULAR RECOMBINATION RATE
MOLECULES / CM³ SEC
10¹⁹
10¹⁷
10¹⁵
10¹³
10¹¹
10⁹
10⁷
10⁵
10³
d(H₂)/dt
P = 0.1 Atm.
1000
2000
3000
4000
5000
T° K

Figure 34

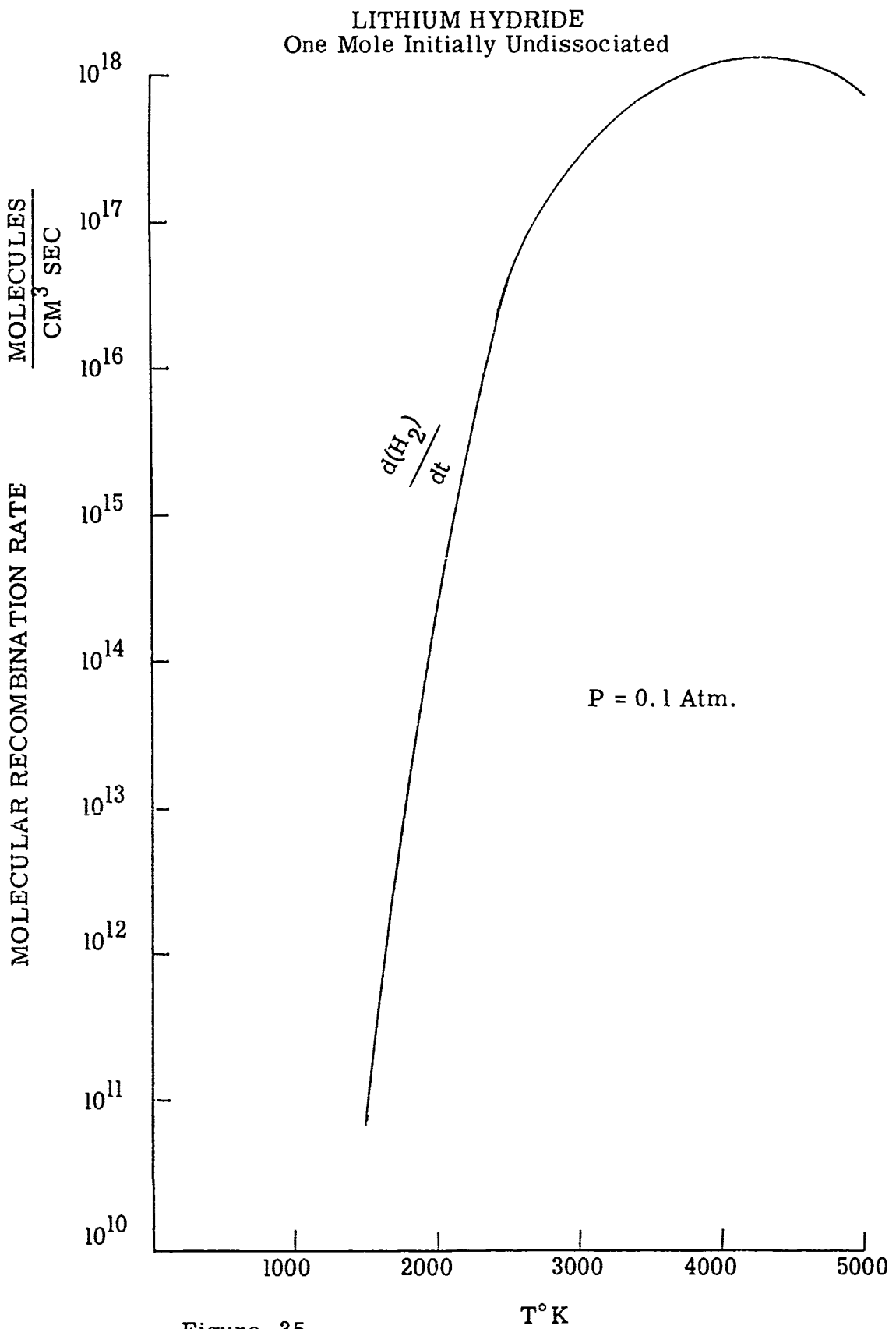
LITHIUM HYDRIDE
One Mole Initially Undissociated
MOLECULAR RECOMBINATION RATE
MOLECULES / CM³ SEC
10¹⁸
10¹⁷
10¹⁶
10¹⁵
10¹⁴
10¹³
10¹²
10¹¹
10¹⁰
d(H₂)/dt
P = 0.1 Atm.
1000
2000
3000
4000
5000
T°K

Figure 35

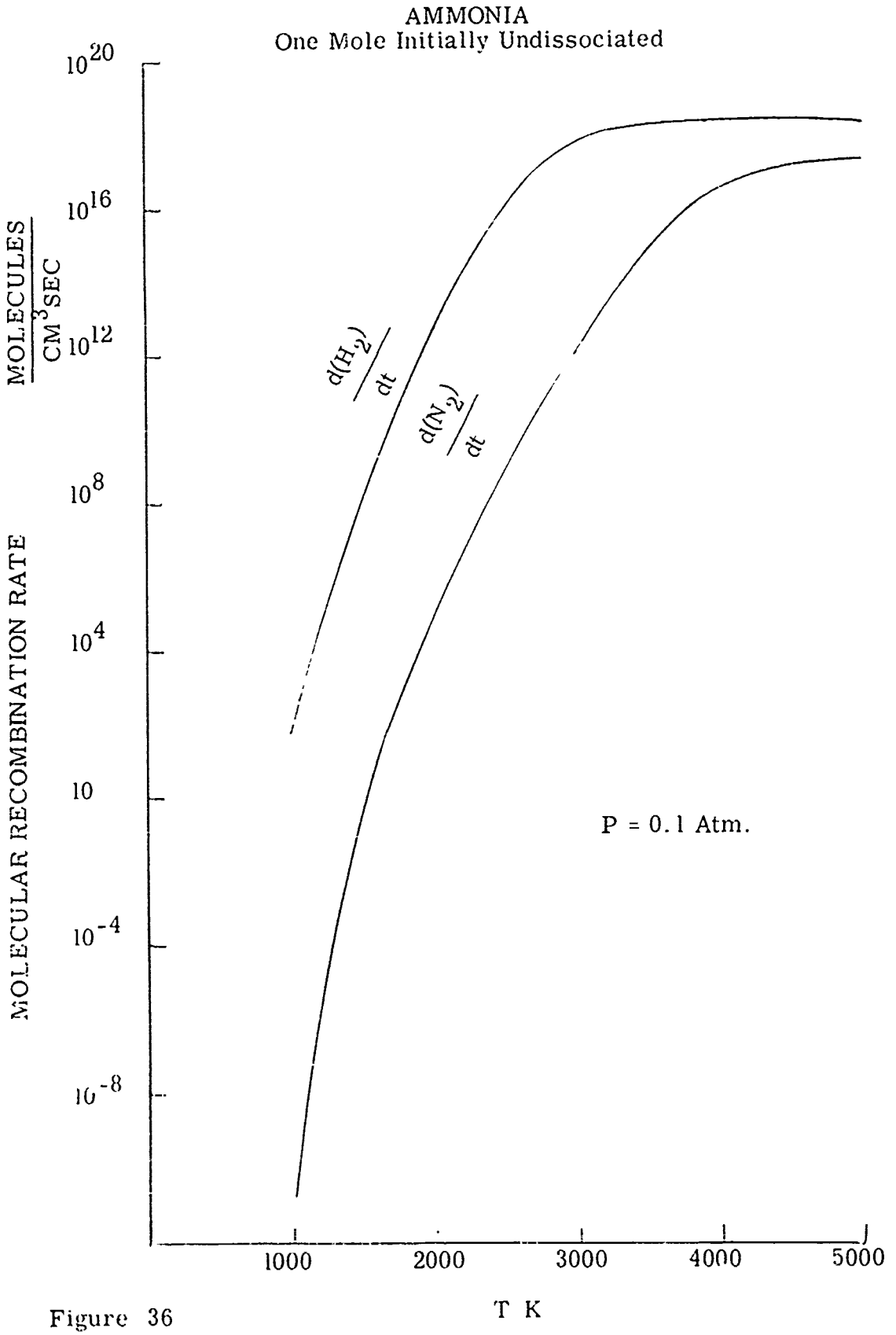
AMMONIA
One Mole Initially Undissociated
MOLECULAR RECOMBINATION RATE
MOLECULES / CM³ SEC
10^20
10^16
10^12
10^8
10^4
10
10^-4
10^-8
d(H2)/dt
d(N2)/dt
P = 0.1 Atm.
1000
2000
3000
4000
5000
T K

Figure 36

RECOMBINATION IN NOZZLE FLOW

General

If the time required for the flow in a rocket nozzle to achieve equilibrium is of the same order of magnitude as the time for a typical particle to pass through the nozzle, then deviation from equilibrium is likely. Conversely, if the equilibrium time is orders of magnitude less than particle flight time, equilibrium may be approached in the nozzle. If equilibrium is approached and the energy recovery associated with the recombination processes represents a significant portion of the total change in gas enthalpy (from entrance to exit), then the thrust can be expected to increase.

For diatomic molecules,

$$t = \frac{1/2 n_A}{\frac{d(A_2)}{dt}} \qquad (14)$$

where t is the time required for recombination of all the atoms (of a particular type) in a unit volume, n_A is the number density of the atoms and $\frac{d(A_2)}{dt}$ is the volumetric recombination rate. If the variation of n_A and of $\frac{d(A_2)}{dt}$ is known in a nozzle flow, the recombination time as a function of nozzle length or area ratio can be estimated.

Particle flight time can be determined by measuring the area under a curve of reciprocal velocity versus nozzle axial distance. Since we are concerned with orders of magnitude of time, such a computation seems to be of undue refinement. A simple estimation of flight time based on the assumption that

$$t_{flight} = \frac{x}{v_{avg}} \quad ; \quad v_{avg} = \frac{v_{exit}}{2}$$

is in order.

Seeding

Molecular recombination rate increases with an increase in the number and size of the third bodies present. Accordingly, foreign particles placed in the nozzle flow may conceivably increase thrust, if the diameter of these particles is much greater than that of the atoms and molecules in the system.

For hydrogen, the recombination rate with foreign third body injection is

$$\frac{d(H_2)}{dt} = \left[\frac{d(H_2)}{dt}\right]_o + 1.52 \times 10^{-5}\, T^{1/2} n_H^2 n_u \left[1.77 \times 10^{-16}\sigma_u + 1/2\sigma_u^4 \left(\frac{1}{M_u}\right)^{1/2}\right] \quad (15)$$

where $\left[\frac{d(H_2)}{dt}\right]_o$ is the recombination rate without seeding, σ_u is the foreign particle diameter, $\sigma_u >> {}_H$ and M_u is the mass of one foreign particle. Inspection of equation (15) indicates that the recombination rate will increase with: an increase in foreign particle concentration and diameter, and a decrease in its mass.

Estimation for Typical Thruster Flow

An estimation was made (see Figs. 37 & 38) of equilibrium time with and without seeding, and particle flight time for two different chamber conditions (1.0 and 10 atmosphere pressure and 3000°K) for hydrogen. The chamber conditions chosen correspond to an impulse of about 1000 seconds. Equilibrium time and time for all atoms to recombine are essentially the same for a nozzle exit area ratio of 100, for the given example. The seeding material considered was one micron diameter graphite particles at a concentration of 10^9 cm^{-3}. The changes in enthalpy for hydrogen in equilibrium flow from chamber to exit at $A/A^* = 100$ for the two cases (1.0 and 10 atmospheres chamber pressure) are about 15,000 and 10,000 calories per gram, respectively. If equilibrium were achieved within the nozzle the energy release would be about 20,000 and 9,000 calories per gram of gas, respectively. Therefore, if equilibrium were attained a considerable increase in thrust would be obtained.

The conclusions drawn from this estimation are:

(1) For hydrogen at an I_{sp} of 1000 seconds and chamber conditions of one atmosphere pressure and 3000°K, significant recombination probably will not occur in a typical arc-jet thruster, with or without seeding. (The same conclusion would be obtained even if the seed concentration and particle size were at practical high limits.)

(2) At ten atmospheres chamber pressure and I_{sp} of about 1000 seconds, significant recombination may take place, with seeding, if the nozzle length is of the order of one foot.

Conclusions on Recombination

1. A reliable evaluation of the recombination characteristics of propellants must be based on experimental measurement.

2. The possible contribution to thrust from recombination of dissociation products is roughly the same for H_2, LiH and NH_3, per mole of initially undissociated propellant. On this basis hydrogen is of course superior because of its low molecular weight.

3. It is unlikely that significant recombination will take place in an arc thruster nozzle unless foreign third body seeding is used in conjunction with high pressure operation ($\sim$ 10 atmospheres chamber pressure).

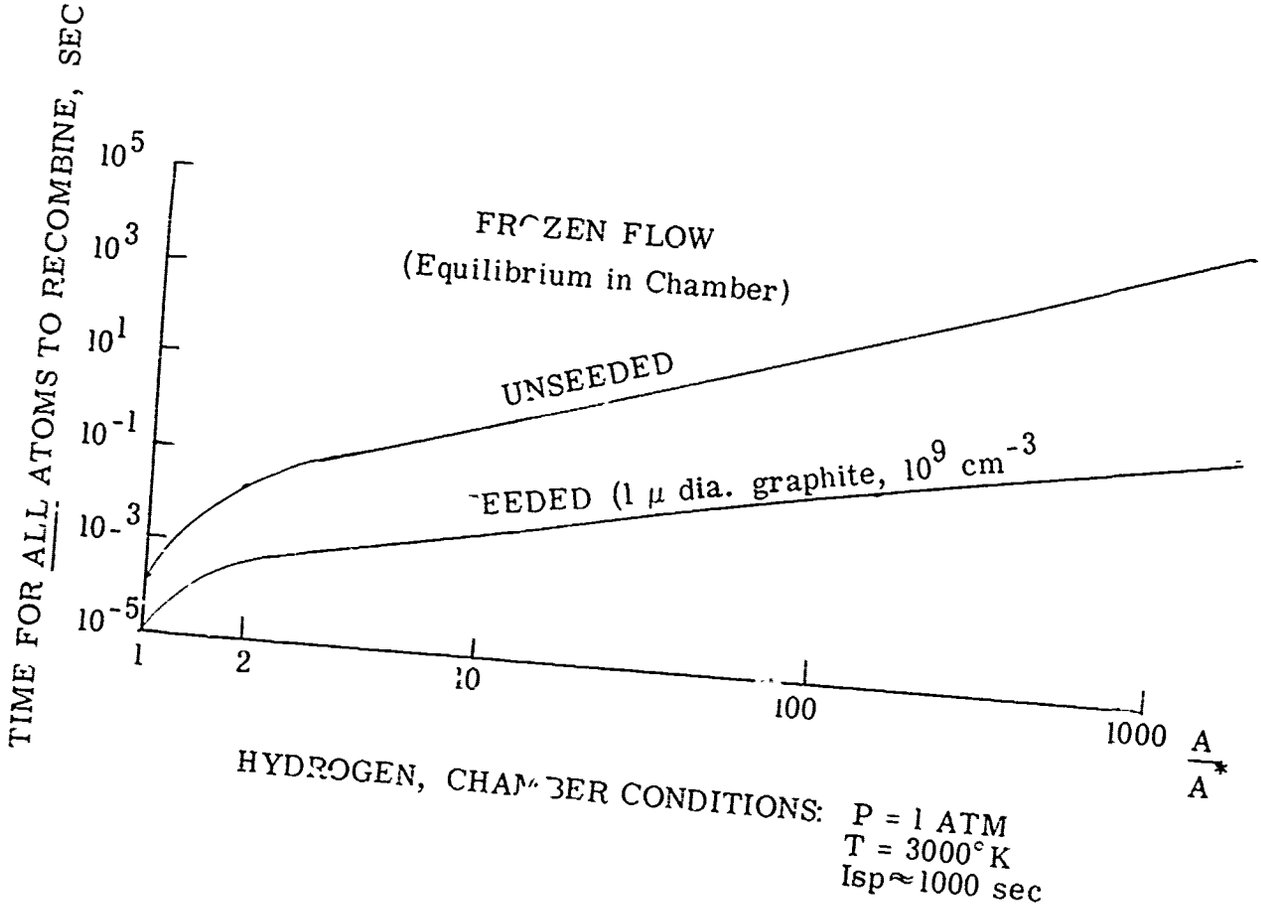
TIME FOR ALL ATOMS TO RECOMBINE, SEC
10^5
10^3
10^1
10^{-1}
10^{-3}
10^{-5}
FROZEN FLOW
(Equilibrium in Chamber)
UNSEEDED
SEEDED (1 μ dia. graphite, 10^9 cm^{-3}
1
2
10
100
1000
A/A*
HYDROGEN, CHAMBER CONDITIONS: P = 1 ATM
T = 3000° K
Isp ≈ 1000 sec

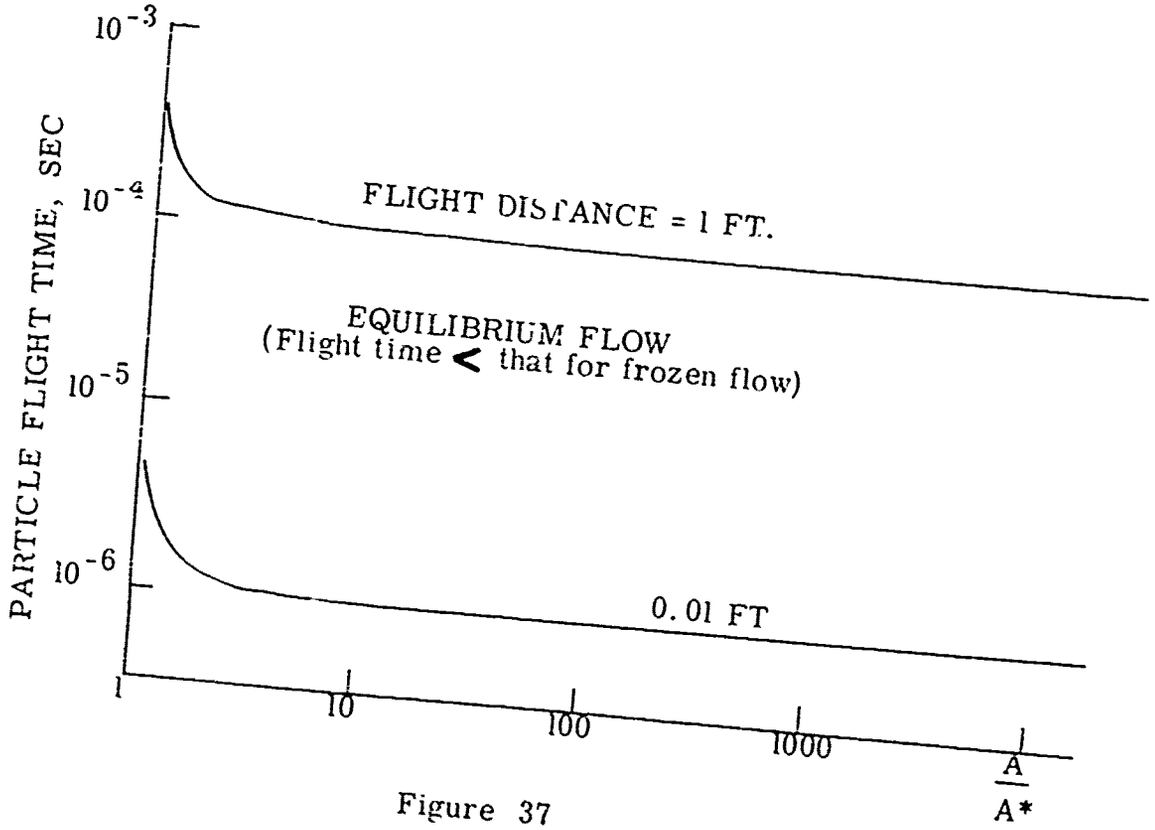
PARTICLE FLIGHT TIME, SEC
10^{-3}
10^{-4}
10^{-5}
10^{-6}
FLIGHT DISTANCE = 1 FT.
EQUILIBRIUM FLOW
(Flight time < that for frozen flow)
0.01 FT
1
10
100
1000
A/A*

Figure 37

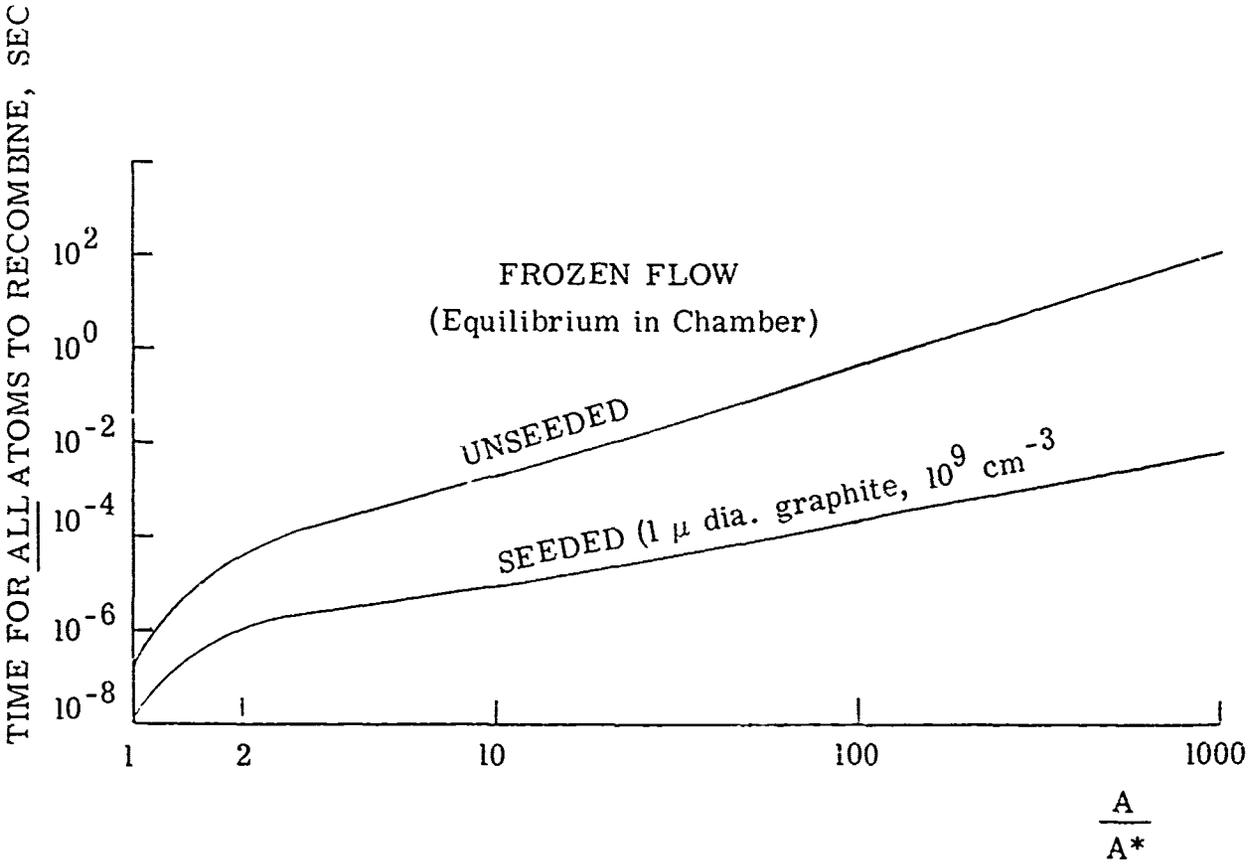

HYDROGEN, CHAMBER CONDITIONS: P = 10 ATM
T = 3000° K
Isp ≈ 1000 sec

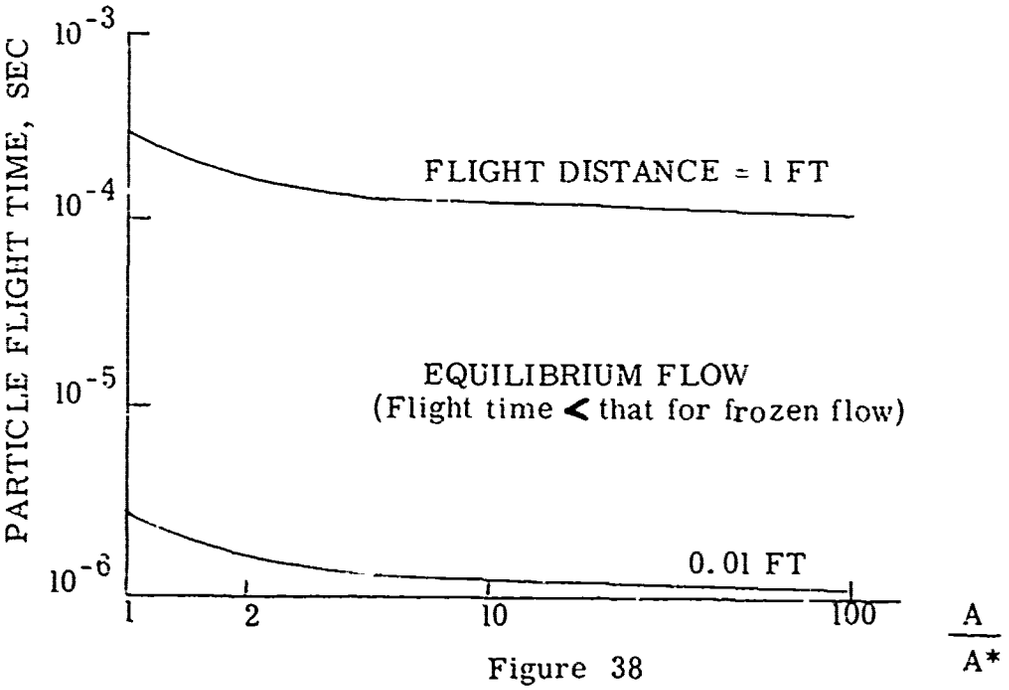

Figure 38

RECOMBINATION EXPERIMENTS

The recombination of hydrogen in nozzle flow has been studied recently at Plasmadyne (NASA Contract No. 8-844).

An arc generated hydrogen plasma was expanded through a water-cooled mixing chamber and converging-diverging nozzle with a conical exit section. Six groups of sapphire windows were located in the side wall of the nozzle, equally spaced along the nozzle axis. In addition, static pressure taps were integrated with each group of windows. A schematic diagram of the apparatus set-up is shown in Figure 39. Two measurements were made at each axial station of the nozzle, static pressure and degree of dissociation.

Pressure Measurements

The static pressure was measured using simple U-tube manometers. One side of each manometer was connected to a fore pump which can evacuate to a pressure of the order of 10 microns of mercury. For such an arrangement the pressure measurement error was estimated to be less than 2 per cent.

Spectrographic Measurements

Spectroscopy was used to identify the species present in the flow. The ratio of the intensity of a hydrogen atomic line to that of a hydrogen molecular spectrum was measured and used to obtain the degree of dissociation.

This method is based chiefly on three assumptions. (1) the partition function is a constant, (2) the upper energy levels of the molecular and atomic species of interest are equal and (3) the portion of the plasma on which the spectrograph is focussed is in local thermodynamic equilibrium.

The partition function Z depends on temperature. But for a moderate temperature range such as that present in this experiment (2000° - 6000° K.), Z can be considered a constant and can be computed by summing over the ground states only.

The spectral lines used to determine α were the H_δ line (4101.735Å) and the hydrogen molecular line at 5615.6Å. These two species have upper energy levels of 13.154 e.v. and 13.191 e.v. respectively. The measured intensities were corrected for self-absorption by the plasma. For given operating conditions the intensity of line radiation is the most important factor in determining the degree of self-absorption.

The self-absorption was determined as follows: A concave mirror was placed so that the plasma was between the mirror and the spectrograph. Then intensity measurements were made both with and without the mirror in place. The absorption coefficients were then computed using the following relation:

$$I = I_o e^{-ad}$$

Where I_o is the intensity of the emitted radiation, I is the intensity after some absorption, d is the distance the radiation travels through the absorbing medium, and a is the absorption coefficient.

The experimental data were compared with the theory of K. N. C. Bray (Ref. 41), which is based on the quasi one-dimensional inviscid isentropic flow of an ideal dissociating gas. See Figure 40. Bray's theory is probably not applicable to our case because viscous effects in our nozzle may have been great and the flow was obviously non-isentropic. However, the degree of dissociation did decrease by more than one order of magnitude between the nozzle throat and exit, according to the spectral measurements. The data therefore at least indicate that the flow was approaching equilibrium (not frozen) as it progressed out the nozzle.

Future experiments will be performed using nozzles with improved cooling systems (for example, the portions of the nozzle upstream and downstream from the throat will be separately cooled to simplify analysis) higher expansion rates and increased gas flow rates. Viscous effects will thus be decreased. The viscous effects will be studied by means of radial survey measurements of various gas dynamic properties. The effects of seeding on recombination and on plasma electrical conductivity will also be examined.

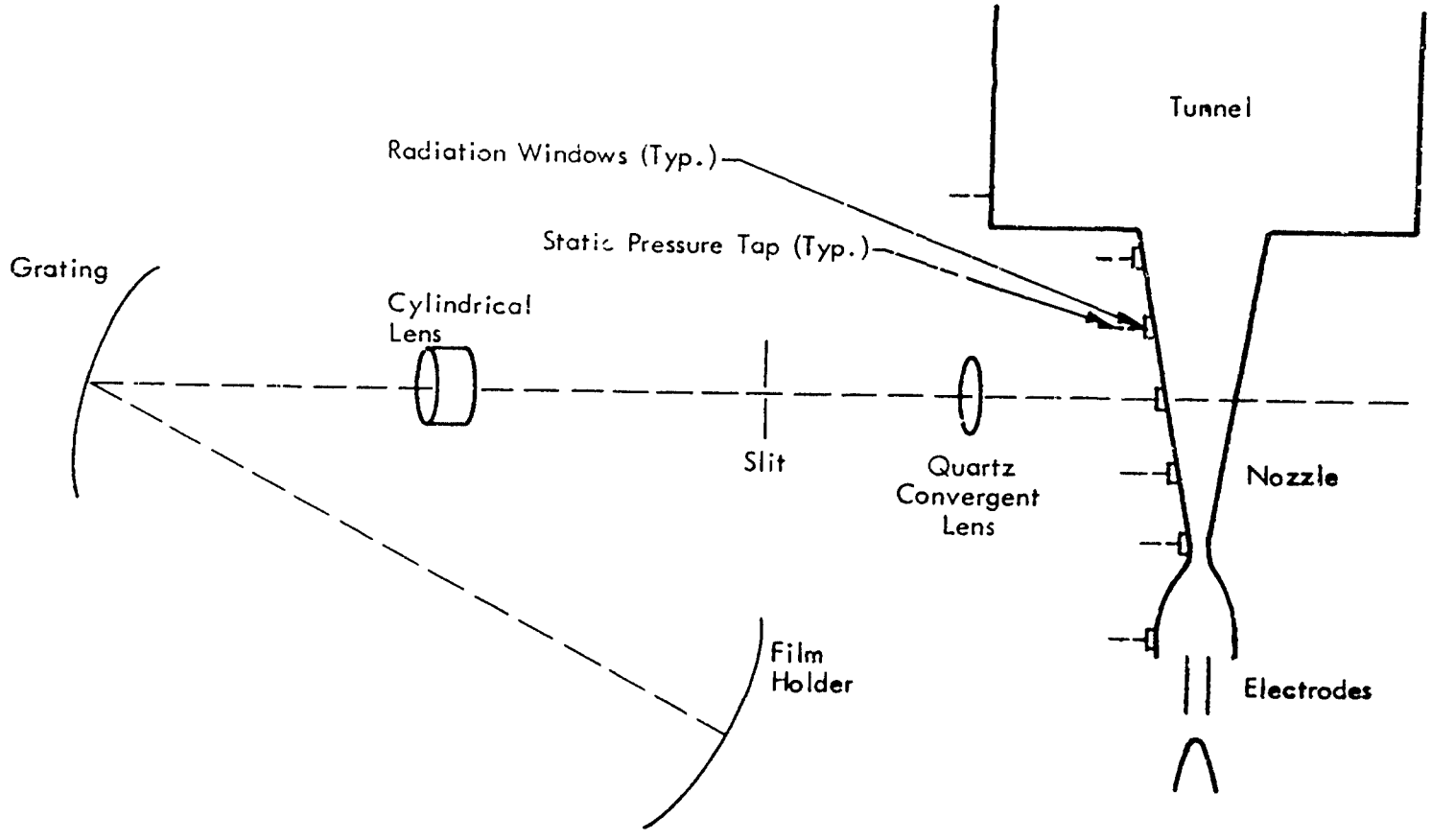

Figure 39 SCHEMATIC OF RECOMBINATION EXPERIMENTAL APPARATUS

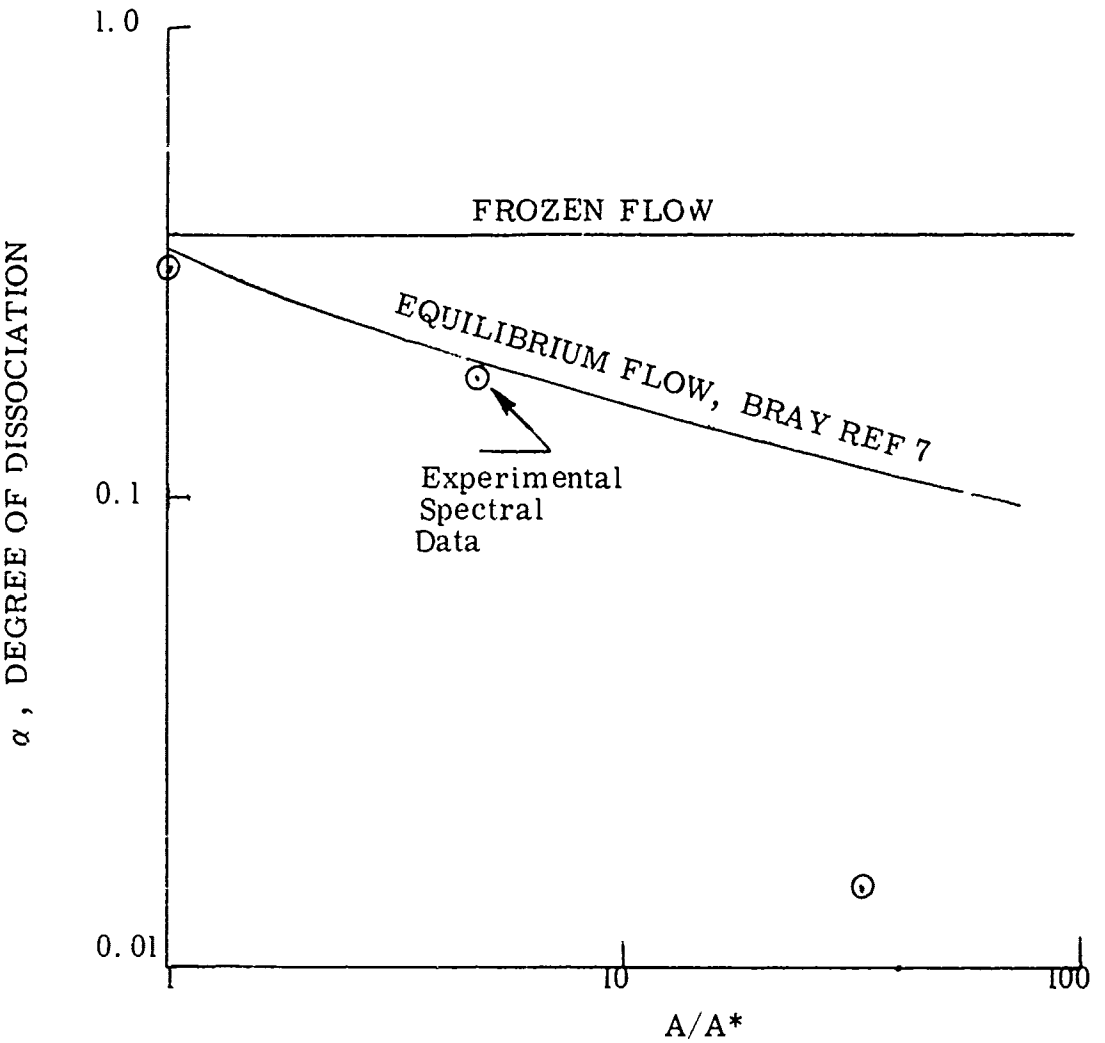

HYDROGEN NOZZLE FLOW

MIXING CHAMBER CONDITIONS: P_o = 20 cm Hg

H_o = 60,000 BTU/lb

α_o = 0.37

Figure 40

Measurement Made on NASA Contract No. 8-844

HEAT TRANSFER PROBLEMS

The heat transfer analysis of an arc-jet engine can be quite extensive. The performance of the entire engine is very closely related to heat transfer phennomena. The arc itself transfers heat into the incoming propellant by convection and radiation. It also radiates to the chamber and tunnel walls and to the surroundings. Concentrated heat loads are transferred to the electrodes from the anode and cathode arc fall regions. The hot plasma transfers heat by convection to the throat and nozzle walls and also loses energy to the surroundings by radiation. The engines are usually cooled by radiation from the external body and also the situation is complicated in most cases by regenerative cooling systems. In this section a few of these problems will be briefly discussed.

Thermal and Viscous Losses (Taken in part from Ref. 43)

The strong influence of Reynolds number on heat transfer and viscous losses may be illustrated by a simple model where the nozzle is sufficiently long that equilibrium temperature and velocity profiles may be assumed as in pipe flow. Usually only the liminar flow case is considered since it is in the low Reynolds number regime where losses are most severe. Most of the arc engine nozzle designs fall in low Reynolds number regime and laminar flow is expected in the nozzle. This is true at both high and low powers when high specific impulse operation is required. An examination of Figure 41 shows that for a 300 KW, 2000 second engine the nozzle throat Reynolds number is only 1500 at an arc chamber pressure of one atmosphere. Plasmadyne's one KW engine operates at a Reynolds number of 400. This low number is because of the high viscosity, and thermal conductivity associated with these high gas temperatures.

For the case discussed the viscous loss ratio can be expressed

$$\frac{\text{Viscous loss rate}}{\text{Kinetic Energy rate}} = \frac{64\,\frac{L}{D}}{R_e}$$

while the heat transfer loss ratio may be written

$$\frac{\text{heat transfer loss rate}}{\text{energy input rate}} = 17.5\left(\frac{L}{D}\right)\left(1 - \frac{T_{wall}}{T}\right)\frac{1}{R_e P_r}$$

where

(L/D) = Length to Diameter ratio
R_e, P_r = The Reynolds and Prandtl numbers
T = Temperature

In both cases the percentage loss varies inversely as Reynolds number. For short nozzles a better model might be one considering a thin boundary layer building up as it does on a flat plate. In this case, the percentage losses vary inversely as the square root of the Reynolds number. For the scale of thermal losses shown in Figure 41 an intermediate case is assumed where losses vary inversely as the three fourths power of the Reynolds number. This scale only indicates trends. The viscous losses have been found approximately equal in magnitude to the thermal losses for the simplified cases that have been calculated.

Radiation Heat Loss

In addition to the convective heat loss discussed above, heat is also lost from the gas to the nozzle and arc chamber walls by radiation. There are two types of radiation which must be considered, continuum radiation and line radiation. The continuum radiation is caused by the encounters of electrons and ions and is so named because the energy distribution is a continous function of frequency and therefore yields a continuous spectrum. It includes both Bremsstrahlung (caused by free encounters in which the electron is not captured by the ion) and recombination radiation (caused by free-bound encounters in which the electron is captured by the ion). The line radiation, by comparison, is a result of the transition of bound electrons between various discrete energy levels, resulting in a line spectrum. Determining the total energy radiated from the plasma then consists of determining the sum of the continuum and line contributions. Continuum has been investigated by many authors.

Reference 44 contains a fairly complete summary for hydrogen. The result for the Bremsstrahlung radiation is that the radiated power per unit volume is proportional to the product of the electron number density times the ion number density times the square root of the temperature. It should be noted that this is also proportional to the number of collisions per unit time and volume since the mean velocity of an electron is proportional to the square root of the temperature and therefore for a given mean free path (number density) the frequency of collisions is proportional to the velocity.

The Bremsstrahlung radiation flux out of the surface of a 1 cm diameter cylinder is shown for a fully ionized gas in Figure 42. These curves are, of course, only valid for pressures and temperatures at which the gas is fully ionized. At lower temperatures these curves should be modified to account for the lower ionization fraction. These lines then represent the upper limit of radiation from a fully ionized hydrogen plasma. They have a negative slope because they were calculated for constant pressure and therefore as the temperature increased the number density must decrease. Since, for a fully-ionized gas, the radiation is proportional to the square of the number density, and the temperature to the one-half power the radiation per unit volume varies inversely with the three halves power of temperature.

It should be pointed out that these curves also neglect re-absorption of the radiation which, if included in these calculations, would result in a curve which fairs into the black body limit shown on Figure 42. The calculation, if re-absorption were included, would yield a result somewhat as shown in the dotted line labeled B, depending on the pressure and per cent ionization. Unfortunately, the contribution of the line radiation is more difficult to analyze. The general form of the result, including line radiation as well as recombination radiation, is suggested by dotted line A. At the present time it appears that losses due to continuum radiation will not be large for designs with an arc chamber pressure of one atmosphere. However, losses will increase with increasing pressure, although only as the square root of pressure because the volume radiating is being reduced for constant mass flow. Before final conclusions can be reached, it will be necessary to evaluate the line radiation in this temperature range.

The above discussion is only a brief description of the heat transfer evaluation in the arc engine. A great deal of analysis in this field is required to acquire a full understanding of the interrelation of the various heat transfer processes.

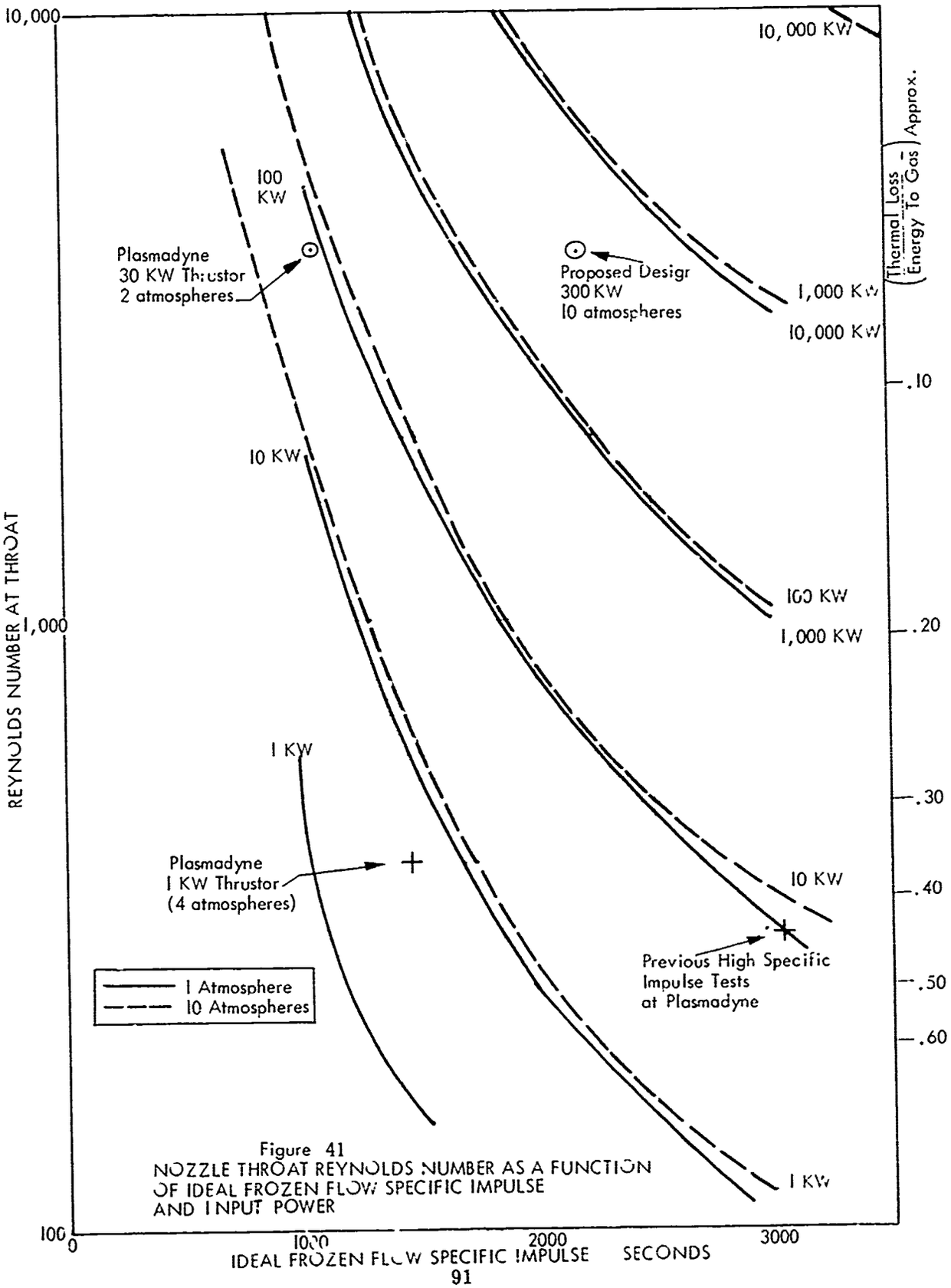

Figure 41
NOZZLE THROAT REYNOLDS NUMBER AS A FUNCTION OF IDEAL FROZEN FLOW SPECIFIC IMPULSE AND INPUT POWER

Figure 42

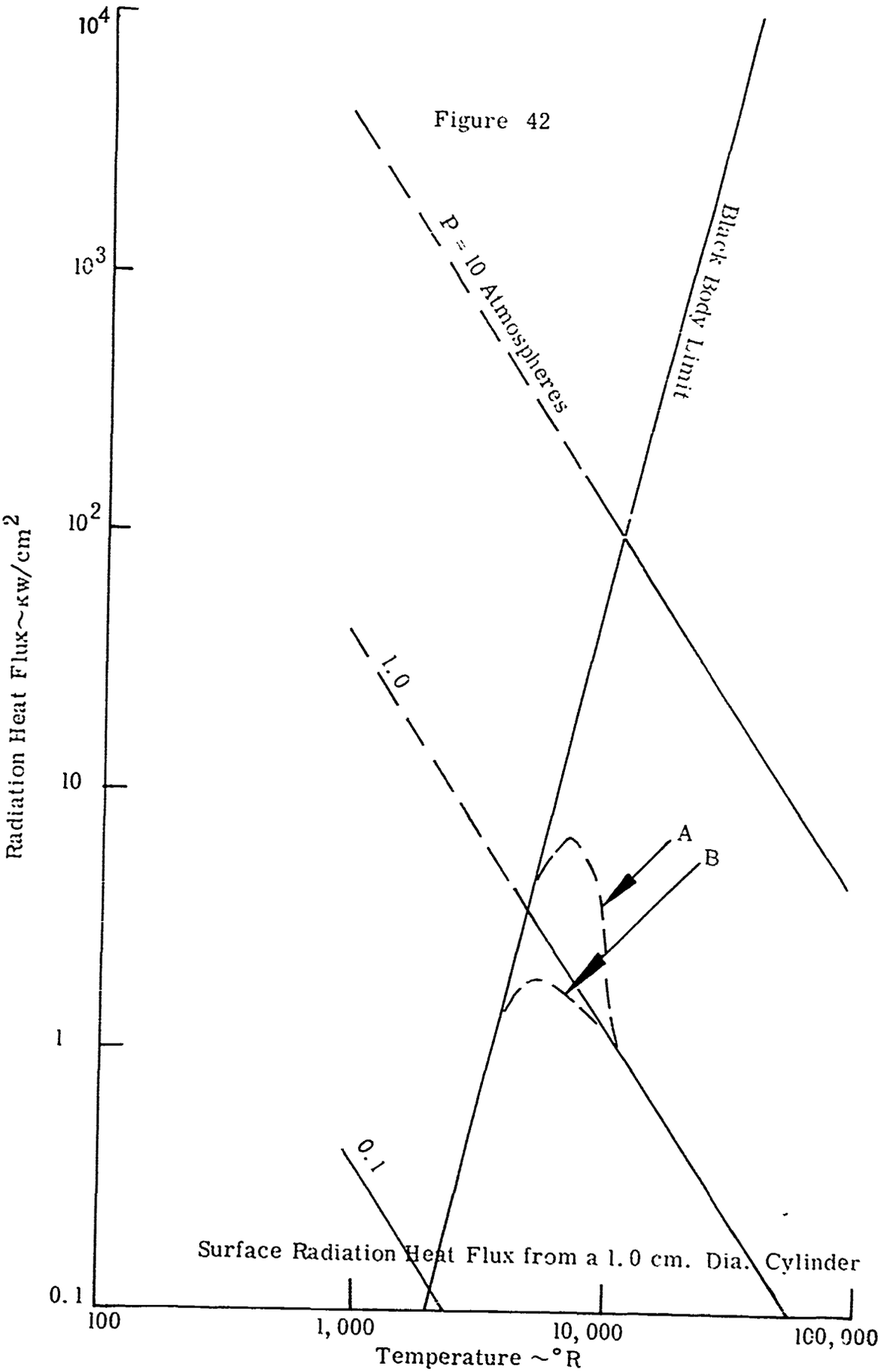
Radiation Heat Flux ~ kw/cm²
10⁴
10³
10²
10
1
0.1
P = 10 Atmospheres
Black Body Limit
1.0
0.1
A
B
100
1,000
10,000
100,000
Temperature ~ °R
Surface Radiation Heat Flux from a 1.0 cm. Dia. Cylinder

THE EFFECTS OF PRESSURE

The effects of chamber pressure on the arc-jet engine operating mode are quite extensive. The various factors which are dependent on pressure have been discussed, somewhat, in many other sections of this report. Here they will be listed to illustrate the importance of this parameter. The discussion as it pertains to the different propellants would be quite lengthy. If one were examining an engine using a particular propellant, optimum designs could only be achieved by making a complete system survey on the effects of pressure variation. Pressure variations effect the following factors:

1. The degree of dissociation and ionization decrease with increasing pressure all else being equal.

2. Conductivity - since the conductivity varies roughly with the degree of ionization - conductivity would decrease for increases in pressure.

3. Frozen flow efficiency - for a given specific impulse, the frozen flow efficiency would increase with increases in pressure.

4. Recombination of particles in the nozzle tends to increase greatly with increase of chamber pressure.

5. Sputtering - The amount of electrode material loss due to sputtering would decrease slightly with greater pressures.

6. Vaporization of the hot metal electrodes and nozzle would tend to decrease as the pressure were raised.

7. The Reynolds Number in the nozzle will increase as the pressure.

8. The viscous loss rate and the heat transfer loss rate will decrease as the Reynolds number is increased and Reynolds number varies with pressure.

9. The radiation heat loss increases as the temperature and pressure.

10. The initiation of the arc will be altered by increases of the pressure. For a given starting voltage the minimum electrode gap will be decreased as pressure is increased.

From the above, it would seem that any increase in pressure would lead to higher performance and longer operating life. Experience to date on arc-jet engine tests has shown this to be true. However, at very high pressure the radient heat loss, it is believed, becomes quite significant. This leads to the conclusion that for each engine geometry, power, flow rate, and propellant there is an optimum pressure to use for best performance.

THE USE OF MISSION STUDIES IN PROPELLANT EVALUATION

The final choice of a propellant will depend on the mission which is being considered. The following mission characteristics should be taken into account in making a selection:

1. Desired Duration of the Mission

The urgency of completing a mission varies widely and depends on such factors as the competitive nature of the mission's purpose; the life of essential equipment, such as the power supply, possible radiation or meteorite damage, the effect of thrust level on the *characteristic velocity needed for performance of the mission, whether or not the vehicle is manned, and, in some cases, timing of the movement of other vehicles or bodies involved in the mission. If the mission must be of short duration, the tendency will be to choose a propellant which provides good performance in a low or moderate specific impulse range so that higher thrust levels may be attained. The storability of a propellant will, of course, be of less importance for shorter missions. Both the operating time and the total mission time including waiting and coasting periods must be considered since one is of importance with regard to power plant life and the other with regard to the propellant storage problem. For a round trip, it may be advantageous to use a cryogenic propellant for the first portion of the mission, and a storable propellant for the return leg.

2. The Vehicle Size

The size of the vehicle affects the propellant choice in several ways. First, it affects the thruster performance. In general, in the larger sizes the losses are reduced and this makes it feasible to operate at a higher specific impulse with a given propellant. Thermal losses and viscous losses are both reduced as size increases; and, if the thruster is large enough, it becomes reasonable to expect some recombination in the nozzle (particularly with high arc chamber pressure). The use of high arc chamber pressure with a cryogenic propellant becomes more practical in large sizes because it becomes reasonable to incorporate cryogenic gas pressurization equipment and liquid metal cooling systems, both of which appear to be necessary if the full advantage of high arc chamber pressure is to be realized.

---

* The characteristic velocity for performance of a mission is herein defined as the ratio of thrust to total vehicle mass integrated over the duration of the mission.

Secondly, the size of the vehicle affects the power plant weight to power ratio. On the basis of present plans, it appears that much more favorable weight to power ratios will be available in the high power ranges. This means that large vehicles will be able to operate at higher specific impulses without too severe a cost in operating time, since the necessary power for high thrust with high specific impulse can be made available. In these cases, a propellant which gives good performance at high specific impulses should be selected.

Finally, the size of the vehicle affects the propellant storage problem, particularly for cryogenic propellants. For example, if we examine the cryogenic storage tank for a one kilowatt arc-jet engine and a one megawatt arc-jet engine (holding other factors the same) the following comparison results:

Ratio of powers (10^6 to 10^3)	1000 to 1
Ratio of propellant masses	1000 to 1
Ratio of tank surface areas	100 to 1
Ratio of practical insulation thicknesses (Fixed ratio of insulation mass to propellant mass)	10 to 1
Ratio of evaporation rates	10 to 1
Ratio of practical storage times	100 to 1

Since the practical storage time for the one megawatt size is roughly 100 times as great as for the one kilowatt size, the storage of cryogenic propellants clearly becomes a much less severe problem as size increases. Cryogenic propellants can be particularly advantageous in the large size ranges.

3. The Orbit Requirements

The total characteristic velocity which the engine must be capable of providing during the mission is a function of the vehicles destination and the time available for travel. A number of approximate solutions (see for example Ref. 45) have been made for determining the characteristic velocity required for spiraling out into desired orbits. In addition, Reference 46 gives machine solutions for a systematic family of spiral paths into orbit. When the characteristic velocity has been summed for all of the powered portions of the mission, the required propellant mass can be determined from the rocket equation:

$$\log_e \frac{M_{initial}}{M_{initial} - M_{propellant}} = \frac{V_c}{I_{sp} g}$$

To avoid having the propellant mass an unreasonably large fraction of the total mass, it is necessary to increase the specific impulse as characteristic velocity increases. Thus, propellants suitable for high specific impulse should be favored for missions requiring large characteristic velocities.

Due to the large number of variables involved, a general study has not been made to indicate the best propellant choice for any particular mission. In making an evaluation for a specific mission, the following procedure could be followed:

1. Choose a number of propellants and a range of specific impulses for each propellant.

2. For each combination of propellant and specific impulse choose a number of power levels and find corresponding power supply weights.

3. For each point (that is, each combination of propellant, specific impulse, and power level), estimate losses in the thruster and determine thruster efficiency and the thrust level.

4. For each point, calculate the powered orbits needed to perform the mission and determine the required characteristic velocity and mission duration.

5. For each point, calculate the propellant weight required using the rocket equation and estimate the tank weight including sufficient insulation to store propellant for the duration of the mission.

6. For each point. estimate the weight of power conversion equipment, the propellant metering system, thruster control equipment, the thruster itself, and structure related to the propulsion equipment.

7. For each point, determine the gross payload weight defined as total initial vehicle weight minus the weight of propulsion related equipment and propellant.

8. Plot the ratio of total initial vehicle weight to gross payload weight as a function of mission duration, and draw an envelope under the resulting family of curves. Since both of these parameters (payload weight ratio and mission duration) are of primary importance, the design selected should lie close to the envelope and be near a "knee" in the envelope curve that represents a reasonable compromise between the desire for a high payload weight and a short mission duration.

The family of curves resulting from the above procedure will indicate preferred propellants since the curves for the most desirable propellants will be close to the envelope in the region of interest. Figures 43 and 44 show two families of curves obtained in this manner but using simplifying assumptions. The curves are for illustration purposes only. Figure 43 is for a one way trip to the moon while Figure 44 is for a round trip to the moon. Only curves for hydrogen are shown. The following simplifying assumptions are involved:

1. The power supply weight factor is taken as 10 pounds per kilowatt for all power levels considered.

2. The thruster efficiency is taken as equal to the ideal frozen flow efficiency for each specific impulse considered.

3. Orbits were estimated using the approximate method outlined in Reference 45. Resulting characteristic velocities and coast times are shown in Figure 45 as a function of thruster operating time.

4. The propulsion system weight is assumed to consist of power supply weight and propellant weight only. The weight of other equipment is neglected.

An interesting result of this calculation is that the 1500 second curve does not touch the envelope because of the reduced frozen flow efficiency occurring in this specific impulse range.

Although a general study using the procedure outlined and carrying a range of mission types would be a major undertaking, an abreviated study covering a few selected missions would be a worthwhile guide to future arc-jet development work.

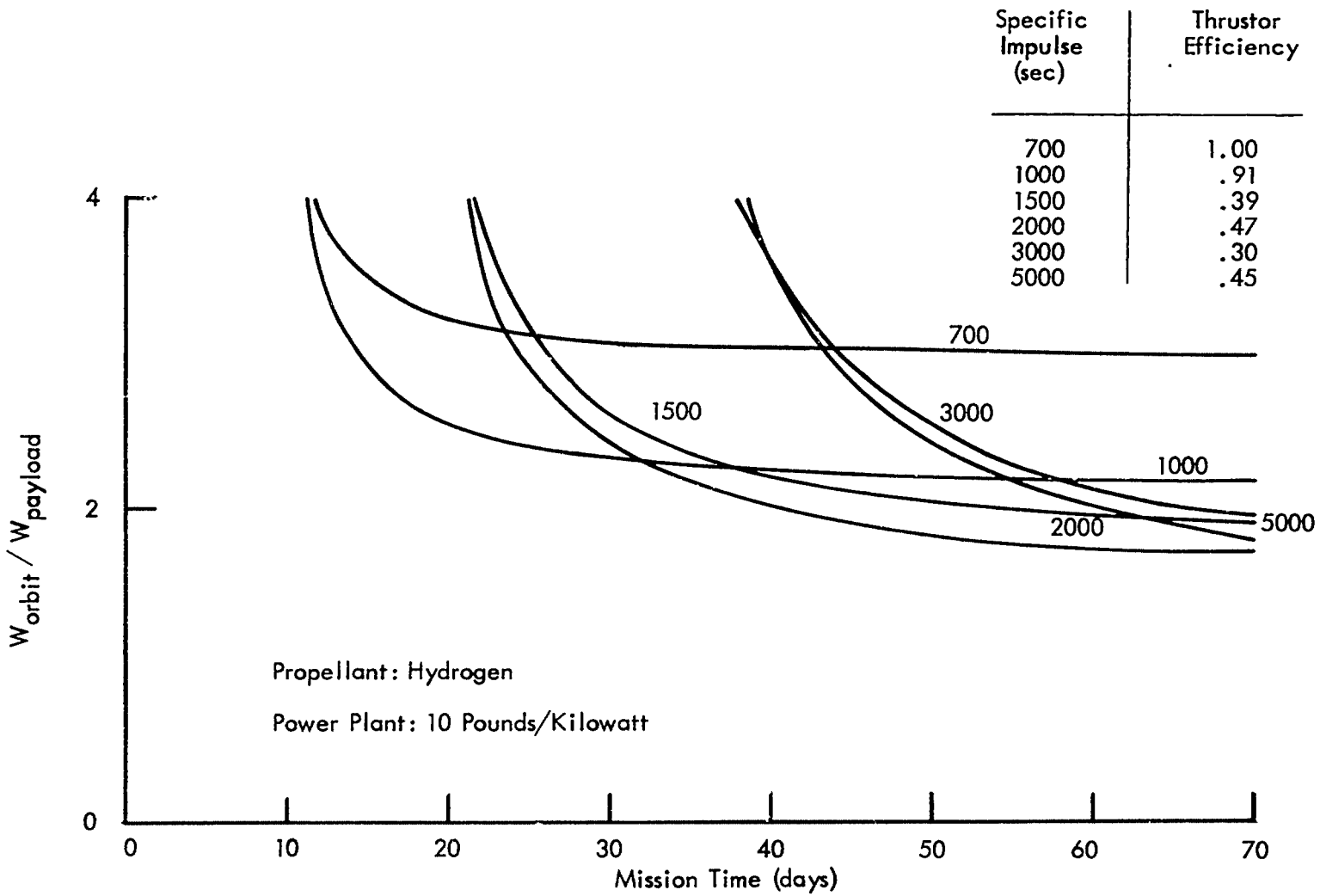

Figure 43 IDEALIZED VEHICLE PERFORMANCE FOR A ONE WAY TRIP TO THE MOON USING A THERMAL ARC JET THRUSTOR (Minimum Energy Orbits)

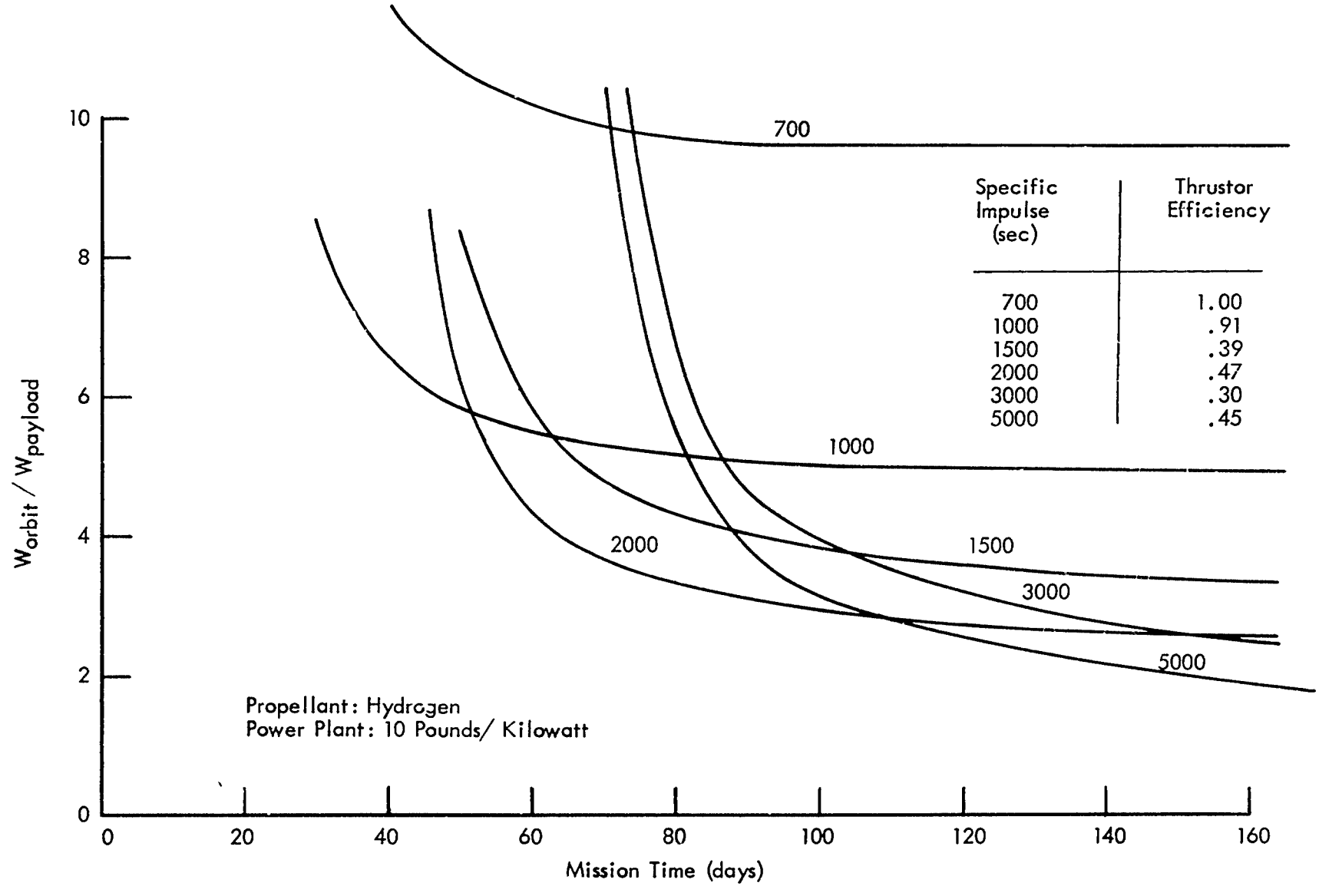

Figure 44 IDEALIZED VEHICLE PERFORMANCE FOR A ROUND TRIP TO THE MOON USING A THERMAL ARC JET THRUSTOR (Minimum Energy Orbits)

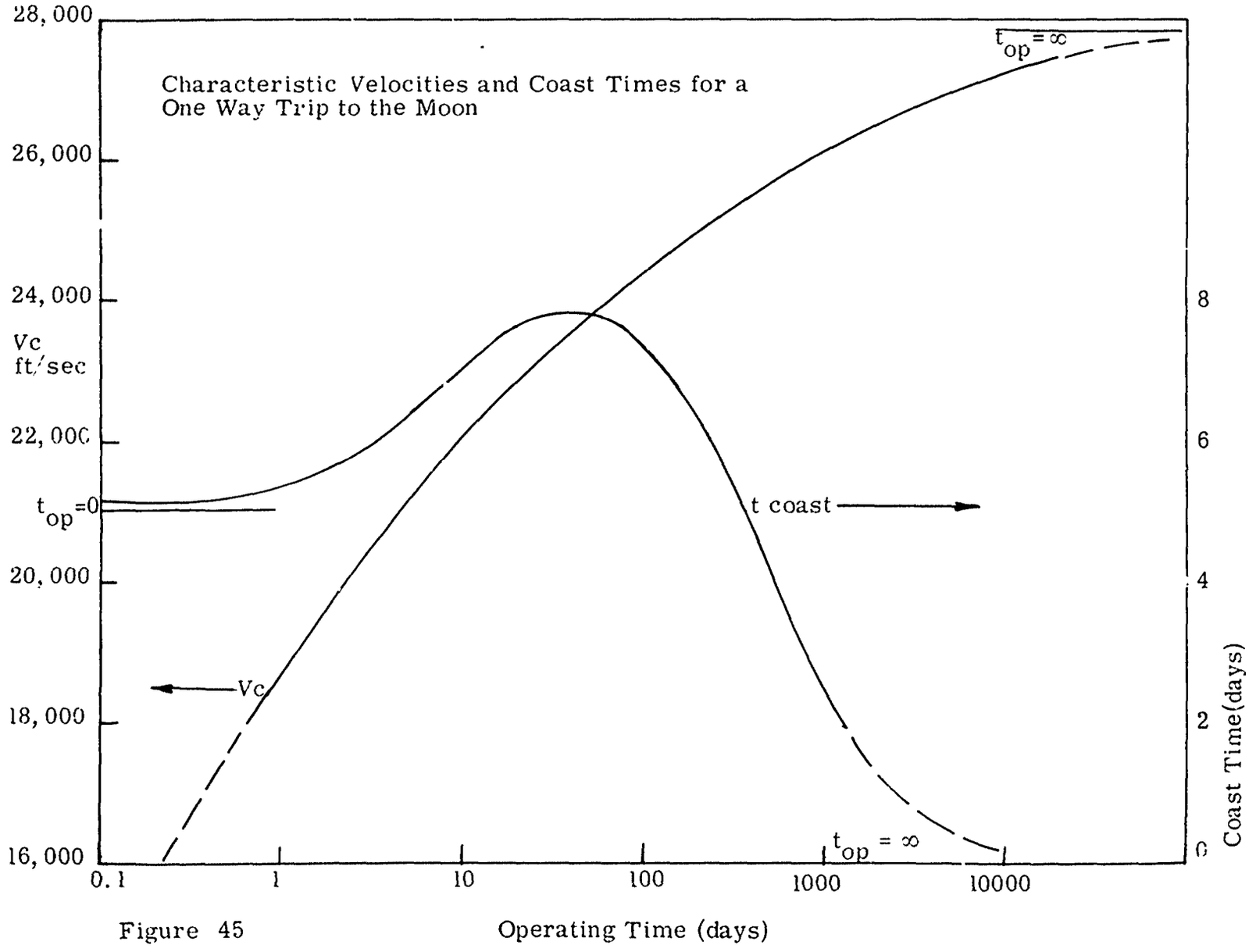
Characteristic Velocities and Coast Times for a
One Way Trip to the Moon
28,000
26,000
24,000
22,000
20,000
18,000
16,000
Vc
ft/sec
$t_{op}=0$
$t_{op}=\infty$
Vc
t coast
$t_{op}=\infty$
8
6
4
2
0
Coast Time(days)
0.1
1
10
100
1000
10000
Operating Time (days)

Figure 45

EXPERIMENTAL THRUSTER PERFORMANCE EXPERIMENTS

Plasmadyne has been engaged in arc-jet engine development programs for the past several years. This includes work on the design of a low thrust engine from 0.01 to 0.1 pound, to operate at a specific impulse of 1000 seconds. (Contract No. DA-04-495-21x4992. 506-ORD-1806.) This study examined overall performance as effected by such things as nozzle geometry, hot or cold wall operation, materials and chamber pressures. In addition, work is now in progress to develop a 30 KW plasma jet for the Air Force. This operates at a mid range specific impulse using hydrogen as a fuel. It is a hot wall design using a tungsten nozzle and anode. The life of the engine is believed to be over 100 hours and life tests are currently being performed. This size thruster (30 KW) has been designed to operate using ammonia as the propellant at AVCO. Because of the more severe operating characteristics involved with using ammonia lower efficiencies at similar specific impulses were measured.

Water-cooled arc-jets were operated with many different propellants, especially early in the engine development programs. Because they are inherently less efficient than the hot wall design, this type of engine was eliminated for use as a space engine. Cold wall tests have been run at high power levels for extended periods of time using hydrogen, helium and ammonia as propellants. For example, using hydrogen, specific impulses as high as 2100 seconds using power levels of up to 130 KW have been achieved. Helium has been operated at power levels of 30 KW and I_{sp} of 1000 seconds. Thrusters using ammonia and 90 KW at I_{sp} as high as 1400 have also been tested (Contract No. AF 49(638)-766).

In this program a series of propellants were tested using a modification of the Plasmadyne 1 KW engine designed under a NASA contract. The modification that was used is less sophisticated and costly to manufacture than the high performance NASA engine. At 1 KW and an I_{sp} of 1100 seconds, the efficiency of the advanced thruster on hydrogen is over 35 per cent (Taken from unclassified Ref. 48). As described in the following sections, the modified Cute V thruster runs at a lower efficiency (25 per cent). The life of these thrusters is controlled by the amount of erosion of the tungsten nozzle-anode insert. Essentially, the same thruster was run for each test using a new insert when required. The replaceable anode allowed the testing of a large number of different propellants in a reasonably short time. The propellant tests using the 1 KW engine were sponsored jointly under this program and the NASA-Plasmadyne 1 KW development program.

The use of this low power engine is an extremely severe test for propellant evaluation. Operating difficulties are magnified and failures occur after very short test runs. Propellants which show marginal performance in these tests might be quite adequate in large powered arc-jet engines.

EXPERIMENTAL ARC-JET ENGINE

The evaluation of the performance data reported for the propellants investigated under this program requires knowledge of the thruster utilized in the program. The thruster is a Plasmadyne developed design designated Cute V and shown in Figure 46 and 47. This thruster was developed under a NASA contract and an extensive description of the thruster and its performance with hydrogen and ammonia as propellants can be found in References 47 and 48. The thruster is basically a radiation cooled unit and was designed to operate on hydrogen at an input power of 1 KW. The Cute V thruster is made with 2 per cent thoriated electrodes, encased in molybdenum housings. Boron nitride was used as the insulator material. Sealing was provided by using high temperature inconel seals. The unit is one and one-half inches in diameter, two and one-half inches long and weighs 600 + grams.

The unit was designed to operate with a negative rear electrode and a positive front electrode, which doubled as the nozzle. The basic arc region geometry consists of a cathode with a 30° half angle and an anode with a 45° inlet half angle, a 0.009 inch diameter throat and a 30° exit cone half angle. The expansion ratio is approximately 200. The gap setting, the distance between electrodes, is normally 0.025 inches. The thruster described above or modifications thereof was used throughout the experimental investigation portion of this program.

Optimized or nearly optimized performance with an electrothermal or plasma device involves a complicated analytical and experimental evaluation of the complete thruster. Of particular importance is the selection of the arc chamber geometry and gap setting. The selection of the proper arc chamber geometry and gap setting requires knowledge of the design flow rate, the input power, the expected performance and the associated arc chamber pressure and temperature under equilibrium operation.

The above mentioned complexities represent only a portion of the difficulties. They are, however, sufficient to show that such an optimization was beyond the scope of the program undertaken. Therefore, the goal of this investigation was to obtain useful data which would permit a valid experimental comparison of propellants without optimization of the design for each of these propellants. The propellants selected for evaluation were hydrogen, helium, argon, nitrogen, ammonia, methane, air and lithium hydride.

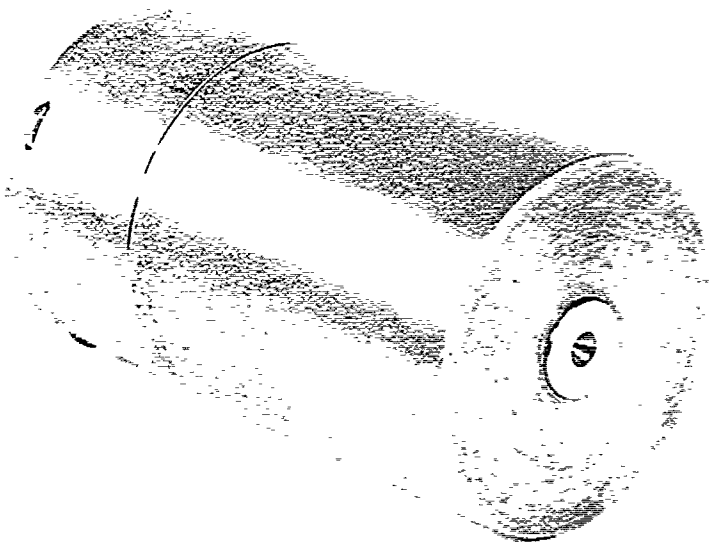

Figure 46 -- CUTE V THRUSTER - FRONT ASSEMBLED VIEW

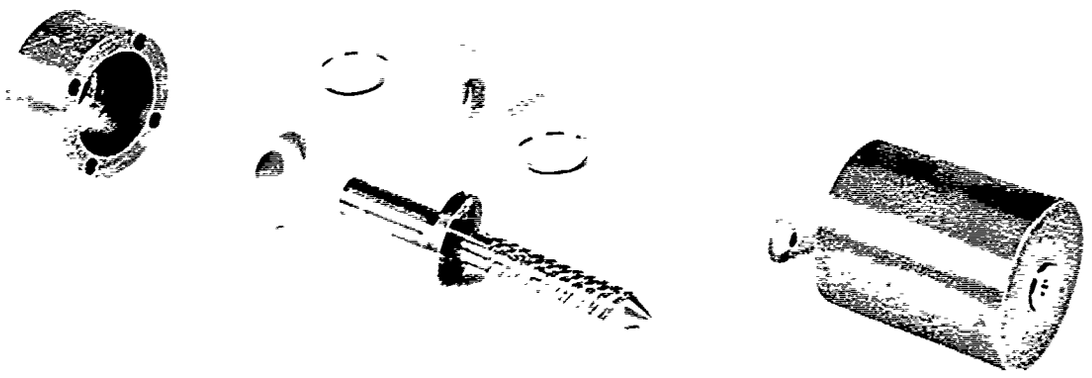

Figure 47 -- CUTE V THRUSTER - FRONT DISASSEMBLED VIEW

HYDROGEN EXPERIMENTAL RESULTS

The operation of the Cute V thruster with hydrogen resulted in good performance. With an input power of 1 KW and a mass flow of 10^{-5} lbs sec. the unit produced approximately 0.01 lbs. of thrust. The specific impulse was approximately 1000 seconds with a kinetic efficiency of approximately 25 per cent. Kinetic efficiency being that percentage of the input power across the thruster found in directed kinetic energy. The normal operation of this design at the above conditions of flow and power were obtained at an 80 to 90 volt and 12 to 14 ampere level. Arc chamber pressure was nominally 5 atmospheres. Under normal operation approximately 60 per cent of the input energy across the thruster is transferred to the gas with the rest accounted for as thermal losses in the thruster. The thermal losses to the thruster result in an equilibrium operating temperature of approximately 975° C on the outside surface. The life of the unit is approximately 10 to 12 hours. The present life limitation of the thruster is due to the slow, steady ablation of the nozzle throat (anode). This decreases the arc chamber pressure causing a corresponding decrease in voltage, an increase in current which results in a deterioration of performance. The hydrogen plume at the above listed operating conditions is approximately 2 to 2-1/2 inches long and 1/2 to 3/4 inches in diameter. The test chamber pressure is 1 mm of Hg in all tests described. The color was an intense reddish pink with a whitish-yellow core at the nozzle exit. Operation is extremely stable and the erosion or ablation rate is very low so that molten electrode discharge is not noticeable.

HELIUM EXPERIMENTAL RESULTS

Operation with helium as the propellant was sustained in four separate tests. Total operating time was in excess of one and one-half hours. All units operated between 20 to 40 volt and 10 to 20 amperes. The input power varied between 750 and 300 watts. Several arc region geometries were tried. Flow rate operation was between 1.3×10^{-5} and 4.0×10^{-5} lbs/sec. The flow rate could not be reduced for any of the tests; attempts to do so resulted in operation at an extremely detrimental (high erosion) thruster condition. Performance data was obtained for all tests and is reported below.

Helium Test No. 1 -- This unit was tested with the normal arc chamber geometry. The cathode inlet half angle was 30°, the anode inlet half angle was 45°, the throat diameter was 0.009 inches, the throat length 0.010 inches and the gap was set at 0.025 inches. For all tests in this program the nozzle exit cone half angle and expansion ratio were unchanged. The test duration was in excess of 30 minutes. The thruster was operated at a mass flow of 2.2×10^{-5} lbs/sec. with an input power

of 600 watts and produced approximately 0.01 lbs. of thrust. The specific impulse was approximately 450 seconds with a kinetic efficiency of 16 per cent. The unit operated at the 35 volt and 17 ampere condition with an arc chamber pressure of 7 atmospheres. Molten expulsion of tungsten was observed throughout the test. The helium plume was short (about 1 to 1-1/2 inches in length) and very dispersed (approximately 1+ inch in diameter). The plume was pinkish with a whitish core at the throat.

Helium Test No. 2 -- This test was a continuation of Test No. 1. The exit was not modified between runs. The arc-region geometry was unchanged except for the erosion of the nozzle throat. The test duration was in excess of 24 minutes. The thruster was operated at a mass flow of 1.3×10^{-5} lbs sec. with an input power of 360 watts and produced approximately 0.006 lbs. of thrust. The specific impulse was approximately 475 seconds with a kinetic efficiency of 18 per cent. The unit operated at the 30 volt and 12 ampere condition with an arc chamber pressure of 5 atmospheres. The thruster expelled molten tungsten throughout the test indicating a very high erosion or ablation rate. The plume size, shape, and color was as described for Test No. 1.

Helium Test No. 3 -- The thruster utilized for this test was modified from the standard arc-region geometry. The modification made was to increase the gap to 0.035 inches. It was thought that this modification would increase the operating voltage permitting higher input power to the thruster. The test duration was in excess of 24 minutes. The thruster was operated at a mass flow of 1.5×10^{-5} lbs. sec. with an input power of 400 watts. The unit produced approximately 0.006 lbs. of thrust at a specific impulse of approximately 375 seconds and a kinetic efficiency of 11 per cent. The operating voltage was 36 volts with a current of 11.5 amperes. The arc chamber pressure was approximately 6 atmospheres. The plume size, shape and color was as previously described. Expulsion of molten tungsten was continuous and appeared more severe than in the previous tests. The changing of the gap length did not increase the operating voltage level of the unit. It is felt that the decrease in performance (both specific impulse and efficiency) was due to the gap length. It is felt that the change caused the arc foot to strike the anode upstream of the nozzle throat increasing both the heat transfer and viscous losses.

Helium Test No. 4 -- For this test the normal arc chamber geometry was modified. The modification included the reduction of the cathode half angle to 15 degrees and the setting of the gap to 0.014 inches. These modifications were made to simulate the design existing on commercial water-cooled units utilizing helium. The test duration was in excess of 15 minutes. Operation was conducted at a mass flow of 1.0×10^{-5} lbs sec. and an input power of 370 watts. The thrust produced was 0.005 lbs. at a specific impulse of approximately 550 seconds and a kinetic efficiency of 17 per cent. The unit operated at the 30 volt 12+ ampere condition at an arc chamber pressure of 4 atmospheres. The thruster continuously expelled molten tungsten. The plume size, shape and color was as previously described. The increased performance of this test appears to be the result

of the arc region geometry changes made, but confirmation of the test results (with a unit of similar geometry) are necessary before a definite conclusion could be reached.

ARGON EXPERIMENTAL RESULTS

Operation with argon as a propellant was sustained in four separate tests. Total operating time was in excess of 30 minutes. All units operated at an 18 to 20 volt and a 7.5 to 15 ampere level. The input power varied from 130 to 300 watts. Two different arc region geometries were tried at flow rates of 2.0×10^{-5} to 5.7×10^{-5} lbs sec. The geometries were (1) the standard hydrogen configuration and (2) the geometry described in helium Test No. 4.

At the above power to flow ratio it is extremely difficult to obtain satisfactory performance (regardless of the variety of propellant used). Consequently, the performance obtained was only slightly above cold flow specific impulse with negligible kinetic efficiencies (approximately 3 per cent). The power to flow ratio could not be increased (by reducing flow) because operation, even at the above designated levels, was extremely severe. The maximum test duration sustained was 15 minutes. The failure mode for all the units was plugging of the nozzle throat. "Plugging" is the term used to describe the plating of both anode and cathode electrode material in the nozzle throat which ultimately completely closes the throat. This mode of failure is due to the fact that the molten electrode material is not expelled with the nozzle exhaust as it was in operating with helium. It is felt that plugging results when the anode arc foot is upstream of the nozzle throat permitting ablated or eroded tungsten to solidify prior to expulsion from the unit.

NITROGEN EXPERIMENTAL RESULTS

Operation with nitrogen as the propellant was sustained in four separate tests. The total operating time was in excess of one hour with the longest test in excess of 25 minutes. Three different arc region geometries were tried. Data was obtained at voltage levels between 54 and 30 volts and currents ranging from 12 to 33 amperes. The input power varied from 400 to 1200 watts. Flow rates were varied between 2.75×10^{-5} to 3.00×10^{-5} lbs sec. Performance data and operation is reported separately for each test.

Nitrogen Test No. 1 -- This unit was tested with the normal or standard arc chamber geometry (see description in Helium Test No. 1). The thruster was operated at a mass flow of 2.8×10^{-5} lbs sec. with an input power of 1.2 KW. The arc chamber pressure was 1.5 atmospheres, due to the nozzle throat erosion of previous tests. The unit produced approximately 0.008 lbs. of thrust at a specific impulse of 270 seconds and a kinetic efficiency of 4+ per cent. The thruster operated at 34 volts and 34 amperes. The thruster continually expelled molten tungsten material. The plume was approximately two inches long and one inch in diameter (similar to hydrogen). It was basically pink in color with overtones of an orange hue. Nitrogen and hydrogen were the only propellants operated with a satisfactory plume shape (i.e., a long, concentrated and intense plume as opposed to the short, diffused plume experienced with the other propellants).

Nitrogen Test No. 2-- This thruster had the standard arc chamber geometry and was operated at a mass flow of 2.6×10^{-5} lbs sec. with an input power of 230 watts. The arc chamber pressure was approximately 3.5 atmospheres. The test duration was in excess of 10 minutes. A thrust of 0.01 lbs. was obtained at a specific impulse of 260 seconds and a kinetic efficiency of 7.5 per cent. The thruster operated at a 54 volt and 15 ampere condition. The different operating mode from that of nitrogen Test No. 1 is primarily due to the (1) higher arc chamber pressure and (2) the different geometry (newly fabricated unit was used for this test). The plume size, shape and color was similar to the plume described in the first nitrogen test.

Nitrogen Test No. 3 -- The arc chamber geometry of this unit was modified. The modification included the change of the cathode half angle to 20° and the gap to 0.014 inch. The thruster was operated at a mass flow of 2.9×10^{-5} lbs sec. with an input power of 510 watts. The unit produced 0.008 + lbs. of thrust at a specific impulse of 280 seconds and a kinetic efficiency of 10 per cent. The unit was operated for a duration of 12 minutes. The arc chamber pressure was 1 atmosphere and was caused by a short period of extreme erosion early in the test. The thruster operated at 30 volts and 17 amperes. Expulsion of molten material was evident throughout the test and the plume shape, size and color was as previously described.

Nitrogen Test No. 4 -- This thruster was modified to have a cathode half angle of 15° and a gap setting of 0.014 inch. The mass flow was set at 2.75×10^{-5} lbs sec. with an input power of 550 watts. The thrust produced was 0.009 lbs. at a specific impulse of 350 seconds and a kinetic efficiency of 13 per cent. The thruster operated at the 40 volt and 13 ampere condition at an arc chamber pressure of 4+ atmospheres. The plume was as previously described. The expulsion of molten tungsten was evident, but did not appear as severe as in the other tests conducted with nitrogen.

AMMONIA EXPERIMENTAL RESULTS

Although many attempts were made to obtain experimental data, only two could be classified as successful. One was a prolonged duration test which will be described below. The second was a short duration operation conducted as part of an extensive hydrogen test. Operation was conducted at points similar to those of hydrogen because of the specific attention lately given to this propellant. Complete coverage of these tests is reported in Reference 47.

Ammonia Test No. 1 -- This test was conducted with a unit of standard geometry. The mass flow was set at 1.4×10^{-5} lbs/sec. at an input power of 840 watts. The thrust produced was 0.0057 lbs. at a specific impulse of 390 seconds and a kinetic efficiency of 6 per cent. Operation was sustained at 60 volts and 14 amperes with an arc chamber pressure of 3 atmospheres for a duration in excess of 83 minutes. The plume was diffuse and a whitish-yellow in color. Molten expulsion of electrode material was evident but appeared sporadic indicating an instability in the operating mode.

Ammonia Test No. 2 -- The unit was operated with the standard arc region configuration. The ammonia operation, however, was not begun until operation with hydrogen had eroded the throat considerably. Operation was sustained for 22 minutes. The ammonia flow rate was set at 1.1×10^{-5} lbs/sec. with an input power of 920 watts. The unit produced 0.006 lbs. of thrust at a specific impulse of 550 seconds at a kinetic efficiency of 8 per cent. The unit operated at 59 volts and 15 amperes at an arc chamber pressure of 2+ atmospheres. The plume size, shape and color was as previously described. The expulsion of molten material was continuous and more severe than that which occurred in Test No. 1.

METHANE EXPERIMENTAL RESULTS

Two successful tests were conducted utilizing methane as the propellant. Each test was approximately 4 minutes in duration. Reliable performance data, however, could not be obtained because operation was at an extremely detremental condition. The standard arc region geometry was used for both tests. The mass flow was set at 1.55×10^{-5} lbs/sec. and the thruster power input was 1200 watts. This operating condition was sustained at 60 volts and 20 amperes. The units, when started, sustained a rapid increase in pressure indicating a build-up of electrode material in the nozzle throat. The build-up continued until the throat was completely plugged.

Both units tested operated in the above described manner and the failure mode was the same in both tests. The plume was short and diffuse. It was whitish-blue in color and appeared to have a hot core. Large quantities of electrode material were expelled through the nozzle during the entire test.

AIR EXPERIMENTAL RESULTS

The attempts to operate a thruster on air were unsuccessful. The units, in all cases, plugged on start. The mode of failure indicated extremely high current density in the throat region liquifying the tungsten electrode, resulting in plugging of the throat. Further testing to obtain operation could not be conducted due to limited facility time.

LITHIUM HYDRIDE EXPERIMENTAL RESULTS

Operation with lithium hydride as a propellant provided difficulties and complexities not normally encountered. These difficulties were due to the fact that lithium hydride is a solid under ambient conditions and because of the toxicity and other hazards associated with the material. The use of this propellant also provided problems as to the obtaining of useful data. These problems were primarily due to the incorporation of the propellant storage tank and the associated heater to the thruster. This mounting of the complete test unit (thruster, propellant tank, heater and counterbalance) required that the center of gravity (cg) of the propellant fall right under the cg of the beam so that there would be no zero shift with change in propellant weight when utilizing the pendulum thrust beam (see experimental test equipment). Figure 48 shows the schematic of the lithium hydride thruster experimental test set-up. The major portion of the equipment shown is part of Plasmadyne's 1 KW experimental test facility. The equipment unique for this test consists of the thruster, propellant tank, heater and counterbalance. The disassembled components are shown in Figure 49 (prior to installation of heater coil). The assembly is shown in Figure 50, again prior to heating coil installation. The thruster shown is basically a modification of the Cute V thruster previously described. The unit was scaled down and excess anode housing material removed to cause higher operating temperature The thruster had molyb- anode and cathode housings with the electrodes of 2 per cent thoriated tungsten. Boron nitride was used for the insulators. Serrated surfaces on the molybdenum provided the sealing with the boron nitride insulators. The propellant tank was made of molybdenum and consisted of casing, cap, seal, and retainer ring. The tank seal was to have been provided by serration on the molybdenum in contact with a boron nitride sealing ring

(shown in Fig. 49). The technique, however, was not successful in this instance and an inconel seal was used in the actual test. The counter-balance was fabricated from molybdenum and consisted of a simple threaded shaft with adjustable knurled weights. The heater element consisted of six pieces of boron nitride and approximately 20 feet of 0.017 inch diameter tungsten wire. The main portion of the heater being the two interlocking boron nitride cylinders. The inner cylinder was grooved to hold the tungsten heating coil. The cylinder was wound from bottom to top. The assembly procedure required complete fabrication of the thruster components prior to installation with the stainless steel Swaglock tee fitting. The counter balance (unadjusted) was then connected to the fitting. The main heater component was wound and slipped over the open-ended propellant tank. The propellant tank was then secured to the tee fitting. The fitting was taped with glass to electrically insulate the heater coil from the negative potential of the fitting and propellant tank. The inner boron nitride shells (grooved) were placed around the fitting and then the heating coil wound. The outside shells were installed and secured with glass tape. The heater wires were secured to the outside of the heater with a clamp (not shown).

Prior to filling the propellant tank, the thrust beam center of gravity was checked. The thruster assembly was then placed on the beam and the counterweights adjusted so that the center of gravity of the propellant tank was in line with the cg of the thrust beam. The assembly was then removed from the beam, the lithium hydride placed in the propellant tank (propellant wt. of 4.175 grams), the propellant tank closed and sealed, and the assembly reinstalled on the beam. The cg location was rechecked and the thrust transducer and electrical power and propellant leads connected. The experimental test chamber was then closed, evacuated and pruged with helium.

The test was initiated by applying power to the thruster and introducing hydrogen flow. The operation appeared stable and normal for approximately 6+ minutes. At this time the plume shape changed from the normal hydrogen plume. The new plume was almost invisible to the naked eye, but had a slightly blueish-purple hue. The thruster was shut down at this point. The decision was made to continue operation although operation with hydrogen was not normal (but satisfactory in performance). The thruster was restarted and operated at increased hydrogen propellant flow. Power to the heater was initiated and slowly brought up to the 90 volt, 9 ampere input power level. There was no noticeable color to the boron nitride casing of the heater but the ends of the coil indicated operation at about 1200°C. Since no evidence of lithium hydride appeared in the plume, it is assumed that the propellant at this point was somewhere in the liquid range. Power to the heater was increased to the 136 volt and 9.5 ampere level. The thruster operation at this point was 15 volts and 10.5 amperes. At this time (approximately 12 minutes after second start) the first noticeable trace of lithium was observed in the plume indicating propellant temperature in excess of 860°C. A bright red or carmine color was observed definitely indicating lithium was passing through the thruster.

At this point the hydrogen propellant was slowly decreased. A succession of minor failures occurred at this point. The phenolic clamp holding the heating element broke due to expansion of the heater, the heater lead connections were not broken. This failure changed the zero thrust position which is cg sensitive. A small leak developed at the bottom of the propellant tank. The lithium hydride flow was sufficient to cause a glow discharge to appear between the cathode of the thruster, the heater lead and the anode of the thruster. In the area of the lithium hydride leak at the bottom of the propellant tank a bright red glow was observed. During the above, the temperature of the assembly was approaching equilibrium. The complete assembly surface, except for the extreme end of the counter balance appeared to be at approximately 1000°C. The plume of the thruster contained a larger amount of lithium and was, therefore, more intense and redder in color. Operation with lithium hydride at this point had been sustained for 9+ minutes. Hydrogen flow was being sustained at a low flow fate and continually being decreased. At this point the bottom of the boron nitride heater case started to bubble and to shower sparks throughout the test chamber. The showering of sparks continued to the end of the test. Test termination occurred when the lithium hydride was completely expended. The complete utilization of the lithium hydride occurred almost immediately after complete termination of hydrogen flow. The increased temperature of the components at this time, due to continued heater power caused a heater failure just prior to shut down of power. At this point helium flow was introduced into both the experimental test chamber and the thruster and the assembly allowed to cool. Figure 51 shows the thruster on the beam after the test was completed. The broken heater clamp is shown. The white coating on the inside of the test chamber is RTV-11 silicone rubber coating. This coating was sprayed on the inside of the tank to simplify the removal of any residual free lithium.

Examination of the unit after sectioning was very helpful in interpreting the failures and phenomena experienced during the test. The completely disassembled thruster is shown with the sectioned propellant tank and heater in Figure 52. As explained previously the clamp holding the heater leads failed. This failure was primarily due to the (1) differential thermal expansion between the heater and the phenolic clamp and (2) the boiling out of the resin of the phenolic clamp. The seal failure of the propellant tank was caused by the failure of the silver surface plated on the inconel seals. This failure occurred when the seal temperature exceeded the melting point of the silver coating. The bubbling and sparking of the lower portion of the boron nitride heater casings is thought to be due to a reaction between the lithium and the boric oxide binder of the boron nitride. This reaction is exothermic and the additional heat input is felt to have caused the failure experienced by the heater at the end of the test.

Examination of the heater parts revealed traces of free lithium deposited on and/or in the boron nitride heater casing. Small amounts of free lithium were also found in the bottom of the propellant heater case. Examination of the tee fitting and the thruster, did not yield evidence of free lithium. All thruster materials performed substantially well (except

the heater clamp and casing). The broken piece of boron nitride (shown in Fig. 52) was not the result of a test failure. Localized melting of the stainless steel fitting occurred, and an embrittlement of the molybdenum connector parts was evident. The tungsten heater coil also underwent recrystalization.

The test was successful in that operation with lithium hydride was sustained for 12+ minutes. The failures, however, prevent the valid reduction of data. The leakage and shifting of the thrust zero point cannot be compensated for and any attempt to do so would yield data which at best could be considered unreliable. From observation of the test, the plume, and from the data that was taken, however, it is guessed that specific impulse between 400 to 800 seconds at a kinetic efficiency between 8 to 12 per cent were reasonable operating conditions.

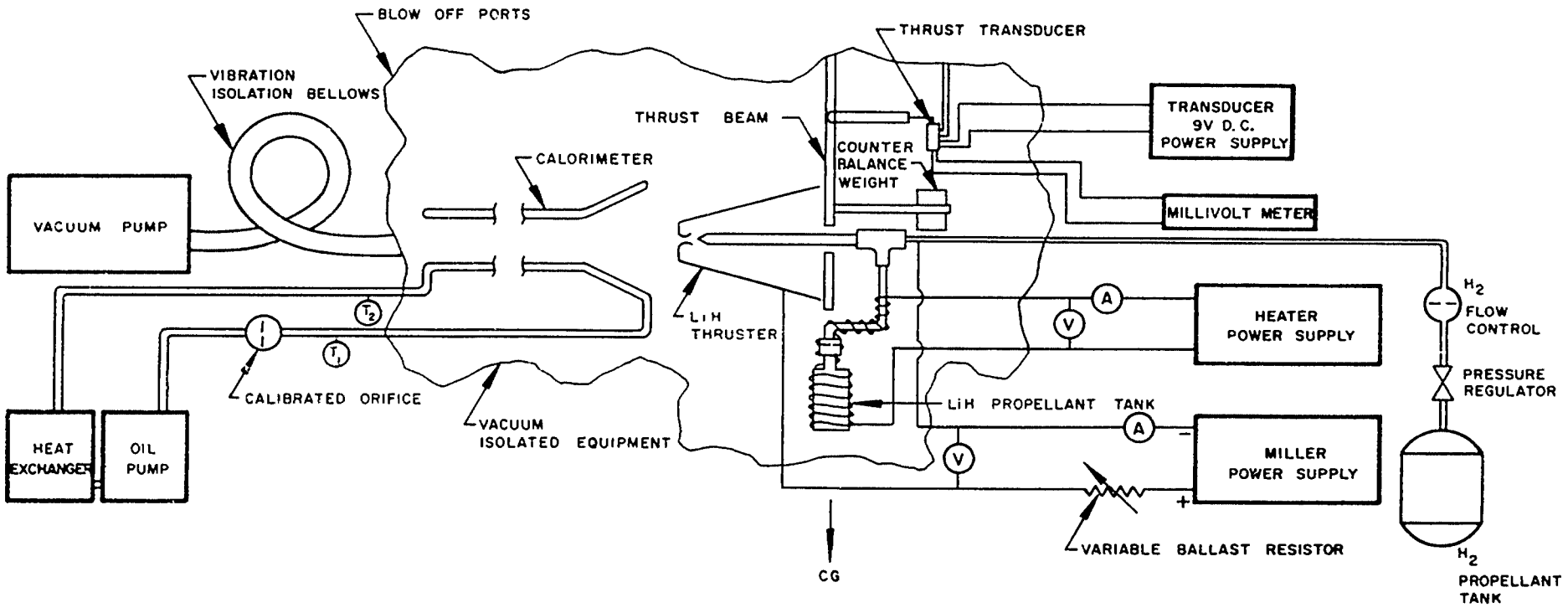

Figure 48 - SCHEMATIC OF LiH THRUSTER EXPERIMENTAL TEST SET UP

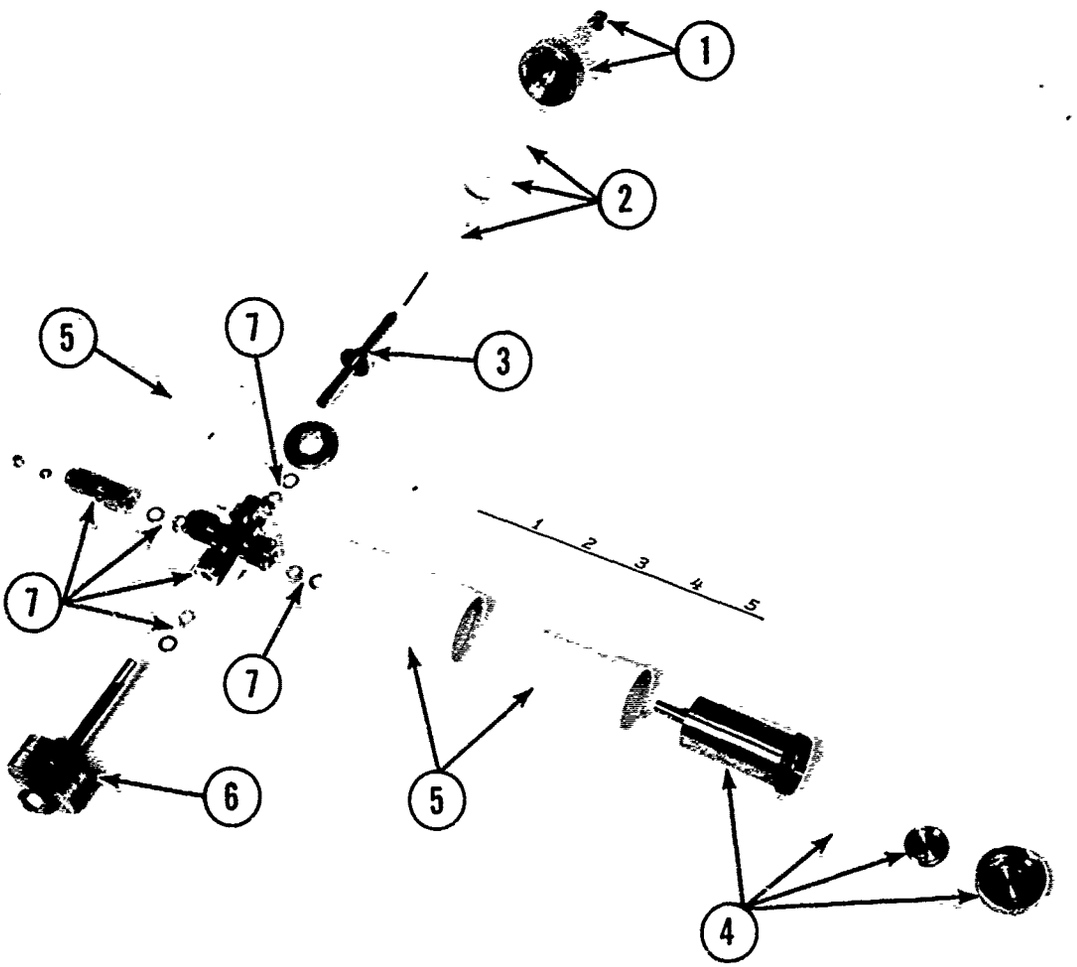

Figure 49 DISASSEMBLED COMPONENTS OF LITHIUM HYDRIDE TEST EQUIPMENT

1) Thruster Anode and Nozzle
2) Boron Nitride Insulators
3) Cathode
4) Lithium Hydride Propellant Tank
5) Heater Components
6) Counter Balance
7) Fittings and Feed Line Connector

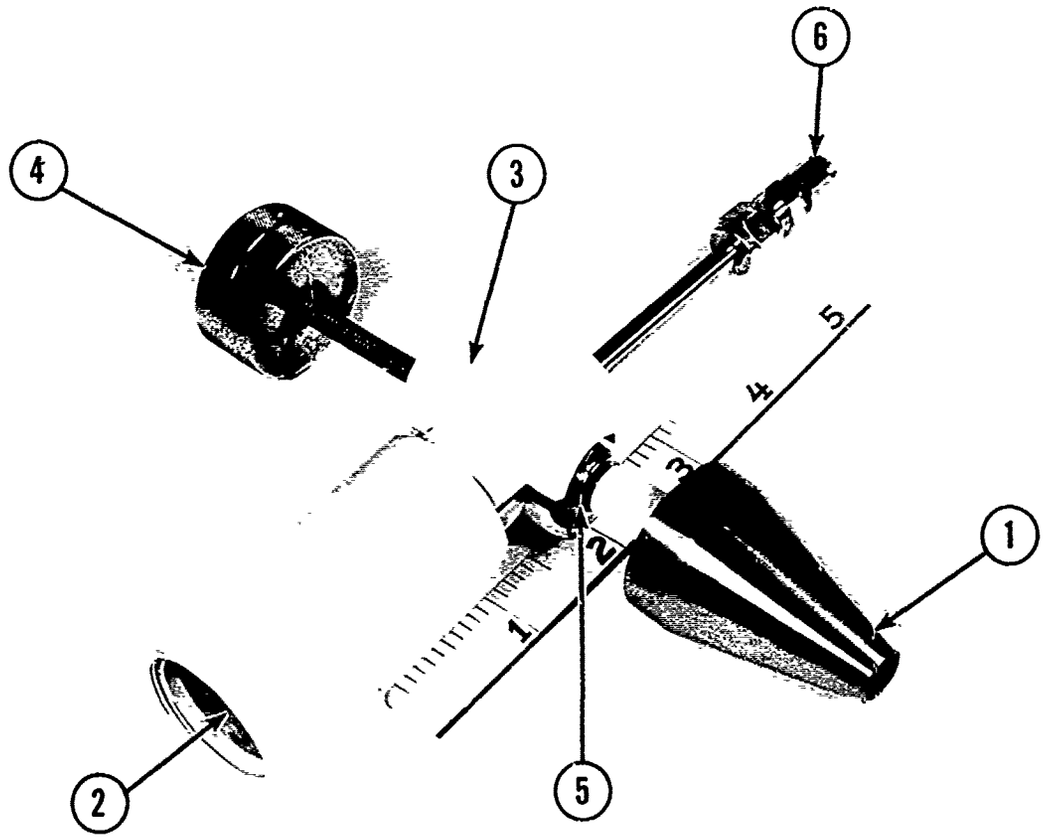

Figure 50 LITHIUM HYDRIDE TEST ASSEMBLY (PRIOR TO INSTALLATION OF HEATER COIL)

1) Thruster
2) Lithium Hydride Propellant Tank
3) Heater Assembly
4) Counter Balance
5) Connector Fitting
6) Hydrogen Feed Line Connector

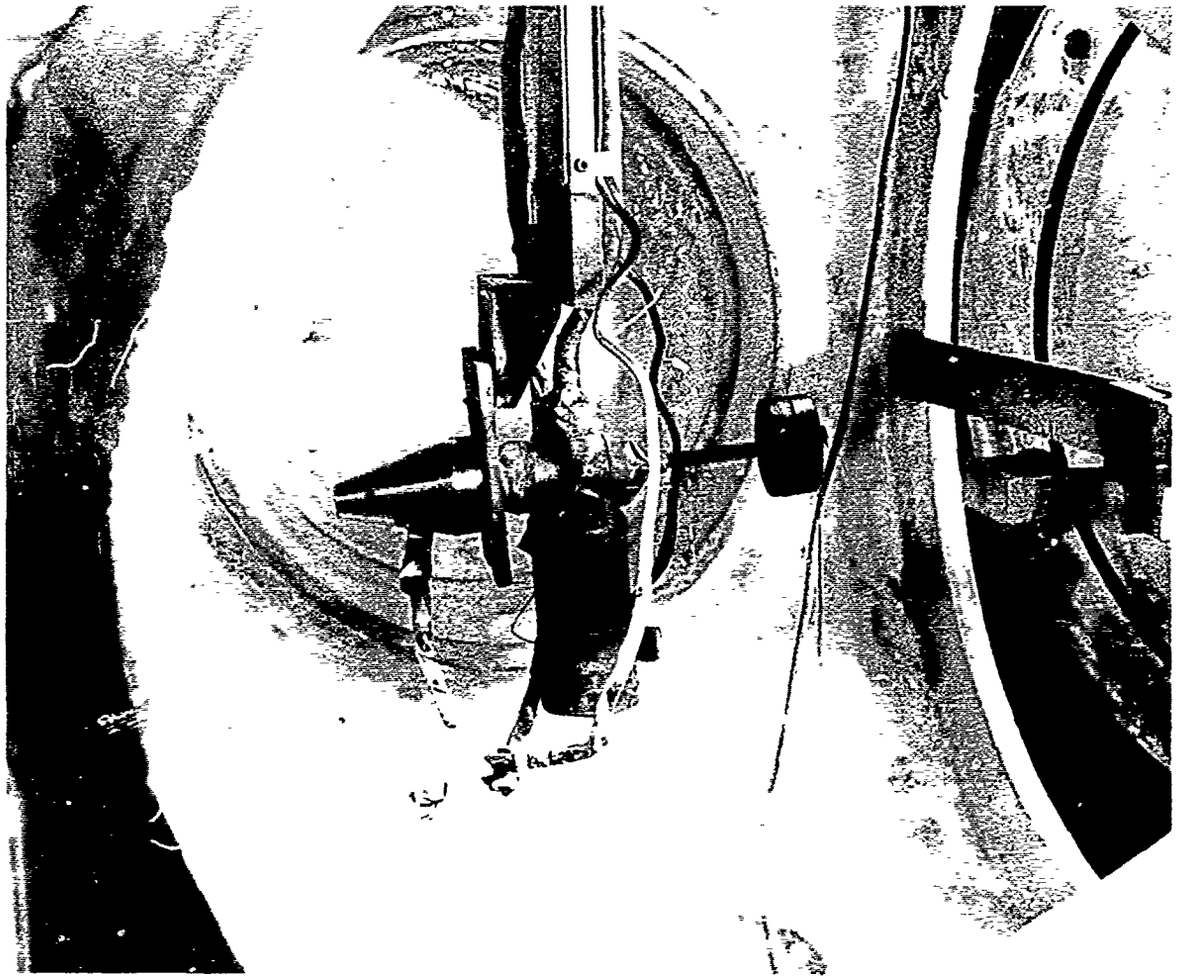

Figure 51 -- LITHIUM HYDRIDE ASSEMBLY AFTER TEST

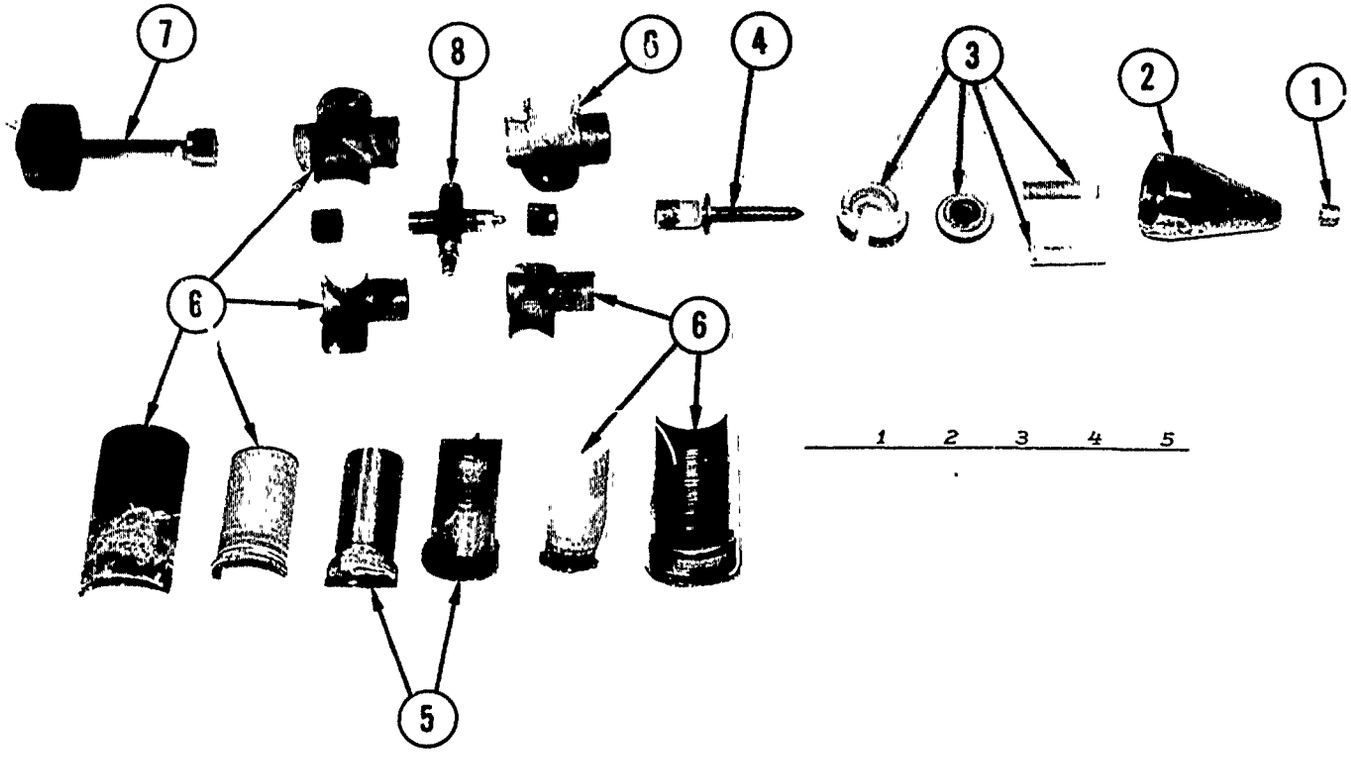

Figure 52 DISASSEMBLED AND SECTIONED COMPONENTS OF LITHIUM HYDRIDE TEST

1) Anode Nozzle Insert
2) Anode Housing
3) Boron Nitride Insulators
4) Cathode
5) Lithium Hydride Propellant Case
6) Heater Components
7) Counter Balance
8) Fitting

CONCLUSIONS ON THRUSTER EXPERIMENTS

A summary of the best test data obtained is shown in Table XIII. Several conclusions can be made concerning the operation of an electrothermal arc-jet with each of these propellants. It is obvious that hydrogen has the highest impulse and efficiency obtained to date. This is due to the concentrated effort expended to obtain performance with this propellant. Hydrogen is a useful propellant because it provides the least severe materials problem, and the lowest operating temperature at a given specific impulse. This decreased severity gives it an advantage of longer useful life. Ammonia and nitrogen appear favorable as propellants but are more detrimental to thrusters than hydrogen. This detrimental condition limits the useful life and provides an extremely severe materials' problem which must be overcome. Helium appears favorable because of the high kinetic efficiency but it is felt that the thruster operating with this propellant would always have a shorter life than a unit utilizing hydrogen. The use of air, argon, and methane provide extreme materials problems even at low specific impulse operation. It is felt that the materials problems cannot be overcome at this time. Reaction of both methane and air with the electrode material at high specific impulse levels will provide further difficulties which would be difficult if not impossible to overcome. Lithium hydride, even if high impulse and kinetic efficiency levels were obtained, has several serious drawbacks. The material requires additional power, other than supplied to the thruster, to obtain the propellant in a useful form (i. e., a gas instead of a solid). If reasonable response times are required the solid propellant must be constantly supplied with heat to keep it in usable form. Use of lithium in the solid state is feasible but a multitude of development difficulties have to be overcome.

Table XIII**

SURVEY OF PROPELLANT PERFORMANCE TESTS

Propellant	Power Input (watts)	Flow Rate (lb/sec x10^{-5})	Voltage (volts)	Current (amperes)	Thrust (lbs.)	Specific Impulse (sec)	Kinetic Efficiency (%)	Life Expectancy at Oper. I_{sp} (hrs.)	Life Expectancy at I_{sp}= 1000 sec. (hrs.)
Hydrogen	1000	1.00	80-90	12-14	0.010	1000	25	10-12	10-12
Ammonia	920	1.10	59	15	0.006	550	8	~ 2 +	~ 1.5
Nitrogen	550	2.75	40	13	0.009	350	13	~ 2 +	< 1
Helium	370	1.00	30	12	0.005	550	17	< 2	< 1
Methane	1200	1.55	60	20	-----	-----	---	~0.1	~0.2
Air	-----	-----	---	---	-----	-----	---	~0.01	~0.0
Argon	130/300	2.00/5.70	18/20	9.5/15	~	80	3	~0.2	~0.05
Lithium Hydride*	700	~	70	10	~	400/800	8/12	~0.25	~0.20

* Since flow of hydrogen was present, it is not possible to accurately define parameters for this propellant.

** All values and comments refer to operating with 1 KW engine and are on the basis of these initial tests.

EXPERIMENTAL TEST FACILITY

The propellant evaluation program was conducted in the facility primarily used for low power thruster development. The selection of this facility was made due to (1) its adaptability to the program and (2) the existence of a developed thruster at this level. The complete experimental facility (pump, propellant and power supply not shown) is shown in Figure 53. The pump is mounted on a separate concrete slab and isolated from the rest of the facility to minimize vibration. The power supply and propellant stroage tanks are separated from the facility due to safety considerations. The instrumentation console contains most of the operation controls for the system. All necessary recorders and gauges excluding those for the calorimeter are contained in the console.

The test chamber, designed by Plasmadyne, has three (3) access doors. Two (2) of these are glass, which permit the viewing of the thruster and its plume. The tank extension is necessary for the pendulum type thrust beam. The top plate of this extension is utilized to bring in the propellant feed line and the power cables. The calorimeter lines and the thrust transducer electrical connections are located in the bottom plate, directly below the thruster test section. The test chamber pressure line is mounted in the center of the rear access door. The test chamber is connected to the pump by means of a bellows. This stainless steel bellows is one and one-half inches in diameter and four feet long. It is connected to the pump with a single loop. The transmission of pump vibration to the test chamber is eliminated by this bellows link. The heater power supply leads were installed in the top plate. The blow off ports are located on the downstream end of the tank.

The vacuum pump utilized is manufactured by Kinney. The model number is KDH-130. The unit is driven with a General Electric induction motor and has a 130 cfm. capacity at standard conditions. This pump maintains a test chamber pressure of 1 mm Hg at a 10^{-5} lbs sec. flow rate of hydrogen.

The power supply is basically a Miller welding supply. The supply is capable of use with an open circuit voltage of 320, 160 or 80 volts DC at up to 12.5 KW output. A variable ballast resistor is used in series with the thruster. The ballast resistor is variable over a range of 0-40 ohms.

The heater supply is a battery cart capable of operation at 240, 120 and 60 volts open circuit. The current limit is 15 amperes. A variable ballast resistance is connected in series with the batteries and is an integral part of the power supply.

The method used to obtain thrust utilizes the pendulum beam technique. The pendulum beam is mounted to the top plate of the test chamber extension. The beam was designed to measure thrust accurately and to minimize the error introduced into this measurement by thermal distortion. The beam is connected to a ± 0.3 ounce Statham transducer by means of a phenolic stirrup. The transducer is driven by a constant voltage power supply (9 volts). The transducer output is presently read from a standard laboratory millivoltmeter. Calibration of the thrust measuring system is performed both prior to and immediately after every test. A dead weight calibration technique is used.

Mass flow calibration is determined by calibration of a critical orifice. The system is filtered and solenoid value operated. The extreme difficulty required to determine lithium hydride instantaneous flow was beyond the scope of this program, and was therefore not attempted.

The input power is measured by recording voltage and current on an Esterline-Angus Recorder. The voltage is measured directly across the thruster. The test chamber pressure is visually read from a Wallace and Tiernan gauge. The time is recorded with a stop watch and a clock is used to provide correlation.

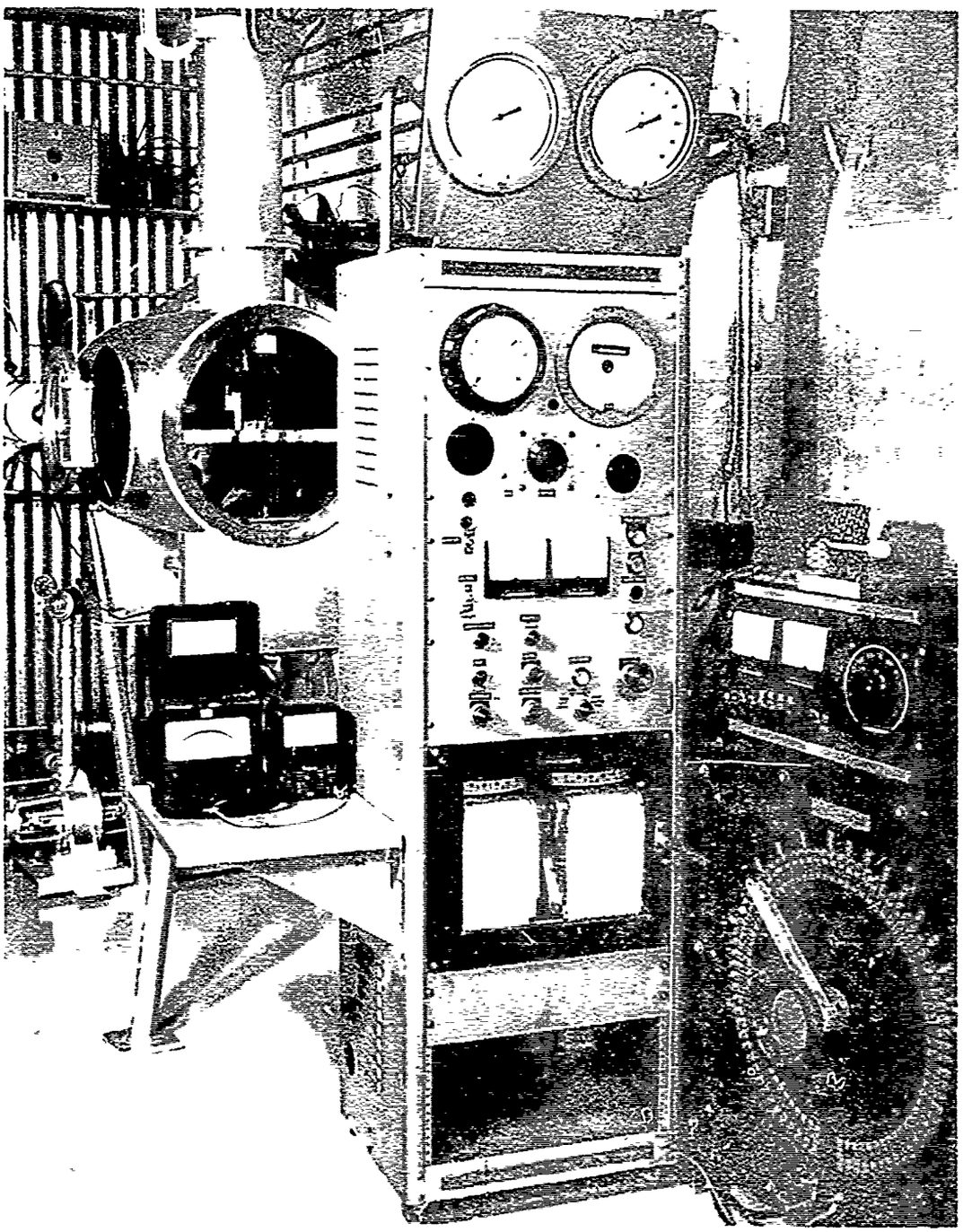

Figure 53 -- COMPLETE EXPERIMENTAL FACILITY
(Pump and Power Supplies Not Shown)

CONCLUSION

A few simple conclusions can be drawn from the preceeding discussion pertaining to the various propellants examined.

Helium - Arc-jet engine performance is moderat ly good using helium, however, because of the extremely high weight penalties involved in storing helium it is not a particularly promising propellant.

Methane and Ethane - The high chemical activity of the carbon in these compounds causes very severe materials problems. In the experiments reported above the erosion rates were extremely rapid. The performance was also hampered by carbon formations in the nozzle regions in several previous tests. The materials problems are difficult enough to classify these as undesirable propellants.

Air - Similar materials problems arise because of the oxygen's attack on electrode and nozzle materials. This plus the relatively high molecular weight resulting in very high operating temperature at desirable specific impulse values classifies this as a poor propellant.

Oxygen, water and hydrogen peroxide can be eliminated for consideration as propellants on similar grounds as air.

Argon - Because of its high molecular weight the operating temperatures for specific impulses in the order of 1000 seconds are so high that significant life can not be obtained.

Hydrogen - The performance is by far the best using a pure hydrogen propellant. Operating temperatures are low, heat transfer and materials problems are the most manageable using it. Very long life should be attainable. The storage of hydrogen places high weight penalties on the system but the high performance on some missions justifies the additional storage weight.

Ammonia - This propellant introduces slightly more difficult materials problems than with hydrogen. Operating temperatures at a given specific impulse are higher than with hydrogen but operation is still feasible for larger size engines for reasonable life times. The storage weight of ammonia is extremely favorable for longer missions. This low storage weight makes it very attractive for many missions.

Nitrogen - Performance and materials problems are moderate. Ammonia however because of its lower molecular weight would always be chosen in favor of pure nitrogen.

Lithium hydride - The high temperatures required to keep lithium in a gaseous state plus the chemical activity of the lithium causes

significant materials damage and makes engine and feed system designs very difficult. The high latent heats also increase the difficulty of obtaining high efficiency operations. The only really attractive point in its favor is its high storage density. The scarcity of both theoretical and experimental work on this compound makes it difficult to completely evaluate it at this time. The value of this type of propellant at present is very questionable.

Lithium - No advantage over a lithium hydride propellant can be noted.

RECOMMENDATION FOR FUTURE PROPELLANT STUDIES

1. From the conclusions drawn in the previous section, the major effort in the study of propellants for arc-jet usage should be placed on hydrogen and ammonia. The effects of various seeding materials should be stressed.

2. The use of a propellant material which can be stored as a solid warrants a small continued effort. The materials problems involved in using a lithium containing compound should be investigated. Designs which use the latent heats of the solid as a means of regeneratively cooling of high heat flux areas should be studied. Several experiments should be studied. Several experiments should be conducted with accurate mass flow and thrust measurements made before a final decision can be rendered concerning this type of propellant.

3. Recombination experiments should be conducted both with and without seeding materials over a range of arc chamber pressure useful for engine operation. The effects of seeding materials and concentrations on the recombination rates and overall engine performance must be determined. Nozzles with various expansion rates and minimized viscous losses should be tested. The data should be taken with emphasis on spectroscopic studies. Radial surveys of pertinent gas dynamic properties must be included in the experiments. In addition, there is always a need for theoretical work on recombination which more closely approaches the actual geometry and operating characteristics of the arc engines being considered.

4. At present the most pressing problems involved in arc-jet engine design are involved with increasing the engine life. Several studies in the area are important, and are listed below.

5. Anode foot erosion - Studies should be made to determine the operating conditions a which cyclic motion of the anode foot is present. Studies should include arc chamber designs which have provision for keeping the arc foot in motion across the anode surface along a non-repeating path. The effect of this on erosion rates and life should be determined.

6. A study of the erosion rates due to chemical causes of the arc chamber and arc-jet engine wall materials is important when long life is needed. With H_2 and NH_3 the problems have not been serious for 10-25 hours of operation, but this will become more important for longer running times; erosion rates are needed in order to design for this. Chemical attack by lithium vapor is a much more serious problem and a great deal of materials compatibility work is needed for engines using lithium hydride propellant.

7. The behavior of arc-jet engine components such as electrodes and nozzles used with the best available grades of gases, such as H_2, A, N_2, and He, have been observed. However, the known impurities such as

H_2O, O_2, CO_2 and hydrocarbons can be expected to contribute to erosion rates and therefore the operating life of the engines. A study should be made using commercial and specially pruified gases in order to determine the effects of the above impurities.

8. Little attention has been given to the effect of residual vacuum tank gases (ambient environment) which are present during experimental tests of arc-jet devices. Since flight testing will put these engines in a "zero" ambient pressure as compared to 10^{-3} to 10^{-5} mm Hg for laboratory facilities, it should be established whether or not small amounts of O_2, H_2O, and CO_2 affect the outcome of life tests.

9. Sputtering - The effects of electrode sputtering should be studied using target materials and surface temperatures normally encountered in arc-jet engines. The propellants must be those considered for use with arc-jets. Parametric measurements of the effects of pressure, surface temperature, ion current and energy on the sputtering ratio should be made. Very limited amounts of experimental data are now available.

10. Heat transfer problems of several types need studying. A more thorough investigation of the type and magnitudes of radiant heat transmission from the arc and plasma is needed. This study becomes increasingly more important with higher operating pressures. Studies which lead to a better understanding of the heat transfer phenomenon occurring in the electrode fall regions should be initiated at this time. They include the determination of magnitude of the fall region heat losses and flux distribution within the foot region itself. Studies on the overall energy balance of the engine system are always recommended. These include the understanding of individual mechanisms involved in the various energy transfers.

11. Recently several gaseous mixtures were used as arc-jet propellants at Plasmadyne. These included hydrogen-helium mixtures and nitrogen-hydrogen mixtures. For a 50-50 mixture of hydrogen and helium performance was significantly superior to that obtained with either pure substance. The experiments were not extensive enough to make this conclusive. In addition, if it is true, the reason for this increase in performance is not understood. It is recommended that some effort be expended in experimental work using gas mixtures with relative concentrations as a variable.

REFERENCES

1. Cann, G., and Ducati, A. C., Plasmadyne Final Report on Air Force Contract AF 49(638)-54, "Propulsive Properties of High Intensity Plasma Jets," Plasmadyne Corp., GRL-TR-9, AFOSR TN 57-748 or ASTIA AD-136 736.

2. Sanger-Bredt, "Uber Arbeitgose fur konventionell Beheizte Raketen," Astronatic Act, Vol 5, 1959.

3. Herzberg, G., "Molecular Spectra and Molecular Structure," New York 1939.

4. Syrkin, Y. K., and Dyatkina, M. E., "Structure of Molecules and Chemical Bonds," Interscience Publishers, New York, 1950.

5. R. R. John et. al., "Arc-Jet Engine Performance - Experiments and Theory," ARS-IAS Paper 61-101-1795, June 1961.

6. Jack, J. R., "Theoretical Performance of Propellants Suitable for Electrothermal Arc-Jet Engines," ARS 1506-60, December 1960.

7. Brandt, P. B., "Partition Functions as they Pertain to Equilibrium Thermodynamic Properties of Gases," Chance Vought Research Report, RE-OR-2, December 1959.

8. Chance Vought Research Report, RE-IR-14, "The Thermodynamic Properties of High Temperature Air," June 1961.

9. Ling-Temco-Vought Research Report, RE-IR-26, "The Thermodynamic Properties of High Temperature Argon," October 1961.

10. McGee, M. A., and Heller, G., "Thermodynamic Properties of Hydrogen, Helium and Lithium Plasmas," ARS 1507-60, December 1960.

11. McGee, M. A., and Heller, G., "Plasma Thermodynamics," ARS 2357-62, March 1962.

12. Gilmore, F. R., "Equilibrium Composition and Thermodynamic Properties of Air," Rand Corp., RM 1543, August 1955.

13. Krieger, F. J., "A Parametric Study of Certain Low-Molecular- Wt Compounds as Nuclear Rocket Propellant," 5 parts IV, Lithium Hydride RM-2403, 1959.

14. Sanger-Bredt, "Uber Arbeitgose fur Konventionell Beheizte Raketen," Astroatic Acta, Vol V/FASC 2 1959.

15. Noeske, H. O., Kassner, R. R., "Analytical Investigation of a Bi Propellant Arc-Jet," ARS No. 2125-61, New York, October 1961.

16. Maecker, H., "About the Characteristics of Cylindrical Arcs," Zeitschrift fuer Physik 157 (1950) pp. 1-29 (In German).

17. Justi, E., "Specific Heat, Enthalpy and Dissociation of Technical Gases," Berlin 1938 (In German).

18. Huff, V. N., Gordon, S., and Morrell, E., "General Method and Thermodynamic Tables for Computation of Equilibrium Composition and Temperature of Chemical Reactions," NACA Report No. 1037 (1951).

19. Rompe, R., and Steenbeck, M., "Der Plasmazustand der Gase," Ergebnisse der exakten Naturwissenschaften 18 (1939) p. 257 (In German).

20. Finkelnburg, W., and Maecker, H., "Elektrische Lichtboegen and Thermische Plasmen," Encyclopedia of Physics, Vol XXII, 1956.

21. Busz-Peuckert and Finkelburg, W., "About the Discharge Mechanism of the High-Temperature Arc," Zeitschrift fuer Physik 146 (1956) pp. 655-663.

22. Ellenbaas, W., "The High Pressure Mercury Vapour Discharge," Amsterdam, 1951.

23. Cobine, J. D., "Gaseous Conductors," Dover Publications, S442, New York.

24. Handbook Dev Physic, Vol XXII, 1956.

25. Scott, R. B., "Cryogenic Engineering," D. Van Nostrnad Co., New York, 1959.

26. Lithium Corp. of America, Products Data Reports, 104-257, and 203-856.

27. Humpel, L. A., Rare Metals Hand Book, Reinhold Pub. Co., New York, 1959.

28. Beech Aircraft Corporation, "Engineering Report 12606," 1962.

29. Patterson, G. N., "Molecular Flow of Gases," Wiley Co., New York, 1956.

30. Stull, D. R., and Sinke, G. C., "Thermodynamic Properties of Elements," American Chemical Society, Washington D. C., 1956.

31. P'tzer, K. S., and Clement, E., "Large Molecules in Carbon Vapor," Journal of American Chemical Society.

32. Weaton, John R., and Dean, Robert C. Jr., "On Anode Gas Sheath Electrical Breakdown in a High Pressure Arc Plasma Generator," Dartmouth Research Report, October, 1961.

33. List, B. H. and Jones, T. B., The Electrical Stability of High Current Arcs in Air and Controlled Gasious Mixtures, AD 1765, ASTIA.

34. Yonts, O. C., Normand, C. E., and Harrison, D. E., "High-Energy Sputtering," Journal Applied Physics, Vol 31, No. 3, March 1960.

35. Herzfeld, Karl F., Uber die Zerfallsgeschwindigkeit der Molekule. Zeitschr. f. Physik., Vol 8, 1922, pp. 132-136.

36. Wood, George P., "Calculations of the Rate of Thermal Dissociation of Air Behind Normal Shock Waves at Mach Numbers of 10, 12, and 14. NACA TN 3634, April 1956.

37. Gibb, Thomas R. P., Jr. and Messer, Charles E., " A Survey Report on Lithium Hydride," A. E. C. Report No. N10-3957, May 1954. (Revised August 1957).

38. Rossini, F. D., et. al., "Selected Values of Chemical Thermodynamic Properties," NBS Circular 500, 1 February 1952.

39. Penner, S. S., "Chemistry Problems in Jet Propulsion," Pergamon Press, New York, 1957.

40. King, Charles R., "Compilation of Thermodynamic Properties, Transport Properties, and Theoretical Rocket Performance of Gaseous Hydrogen," NASA TN D-275, April 1960.

41. Bray, K. N. C., "Atomic Recombination in a Hypersonic Wind-Tunnel Nozzle," Journal Fluid Mechanics, Vol 2, No. 1, 1958.

42. Logan, J. G., "Relaxation Phenomena in Hypersonic Aerodynamics, Institute Aero. Sci., Washington, Preprint No. 728.

43. Stoner, W., Plasmadyne unpublished works on "high specific impulse studies for arc engines," 1961-1962.

44. Van Jaskowsky, W. F., "Brems Continuum Radiation of Hydrogen," Plasmadyne Report PLR-44, January 1960.

45. Stoner, et. al., "Preliminary Engineering Evaluation of Advanced Space Propulsion Systems," Plasmadyne Report PLR-58, AF 33(616) -5709, final report.

46. Moeckel, W. E., "Trajectories with Constant Tangential Thrust in Central Gravitational Fields," NASA TR R-53, 1960.

47. Final Summary Report (Confidential) Vol 1, "Development of a Plasmajet Rocket Engine for Attitude Control," Robert V. Greco, Willis A. Stoner, Plasmadyne GRC 1341-A.

48. ARS Report 2350-62, Electric Propulsion Conference, March 1962, "Research and Development of a 1 KW Plasmajet Thruster," Robert V. Greco, and Willis A. Stoner, (Unclissified).

49. Masser, P. S., "Recent Experimental Plasmajet Thruster Results," Plasmadyne PLR-98, May 1961, and ARS-IAS Conference June 1961, (Unclassified).

50. Skolnik, M. and Jones, T. B., "Characteristics of the Current Tung sten Arc in Argon, Helium and Their Mixtures," Journal of Applied Physics, Vol 23 # 6, June 1952.

TYPING GUIDES; CATALOG CARDS -

This typing guide will be used in preparing catalog or abstract cards for inclusion in Technical Documentary Reports. Format instructions for preparation of catalog cards are contained in AFSC M Nr. 5-1, "Preparation of AFSC Technical Documentary Reports".

All copy typed on this guide should touch the non-photographic blue line limits.

The broken lines and circles will appear on the completed catalog cards and will serve as guide lines in trimming and punching the individual cards for filing.

Typing guides are available from ASAPP, ext. 22239 or 20191.

Aeronautical Systems Division, Dir/Materials & Processes, Nonmetallic Materials Lab, Wright-Patterson AFB, Ohio.
Rpt Nr ASD-TDR-62-451. PROPERTIES OF PLASMAS AS THEY PERTAIN TO THERMAL ARC JETS. Final report, Apr 62, 136 pp, incl illus, tables, & 48 refs.

Unclassified Report

The purpose of this study is to present information which will aid in selecting propellants for use in electro thermal engines. Several potential propellants were examined. These include hydrogen, ammonia, helium lithium hydride, nitrogen, methane, air, argon, and lithium.

(over)

The report includes discussions of important propellant properties and their effect on engine performance and life. The effect of the propellant choice on the operation of the arc jet is considered. This includes examining theoretical thruster efficiency, engine life and the effect of the engine's mission. Experiments were performed for eight propellants using Plasmadyne's one-kilowatt engine. The results of these tests are discussed.

1. Propellant Properties
2. Rocket Propellants
3. Plasma Physics
4. Nuclear Propulsion
I. AFSC Proj 3048, Task 304803
II. Contract AF33(616)-8173
III. Plasmadyne Corp.
IV. Meltzer, Joseph
V. Aval fr OTS
VI. In ASTIA collection